CEREBELLAR INTRACELLULAR CALCIUM SIGNALING AND PROAPOPTOTIC/PROINFLAMMATORY PROTEIN CHANGES COMMON TO MOTOR DYSFUNCTIONS WITH DIVERGENT ETIOLOGIES

By

Matthew G. Lamont

A Thesis submitted to the

School of Graduate Studies

In partial fulfillment of the requirements for the degree of

Doctor of Philosophy

School of Pharmacy

Memorial University of Newfoundland

September 2020

St. John's Newfoundland

Abstract

Introduction

Binge drinking among adolescents is an ongoing public health concern. Although binge drinking can also be harmful to adults, the adolescent population is more susceptible to aberrant neurological changes as their brains are still undergoing significant development. The waddles (*wdl*) mouse is characterized by a namesake waddling gait due to a homozygous mutation of the Car8 gene. Carbonic anhydrase type 8 (CAR8) controls the intracellular release of calcium (Ca^{2+}) from internal stores. Both models display a similar cerebellar based ataxia which is why they were chosen for comparison.

Methods

Groups of pre-adolescent post-natal day (PND 26) and adolescent (PND 34) rats underwent a series of behavioral tests designed to assess memory, anxiety regulation, and motor function. Subjects were first exposed to either ethanol or plain air through a vapour chamber apparatus for five consecutive days (two hours per day). Rota-rod testing was conducted to characterize the wdl mutation and ethanol treatment effects on motor output. Acute cerebellar slices from wdl mice were subsequently utilized for fluorescent calcium imaging experiments. Western blotting was used for protein quantification in the homogenized cerebella of both models.

Results

Behavioral testing using the rota-rod, cage-hang, novel object recognition, light-dark box, and elevated plus maze apparatuses showed significantly decreased object memory and measures of anxiety-related behaviors in ethanol treated subjects. Western blotting indicated elevated levels of proinflammatory/proapoptotic proteins in the cerebella of ethanol treated and wdl animals. Younger homozygous wdl mice outperformed their older cohorts on the rota-rod. Heterozygotes, which were thought to be free of motor impairment, displayed motor learning deficiencies. Calcium imaging revealed significant attenuation of cerebellar granule cell somatic Ca^{2+} signaling in homozygous mice.

Conclusion

Differences on anxiety tests indicate a failure of behavioral inhibition in the ethanol treated group. There are also impairments to motor coordination and object memory, which involve the cerebellar and hippocampal brain regions, respectively. When taken together with work on the wdl mouse, these findings suggest disruptions in cerebellar circuitry hampering proper neuronal communication have drastic consequences for behavioral output of the cerebellum.

Acknowledgments

I would like to acknowledge my supervisor, Dr. John Weber, for his continued advice and support both in conducting experiments for and the writing of this thesis; and my other supervisory committee members, Drs. Noriko Daneshtalab & Qi Yuan, for their helpful comments and guidance. I would also like to thank the many summer students who have come through the lab; especially Catherine Grandy, Nicole Head, Steven Rowe, and Travis Coles for their contributions to behavioral experiments. A special thank you to Dr. Jules Dore for his assistance with the western blotting technique utilized for this project.

Lastly, but certainly not least; thanks to my family and friends who have supported me before, during, and after this work. I would not be where I am today without their love and understanding.

I would like to especially thank my wife Danika for her patience, understanding, support, love, and more than she has provided through this entire process. I am a better person because of her.

This work was supported by grants from the Natural Sciences and Engineering Research Council (NSERC), the Canada Foundation for Innovation (CFI), and the A.G. Hatcher Memorial Scholarship.

Table of Contents

List of Tables

List of Figures

List of Abbreviations

AIDA - 1-Aminoindan-1,5-Dicarboxylic Acid

AMPA - α-Amino-3-Hydroxy-5-Methyl-4-Isoxazolepropionate

ARR – Accelerating Rota-rod

AS – Acoustic Startle

Ca^{2+} - Ionic Calcium

cAMP - Cyclic Adenosine Monophosphate

AUTC – Area Under the Curve

BAC – Blood Alcohol Concentration

Bcl-2 – B Cell Lymphoma 2

CAR8 – Carbonic Anhydrase Type 8

CF – Climbing Fiber

CNS – Central Nervous System

DAG - Diacylglycerol

DHPG - (S)-3,5 Dihydroxyphenylglycine

DLB – Dark/Light Box

EPM – Elevated Plus Maze

EPSC - Excitatory Post-Synaptic Current

ER – Endoplasmic Reticulum

FC – Fear Conditioning

FSRR – Fixed Speed Rota-rod

GoC – Golgi Cell

GC – Granule Cell

GCL – Granule Cell Layer

ICH – Inverted Cage Hang

IkB – Inhibitor of Kappa B

IKK – IkB Kinase

IP_3 - Inositol 1,4,5-trisphosphate

LTD – Long Term Depression

LTP – Long Term Potentiation

MF – Mossy Fiber

mGluR – Metabotropic Glutamate Receptor

NF-kB – Nuclear Factor Kappa-light-chain-enhancer of Activated B Cells

NIK – NF-kB Inducing Kinase

NMDA - *N*-methyl-D-asparate

NOR – Novel Object Recognition

OF – Open Field

OG-BAPTA-1-AM – Oregon Green 488 BAPTA-1AM

PC – Purkinje Cell

PF – Parallel Fiber

PI – Propidium Iodide

PIP2 - Phosphatidylinositol 4,5 Bisphosphate

PKC – Protein Kinase C

PLC – Phospholipase C

PNA – Postnatal Age

PND – Postnatal Day

PP2B - Ca^{2+}/calmodulin-activated protein-phosphatase-2B

PrP^C – Cellular Prion Protein

ROI – Region of Interest

RPM – Rotations Per Minute

VGCC – Voltage Gated Calcium Channel

VOR – Vestibular-ocular Reflex

Wdl – Waddles Mouse

WT – Wild Type

$[Ca^{2+}]_i$ – Intracellular Calcium Concentration

Chapter 1 - Introduction

1.1 Background

Motor coordination and learning are the primary responsibilities of the cerebellum, the cellular basis of which heavily involves the ability of various synapses to undergo plasticity (Ito 2006). Damage to the cerebellum often leads to symptoms such as ataxia, asynergy, dysmetria, and motor learning deficits in humans (Schmahmann 2004; Stoodley & Schmahmann 2010) as well as in other mammalian species such as rabbits or various rodents (Lalonde & Strazielle 2001; Rinaldo & Hansel 2010). Cerebellar dysfunction can be due to acute changes in cellular physiology having a direct effect on function (e.g. significant levels of ethanol in the extracellular environment or an altered intracellular concentration of Ca^{2+} in neurons; Zagha et al. 2010), or to chronic changes in cerebellar physiology inducing permanent/semi-permanent alterations to functionality (e.g. high levels of ethanol over time reducing the number of neurons or a chronically altered intracellular Ca^{2+} concentration changing cerebellar cortex morphology; Lalonde & Strazielle 2001). Ethanol is a commonly consumed substance that can significantly alter neuronal physiology (especially in the cerebellum), even at relatively low levels (50mM; Belmeguenai et al. 2008).

Rates of binge drinking among adolescents have recently been reported to be unexpectedly high (approximately 17% of respondents in the past two weeks) and holding steady since 2017 despite continued declines in other substances of abuse that were surveyed (Johnston et al. 2018). This is therefore an area of concern for public health as binge drinking induced neuroinflammation heavily contributes to the neurotoxicity of ethanol (Hamelink et al. 2005; Crews et al. 2006; Tajuddin et al. 2014). Chronic ethanol

exposure has been shown to cause deficits in motor coordination and learning (Forbes et al. 2013; Teixeira et al. 2014); in addition, ethanol can cause depressed regional brain Ca^{2+} levels (Ross Medina & Cardenas 1974), and at concentrations as low as 10 μM inhibit neuronal Ca^{2+} uptake via N-methyl-D-aspartate (NMDA) receptors in neuronal cultures by approximately 30% (Hoffman et al. 1989). *In vivo* concentrations of ethanol needed to be higher to have the similar effect of inhibiting Ca^{2+} influx via voltage gated channels (in the cerebellum this concentration was 100 mM; Daniell & Leslie 1986). It is likely that alterations of NMDA Ca^{2+} currents would have the most significant effect on behavior as their normal activity is necessary for long-term potentiation (LTP). Alterations in behavior and neuronal Ca^{2+} homeostasis seen in chronic ethanol exposure are comparable to the symptoms seen in a mutant model of cerebellar ataxia, the *wdl* mouse.

The mutant *wdl* mouse is an excellent model to study how a change in cerebellar physiology, specifically physiology involving Ca^{2+} signaling, affects cerebellar development and ultimately motor output. This mutation affecting intracellular Ca^{2+} signaling is localized to the cerebellum within the central nervous system (CNS; Aspatwar et al. 2010). The *wdl* mouse originated as a spontaneous mutant, initially found in Jackson Laboratories, which exhibited a wobbly side-to-side gait and appendicular dystonia from birth (Jiao et al. 2005). Genotyping of this mutant revealed a 19 base pair deletion in the gene encoding carbonic anhydrase type 8 (CAR8; Jiao et al. 2005). The deletion causes a virtual absence of functional CAR8 in homozygous animals which display a phenotypic ataxia. Interestingly, heterozygous animals with only one faulty copy of the gene display normal motor proficiencies. This theoretically translates to the

heterozygotes possessing half of the functional copies of CAR8 seen in non-mutated animals. CAR8 has been shown previously to reduce the release probability of Ca^{2+} from intracellular stores by inhibiting the binding of inositol 1,4,5-trisphosphate (IP_3) to its receptor (inositol 1,4,5-trisphosphate receptor; IP_3R). It is expressed primarily in the cerebellum of mice with particularly high localization in the molecular layer (ML) and peri-somatically in Purkinje cells (PC; Yan et al. 2007; Aspatwar et al. 2010). The IP_3R is located intracellularly on the endoplasmic reticulum (ER) and controls the release of Ca^{2+} from internal stores. As the homozygous *wdl* mice lack functional CAR8, we would expect to see more Ca^{2+} released in the cerebellar cells of these animals in response to stimulation affecting the IP_3 signaling pathway in neurons.

The goal of this dissertation is to compare two models of cerebellar dysfunction: the mutant *wdl* mouse, and an adolescent binge drinking paradigm in rats. This comparison gives us a deeper understanding of alterations to cerebellar physiology and how these give rise to aberrant behavioral output. These important concepts and more are discussed further and with more detail in subsequent sections.

1.2 The Cerebellum

The cerebellum is involved in fine tuning motor output by controlling aspects such as balance, smoothness of movements, and gait (Ito 2006). The cerebellum achieves this by processing a large amount of afferent converging information from areas such as the vestibular and inferior olivary nuclei into a relatively small amount of efferent information. This outgoing signal is conducted by the sole output neuron of the cerebellar cortex, the PC (Ito 2006). PC output is mediated by the chief inhibitory neurotransmitter of the mammalian nervous system, gamma-aminobutyric acid (GABA). GABAergic

output of the PCs inhibits deep cerebellar and vestibular nuclei, modulating cerebral motor commands as they are propagated towards the spinal cord. Before the output signal leaves the cerebellum, there is an enormous amount of internal processing that occurs within the cerebellar circuitry. The first step in the cerebellar circuitry is incoming mossy fibers (MFs) that originate from numerous sources in the peripheral nerves, spinal cord, and brain stem, synapsing onto 400-600 granule cells (GC). Each of these GCs then projects their axon as parallel fibers (PFs) which each synapse with as many as 300 PCs (Eccles et al. 1967). Along with all these connections there are also several types of inhibitory interneurons modulating the afferent signal, further complicating this neuronal circuitry (Fig. 1.1).

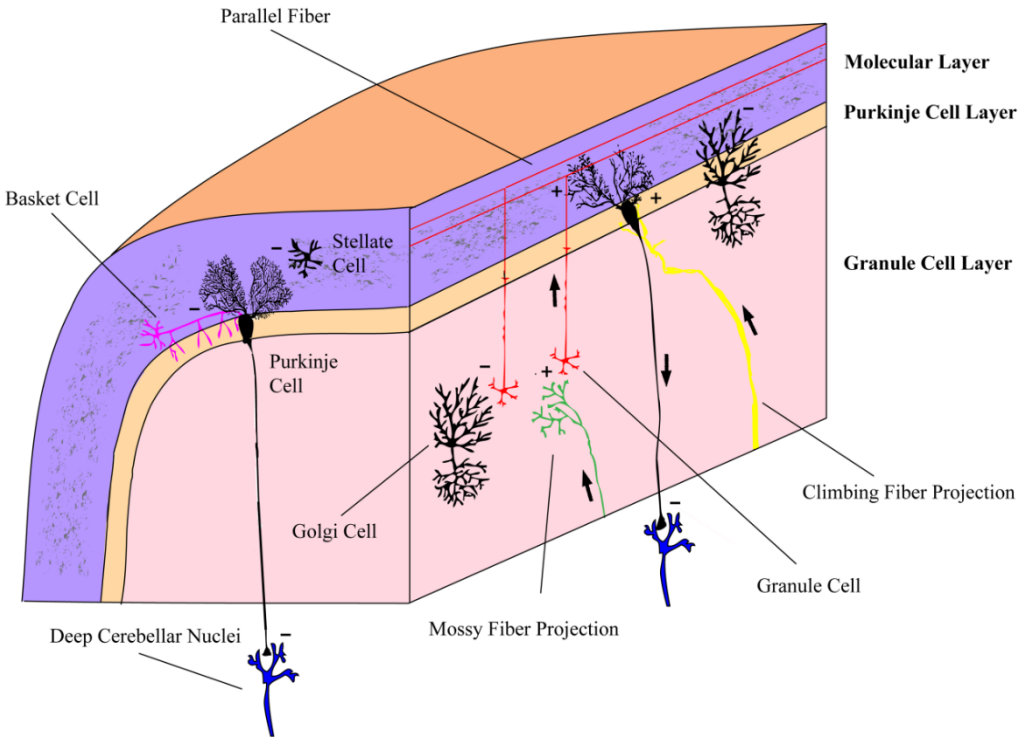

Figure 1.1 - Neurons and circuits of the cerebellum – The main signaling circuit of the cerebellum begins with an incoming stimulus from the mossy fiber (MF; Green), a projection from precerebellar nuclei (e.g. vestibular nuclei, reticular nuclei). The MF forms an excitatory synapse with granule cells (GCs; Red) that is also modulated by Golgi cell (GoC; Black) inhibitory input. When excited the GCs stimulate PCs (Black) via the GC projections called parallel fibers (PFs; Red), which can also be inhibited by neighbouring GoCs. However, the PCs excitability is further modulated by several other types of cells. The inhibitory interneurons (Basket and Stellate cells, magenta/black respectively) are in the ML and provide inhibitory input. PCs receive additional excitatory input from CFs (Yellow) which originates in the inferior olivary complex. Based on the temporal and spatial summation of all incoming signals, the PCs will either continue their tonic inhibition of the deep cerebellar nuclei (Blue) or the inhibition will be temporarily attenuated; generally this is either a result of or will modulate motor behaviour and/or motor learning based in the cerebellum.

1.3 The Importance of Calcium in the Cerebellum

Calcium, in its ionic form, is present throughout the nervous system and carries out a variety of important roles. Ca^{2+} is necessary for proper neuronal growth and development, neurotransmission throughout the central and peripheral nervous system, and can lead to differential patterns of gene expression (Lamont & Weber, 2012). Calcium is also required for several forms of synaptic plasticity in the hippocampus, cerebral cortex, and cerebellum (Bliss & Collingridge 1993; Malenka & Nicoll 1999; Rose & Konnerth 2001). Synaptic plasticity is the ability of either the presynaptic or postsynaptic neuron of a given synapse to either modify the strength of signal released or to respond to a signal more effectively, respectively (Collingridge & Singer 1990). It is theorized that by modifying how strongly a synapse will respond to stimulation, our neural network is encoding salient information from our environment. Long-term depression (LTD), particularly at PF-PC synapses in the cerebellum, is the widely accepted vertebrate model for a cellular mechanism that underlies synaptic changes during motor learning and memory formation in the cerebellum. LTD is said to occur at a synapse when there is activity-dependant reduction in the efficiency of the synapse, which can be due to both pre- and post-synaptic changes. Several molecular components have been identified which appear to be necessary for its induction, including glutamate receptors and various kinases (Massey & Bashir 2007). It was long thought that PF-PC synapses were the only synapses capable of plasticity in the cerebellar cortex, however plasticity has now been described at several other synapses (Hansel et al. 2001; Dean et al. 2010).

In the cerebellum the excitability and signaling in neurons is highly tied to the excitatory glutamatergic neurotransmitter system. Glutamate activates two main receptor types in cerebellar neurons: the ionotropic (AMPA, kainate, and NMDA) receptors and the metabotropic glutamate receptor family.

Ionotropic receptors allow Ca^{2+} influx either directly through their channel when activated by glutamate, or indirectly by contributing to membrane depolarization which affects voltage-gated Ca^{2+} channels (VGCCs). NMDA receptors are well distributed in the brain but were only recently described in adult PCs (Piochon et al. 2007; Renzi et al. 2007). Activation of this receptor subtype primarily causes an influx of Ca^{2+} into the cell. Alternatively, AMPA and kainate receptor activation leads primarily to sodium influx. Although some types of these receptors can also be permeable to Ca^{2+} depending on their subunit combination, AMPA receptors containing a GluR2 subunit are Ca^{2+}–impermeable, while those lacking this subunit are permeable to Ca^{2+} (Liu & Cull-Candy 2005). AMPA receptor activation can also indirectly lead to Ca^{2+} influx by inducing membrane depolarization activating VGCCs. Additionally, membrane depolarization increases the activation of NMDA receptors which are also sensitive to the membrane potential of the cell through their magnesium blockade.

Metabotropic glutamate receptor types are divided into three groups. Group 1 mGluRs (mGluR 1 and 5) lead to intracellular Ca^{2+} increases via a G-protein coupled to phospholipase C (PLC). PLC cleaves phosphatidylinositol 4,5 bisphosphate (PIP2) from the cell membrane, producing diacylglycerol (DAG), which activates the enzyme protein kinase C (PKC) and IP_3, which binds to IP_3Rs on intracellular Ca^{2+} stores located on the ER, resulting in a release of Ca^{2+} from the stores and an elevation of intracellular free

Ca^{2+} (Fig. 1.2). In many types of neurons, the depletion of Ca^{2+} stores also stimulate influx of extracellular Ca^{2+} through channels on the plasma membrane, a process termed "capacitative Ca^{2+} influx" (Weber et al. 2001; Baba et al. 2003). Studies have shown that activation of group I mGluRs can enhance the elevation of Ca^{2+} mediated by NMDA receptors (Bruno et al. 1995; Rahman & Neuman 1996). Group II (mGluR2 and 3) and III (mGluR4 & mGluR6-8) metabotropic glutamate receptors are also G-protein linked and inhibit adenylate cyclase causing lower levels of cyclic adenosine monophosphate (cAMP) and in general lower levels of intracellular Ca^{2+} (Coutinho & Knöpfel 2002).

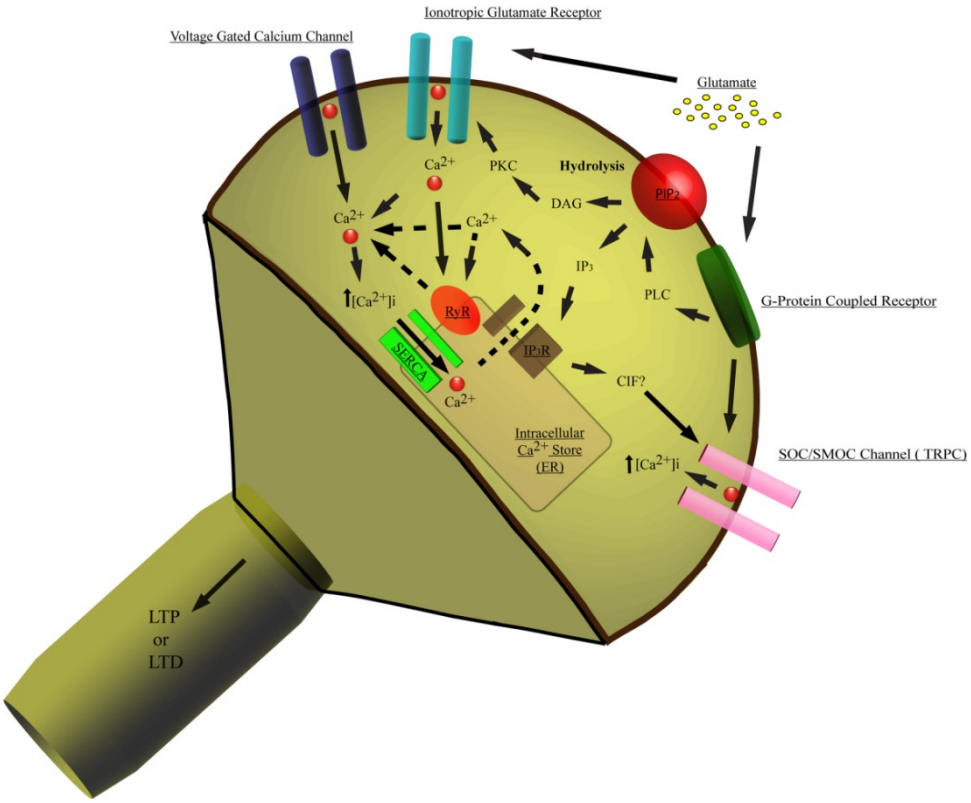

Figure 1.2 - Mechanisms that contribute to elevated intracellular Ca^{2+} *levels at excitatory synapses in neurons - Glutamate can directly activate ionotropic channels, such as NMDA or AMPA receptors, which can lead to* Ca^{2+} *influx. A corresponding change in the membrane potential can activate voltage-gated* Ca^{2+} *channels, leading to further influx of* Ca^{2+}*. Activation of type 1 metabotropic glutamate receptors (mGluRs), which are coupled to G-proteins, produces an intracellular signaling cascade where phospholipase C (PLC) cleaves phosphatidylinositol 4,5 bisphosphate (PIP2) producing diacylglycerol (DAG) and inositol 1,4,5-trisphosphate (*IP_3*). DAG activates protein kinase C (PKC), while* IP_3 *binds to receptors (*IP_3R*) on the endoplasmic reticulum (ER) and releases stored* Ca^{2+}*. Ryanodine receptors (RyR) can also be bound by* Ca^{2+} *and cause* Ca^{2+}*-induced* Ca^{2+} *release. In some types of neurons, release of* Ca^{2+} *from intracellular stores causes additional influx of* Ca^{2+} *through store-operated/second messenger-operated channels (SOCs/SMOCs), which may be mediated by a* Ca^{2+} *influx factor (CIF). SOCs/SMOCs are believed to be transient receptor potential channels (TRPs) in many cells. In Purkinje cells, activation of mGluR1s causes influx of* Ca^{2+} *through TRPCs. Calcium levels are returned to baseline levels by uptake through the sarcoplasmic-endoplasmic reticulum* Ca^{2+}*-ATPase (SERCA) into the ER, by extrusion through membrane pumps, by binding to cytosolic proteins, or by uptake into organelles such as the nucleus and mitochondria.*

Some of the best understood forms of synaptic plasticity involve the PCs. LTD represents a persistent decrease of postsynaptic sensitivity to glutamate caused by the removal of AMPA receptors from the membrane via endocytosis (Ito 2006). This endocytic mechanism is thought to be the primary method for plasticity-mediated memory encoding in PCs, as an input-specific type of synaptic plasticity. Both PF-LTD and CF-LTD on PCs are dependent on an AMPA-receptor induced membrane depolarization and subsequent Ca^{2+} influx through VGCCs (Hansel & Linden 2000; Hansel et al. 2001). Activation of mGluRs also appears to be necessary for expression of LTD at both synapses, most likely via the above-mentioned coupling of group I mGluRs to the IP_3 pathway (Daniel Levenes & Crépel 1998; Kohda Inoue & Mikoshiba 1995). PC synaptic plasticity was thought to be NMDA receptor-independent, until recently when their activation at CF-PC synapses was found necessary for PF-LTD induction (Piochon et al. 2010). In addition to large Ca^{2+} transients, PF-LTD expression is dependent on activation of the enzymes α-Ca^{2+}/calmodulin-dependant protein kinase II (α-CaMKII) and PKC (Piochon et al. 2010).

A stable cellular mechanism for memory could not be established without an opposing force of plasticity, as synaptic strength can only be depressed so far. LTP provides this opposing force of plasticity by strengthening synapses. In cerebellar PC synapses LTP is observed to occur with PF stimulation alone and this effect is ascribed to increased glutamate release from PF terminals (Salin Malenka & Nicoll 1996). It was recently shown that there is also a postsynaptic LTP effect that occurs with PF simulation that is cAMP independent and relies on nitric oxide (Lev-Ram et al. 2002).

The interplay between LTP and LTD of the PF-PC synapse indicates that it operates bi-directionally (i.e. PF stimulation alone leads to LTP of the synapse, while paired stimulation from PFs and CFs causes LTD.). The bi-directionality is controlled by intracellular Ca^{2+} concentration ($[Ca^{2+}]_i$), where a high $[Ca^{2+}]_i$ favors LTD induction and a low $[Ca^{2+}]_i$ favors LTP induction (Coesmans et al. 2004). This is the opposite result to the effect levels of observed $[Ca^{2+}]_i$ have on plasticity at other known bidirectional synapses in the brain, such as those in the cerebral cortex and hippocampus (Hansel Artola & Singer 1997; Mulkey & Malenka 1992). Together this indicates that bi-directional plasticity of the PF-PC synapse has a significant functional role as it modulates the excitability of the sole output neuron of the cerebellar cortex, the PC. Changes induced in the cerebellar circuitry surrounding PCs as well its output targets, the deep cerebellar nuclei and vestibular nuclei, signify a change to the internal representation of a stored memory (i.e. various types and degrees of plasticity in different synapses throughout the cerebellar cortex interact to produce an output signal that fine-tunes our motor movements; D'Angelo & DeZeeuw 2008). This highlights the significance of proper GC function for overall cerebellar function, as they provide these important PF projections synapsing onto and affecting the firing of PCs.

1.4 Calcium and Cerebellar Based Ataxia

The cerebellum plays a critical role in learning sensorimotor tasks or skills (Kandel et al. 2000). For instance, it is widely accepted that the olivo-cerebellar tract is a key pathway contributing to motor learning (Ito 2006). Although the involvement of cerebellar circuit is critical, its precise role in this process is undetermined. There is a growing awareness that many neurodevelopmental disorders are associated with

functional cerebellar deficits and learning impairments (Manto & Jissendi 2012). The cerebellum is an excellent platform for studying neurodevelopment as its structural development occurs in a heavily stereotyped pattern and additional development occurs after birth. In addition, the anatomy of the cerebellum has been highly conserved from rodents to humans, suggesting that studies of cerebellar phenomena in rodents should be at least partially applicable to humans (Manto & Jissendi 2012).

Calcium signaling plays a prominent role in long-term changes in PC synapses with PFs. In Marr-Albus-Ito models of cerebellar function, LTD at PF-PC synapses provides a cellular substrate of certain forms of cerebellar motor learning (Marr 1969; Albus 1971; Ito 1984). Marr proposed that PF synapses onto PCs are potentiated when they are activated simultaneously with a CF (Marr 1969). In Marr's theory the cerebellum learns motor skills by storing memory traces at the PF synapse under instruction of the olivary nucleus, which signals correct performance via CF activation. A few years later, Albus (1971) refined this theory by suggesting that the cerebellum functions on a modified classical conditioning paradigm, with a complex spike as the unconditioned stimulus and MF input as the conditioned stimulus. This last hypothesis became known as the Marr-Albus theory, which predicted the existence of LTD before any plasticity of synapses onto PCs was found. A prominent experimental model of classical motor conditioning is eye-blink conditioning (Medina et al. 2002). In this model, the conditioned stimulus is a tone which is paired with the unconditioned stimulus of a puff of air. The resulting conditioned response is the closing of the eyelid when only a tone is presented, and it is this learned response that is believed to be mediated by PF-LTD. PF-LTD can be induced *in vitro* by simultaneous activation of PFs and CFs at low

frequencies (Ito & Kano 1982; Coesmans et al. 2004). In these cerebellar network models, it was assumed that PF-PC synapses carry contextual information and that signaling at CF-PC synapses represents error signals in motor performance that could alter subsequent behavior.

During ataxia, movements are usually characterized by abnormal timing, delayed muscle activation, sudden interruptions, and exaggerated corrections. These dysfunctions, which are fundamentally of timing and coordination, are often due to a lack of cooperation between agonist and antagonist muscle activation (Garwicz 2002). The deficit in timing likely reflects an abnormal pattern of activity in deep cerebellar or vestibular nuclei, which is thought to encode relative phases of muscle contraction (Sánchez-Campusano Gruart & Delgado-García 2007). Interruptions or alterations in cerebellar circuitry usually leads to some form of ataxia, and more subtle changes that do not interfere with the structure of the circuitry usually do not affect motor performance, only motor learning (DeZeeuw & Yeo 2005). Mutant mouse models with a disturbed Ca^{2+} homeostasis all experience ataxia, at least to some degree (Draski et al. 1994; Lalonde & Strazielle 2001; Mistumura et al. 2011).

Although the PF-PC is arguably the most studied synapse in the cerebellum with respect to plasticity, there are other important synapses with possible functional significance that have been previously described, such as the MF-GC synapse (D'Angelo et al. 1999). Plasticity of the MF-GC synapse is bi-directional and has been observed to be NMDA-receptor-dependent. Both LTP and LTD of this synapse are expressed presynaptically via an increase in glutamate release probability as detected by an increased electrophysiological NMDA-receptor-mediated current (Nieus et al. 2006).

Unlike the reversal in the PF-PC synapse, a lower $[Ca^{2+}]_i$ will cause the induction of LTD and a higher $[Ca^{2+}]_i$ will lead to LTP induction (Gall et al. 2005). This indicates that the hypothesized abnormal Ca^{2+} levels in *wdl* mice would drastically alter synaptic plasticity and therefore the information processing capabilities of the cerebellum.

The review by D'Angelo & De Zeeuw (2008) put forward a 'time-window matching' hypothesis which states that MF inputs to the granule cell layer (GCL) are transformed into "well-timed spike bursts" by intrinsic GCL processing, the duration of which is controlled by Golgi cell (GoC) feed-forward inhibition. The oscillation of these spike bursts is differentially spread over various fields of GCs to generate ongoing time-windows from interacting motor domains (D'Angelo & De Zeeuw 2008). Synaptic plasticity at this synapse would therefore serve the purpose of fine-tuning certain pre-wired circuits, with the result of favoring certain granule cell groups with respect to time windows. This phenomenon demonstrates that plasticity at GC synapses is as important for proper cerebellar function as the plasticity at the heavily studied PC synapses.

As many types of cerebellar plasticity at various synapses rely on differential Ca^{2+} concentrations to drive either the strengthening or weakening of that synapse, the importance of proper Ca^{2+} homeostasis becomes clear. Modifications to the above-mentioned synapses via altered plasticity would affect the cerebellums' ability to integrate existing motor function with novel incoming information (i.e. vestibular input being integrated with balance motor programs). The effects on plasticity would almost certainly affect motor learning that is known to require cerebellar involvement (Ito 2006).

1.5 Mutant Ataxic Animal Models

Immense strides have been made in advancing techniques used to research the involvement of Ca^{2+} in cerebellar plasticity and motor learning. One of these novel techniques is the use of genetic knock-out, knock-in, or mutant mice which allows for this phenomenon to be studied *in vivo*. At the center of most types of synaptic plasticity in the cerebellum is the Ca^{2+} ion. Calcium appears to be necessary for the induction of LTD and LTP at most synapses, and a wide variety of animal models (mutant or transgenic) that elicit disruptions in motor function have alterations in various components of Ca^{2+} signaling pathways.

Many varieties of ataxic mutant mice are suitable for studies of cerebellar plasticity and signaling, such as the hotfoot mouse (Draski et al. 1994; Mandolesi et al. 2009). The hotfoot mouse has a single recessive gene (*ho*) causing a resting body tremor and a high quick-stepping pattern during movement due to alterations in monoaminergic neurotransmission (Draski et al. 1994). There are also more recently discovered models with altered plasticity in the cerebellum, such as the voltage gated $K_{V3.3}$ channel knockout mouse that experiences irregular Ca^{2+} dynamics and electrical conductance in PCs (Zagha et al. 2010).

Schonewille et al. (2010) reported that LTD may not be the only process responsible for motor learning in the cerebellum. This study employed a PC-specific knockout of Ca^{2+}/calmodulin-activated protein-phosphatase-2B (PP2B) based on previous research indicating that PP2B interacted with α-CaMKII to change the phosphorylation state of AMPA receptors (Lisman & Zhabotinsky 2001). By disrupting PP2B production

in PCs LTP was abolished and motor learning was impaired, while LTD remained unaffected (Schonewille et al. 2010). Previously, much of the focus of cerebellar learning researchers was exclusively on LTD. However, Schonewille et al. (2010) indicated that LTP is also an important facet of motor learning and may complement other types of plasticity by controlling excitability. Since LTD alone was found insufficient for proper vestibule-ocular reflex (VOR) conditioning and the kinetics of VOR were unaffected, it may be that LTP has a 'priming' effect.

Other transgenic animals available for ataxic research involving plasticity within the cerebellum include an mGluR null mutant (Alba et al. 1994) and the *stagger* mouse (Mistumura et al. 2011). The *stagger* mutation results in a functional loss of a transcription factor, Retinoid-related Orphan Receptor α (RORα), which is typically prevalent in cerebellar PCs. The most prominent result of the lack of RORα at PC synapses is the complete loss of mGluR-mediated EPSCs, like what is observed in the mGluR-null mutation, thus providing complementary data. Animals bred from these models exhibit similar ataxic behaviour, and an impairment of LTD (Alba et al. 1994; Mistumura et al. 2011). The key difference is that the mGluR-null model is completely devoid of any mGluR protein, whereas the *stagger* model is missing the mGluR-mediated retrograde suppression of PF EPSCs via endocannabinoids and mGluR-mediated slow EPSCs in PCs. Therefore, the functions of the mGluR that are impaired in *stagger* mice may be responsible for the similar ataxia and LTD impairment in mGluR-null mice. Although VGCCs were shown to not be affected by Alba et al. (1994), Ca^{2+} release has been shown to be important for LTD and there may be a dysfunction of IP_3-mediated intracellular Ca^{2+} store release in these two models. The reason for this is that the mGluRs

found in PCs have been shown to activate the IP_3-mediated intracellular Ca^{2+} store release (Okubo et al. 2001), leading to LTD.

Some transgenic models have allowed us to discover and study novel phenomena *in vivo*. Cellular prion protein (PrP^C) is an excellent example, since despite years of research there is little known about its role in maintaining physiology or the in neurodegenerative diseases. In a study utilizing PrP-knockout mice to investigate the involvement of PrP^C in Ca^{2+} dynamics (Lazzari et al. 2011); the PrP-knockouts had a dramatic increase of store operated Ca^{2+} entry, which was found to be due to a lower expression of Ca^{2+}-ATPases in the plasma membrane as well as ER. Dysregulation of extracellular Ca^{2+} influx led to an increased susceptibility to excitotoxicity and to cell death (Lazzari et al. 2011). This is a likely mechanism by which bovine spongiform encephalopathy and other related prion diseases progress so rapidly and aggressively. Although these mice experience disruption of cerebellar Ca^{2+} homeostasis, there is only a small effect on learning and memory in the cerebellum (Steele et al. 2007). This is likely due to LTD being intact, with only the pace making ability of PCs being affected.

Since the mechanisms underlying plasticity of the cerebellum are numerous, generally sensitive to modulation, and are best studied *in vivo*, cerebellar plasticity research lends itself to the use of transgenic models. The continued use of these models and other approaches will aid in evolving this field of research towards a greater and more in depth understanding of how cerebellar circuits work to store motor memories.

1.6 The Waddles Mouse and CAR8

The spontaneous mutation which yields the *wdl* mouse is due to non-functional expression of a protein, CAR8 (Jiao et al. 2005). The absence of CAR8 appears to cause

ataxia with a side-to-side 'waddling' gait as it is the only protein altered by the *wdl* mutation, even though functional CAR8 lacks any known enzymatic activity due to the lack of zinc residues observed in other carbonic anhydrase family members (Dodgson et al. 1991). However, functional CAR8 has been shown to have a high affinity for the IP_3R which gates intracellular ER Ca^{2+} stores (Hirota et al. 2003). It therefore seems plausible that the *wdl* mice are experiencing ataxia due to Ca^{2+} dynamics-related interference with plasticity. Supporting this hypothesis, a study conducted with IP_3R1 null mice found that normal cellular signaling and LTD were impaired by the lack of this receptor (Nagase et al. 2003).

The family of carbonic anhydrases are metal-containing enzymes which are fundamental to many biological phenomena such as photosynthesis, respiration, and bone mineral reabsorption (Dodgson et al. 1991). CAR8 is one of three acatalytic proteins within the sixteen members of the family. The CAR8 protein is expressed most abundantly in the cerebellum in the CNS with high levels in PCs and ML, indicating a strong possibility for a role in brain functions. There was also a low, but still significant, levels of CAR8 expression in the GCL (Aspatwar et al. 2010). Immunohistochemistry showed CAR8 protein in neural cell bodies as well as neurites in the adult mouse cerebellum (Taniuchi et al. 2002). Although there is detectable expression throughout bodily tissues, CAR8 is expressed at only one fifth the level seen in cerebellar tissue in the lungs and liver, which are the only two other tissues expressing significant levels (Aspatwar et al. 2010). A recent developmental expression study of CAR8 indicated it is widely distributed throughout all developing tissue at early stages (0 – 11.5 days post-impregnation) of development (Lakkis O'Shea & Tashian 1997). The level of expression

appeared to be regulated temporarily in a tissue-specific fashion and as development progressed, the expression became more restricted (similarly to the adult expression profile).

IP_3 and its receptor are integral components of the Ca^{2+} system keeping intracellular Ca^{2+} dynamics balanced (Fig. 1.2). This signaling pathway is clearly important for normal Ca^{2+} signaling since it relates to group I mGluRs which would be activated often by glutamatergic transmission. CAR8 normally inhibits the binding of IP_3 released from group I mGluR activation to the IP_3R and therefore regulates the amount of Ca^{2+} released from intracellular stores. There is evidence that CAR8 is also an important protein for proper development of the cerebellar cortex and the arrangement of excitatory synapses (Aspatwar et al. 2010). A previous study of *wdl* mice found abnormal extension of CFs into the ML of the cerebellar cortex in *wdl* mutants, a significant number of PC spines not forming synapses with PFs, and multiple synapse varicosities at many PF-PC synapses (Hirasawa et al. 2007). These structural abnormalities are likely caused by the decreased responsiveness of IP_3-mediated ER Ca^{2+} stores in the *wdl* mutant since changes in Ca^{2+} concentrations are known to alter neurodevelopment in the cerebellum (Ichikawa et al. 2002). The ataxia could also be related to the lower number of functional synapses formed in the cerebellar cortex of homozygous animals. This would once again indicate that altered Ca^{2+} levels are not only affecting proper signaling, but proper development of the cortex and synapses within it. The ataxia experienced by *wdl* mice could be due directly to the suspected atypical Ca^{2+} signaling, but more likely to the abnormal development linked to the atypical Ca^{2+} signaling at both pre- and postnatal time points.

Other ataxic mice, such as the *tottering* and *leaner* mutants, have similar issues to the *wdl* with respect to the aberrant cerebellar morphology and altered Ca^{2+} levels (Lalonde & Strazielle 2001). *Cacna1a* encodes for the α-1a subunit of P/Q type VGCCs, the knockout of which causes the ataxic syndrome seen in *tottering* mice. *Tottering* mice exhibit a disruption in PC firing and display motor deficits, which are similar to ataxic syndromes in human patients (Hoebeek et al. 2005). Like the *wdl* mutants, *tottering* mutants also display multiple synaptic varicosities and abnormal expansion of PF territories (Miyazaki et al. 2004). In both the *tottering* and the *wdl* mice there is a similar underlying issue of abnormal intracellular Ca^{2+} signaling (Kurihara et al. 1997). This provides evidence that the development of cerebellar cortex is sensitive to changes in Ca^{2+} concentrations and that this can significantly affect motor output. *Leaner* mice also exhibit disrupted motor function, like CACNA1A knockout mice (Rhyu et al. 1999). This P/Q-type channel subunit is highly expressed in both cerebellar PCs (approximately 90% of VGCCs) and GCs (approximately 45% of VGCCs; Randall & Tsien 1995).

All the mutations mentioned above are linked as they feature significant disturbances in cerebellar Ca^{2+} signaling as an underlying pathophysiology and multiple synaptic varicosities being formed at PF-PC synapses (Rhyu et al. 1999). Multiple synaptic varicosities represent a similar morphological phenotype to that seen in the *wdl* mice which progresses over the first three weeks postnatal. The similarities between the *wdl* phenotypic morphological abnormalities and those displayed by many other ataxic mutants with altered Ca^{2+} signaling indicate an important developmental role for Ca^{2+} in the juvenile murine cerebellum. Disturbing the natural homeostasis of Ca^{2+} in the cerebellum seems to inevitably lead to some form of ataxia.

1.7 Binge Drinking

Binge drinking of ethanol among adolescents is an ongoing public health concern (Johnston et al. 2018). Although binge drinking can also be harmful to adults, the adolescent population is more susceptible to aberrant neurological changes as their brains are still undergoing significant development (Han et al. 2005; Spear 2013). Brain regions which are particularly susceptible to modulation by ethanol include the hippocampus and cerebellum (Belmeguenai et al. 2008; Nixon & Crews 2002; Phillips & Cragg 1982; Urrutia & Gruol 1992). Adolescent binge drinking also alters motor function which may be due to cerebellar neurodegeneration (Forbes et al. 2013). Even transient exposure of infant rats to ethanol during the period of synaptogenesis triggers widespread neuronal loss in a wide variety of brain regions (Ikonomidou et al., 2000). Furthermore, people with adolescent-onset alcohol use disorder have decreased cerebellar volumes (De Bellis et al. 2005). This decrease in cerebellar volumes reflects a form of neurodegeneration which can likely be attributed to neuronal apoptosis.

Ethanol itself is a psychotropic drug with wide ranging effects on the body, but particularly in the brain where chronic use can cause issues such as visual, motor, and memory impairments (Nutt, 1996). These results are mediated by ethanol's ability to influence various neurotransmitter systems, cell membranes/receptors, and modulating proteins regulating gene expression and intracellular signaling pathways (Alling 1999, Dahchour et al. 2000, Schummers et al. 1997).

The strength of the effect's ethanol has on the body are directly related to the amount consumed, route of administration, and the length of time over which the ethanol is absorbed. Metabolism of ethanol is the major element underlying the importance of the

three factors listed above. The rate at which a given organism can metabolize ethanol controls how quickly it will accumulate in the fluids/tissues, and the route of administration controls the amount/subtype of alcohol dehydrogenase present to begin breaking ethanol down for excretion. There are various genetic models (e.g. knock-out/knock-in of alcohol/aldehyde dehydrogenase) which exist to study the effects of altered metabolism on the effects of ethanol on the body. This dissertation uses animals with a common genetic background which had no known issues with ethanol metabolism as alterations to metabolism are outside the scope of this project.

Subjects for this study were chosen at two different ages, PND 26 to represent a pre-adolescent development and PND 34 to represent adolescence (Sengupta 2012). Subjects ages were determined to reflect a period of neurodevelopment during which previous studies indicate the brain is susceptible to damage from ethanol (Spear & Brake 1983; Spear 2000; Spear 2013). Rats begin the process of sexual maturity after weaning begins (PND 21) and will reach sexual maturity around PND 42 (Adams & Boice 1983). The accepted period of synaptogenesis in rats is over the first two weeks of life and the third trimester of pregnancy in humans (Dobbing & Sands 1979); during which ethanol exposure is known to cause long lasting effects such as microencephaly and psychotic disorders (Streissguth & O'Malley 2000). Ethanol was administered using a vapour chamber apparatus that is often used to induce a state of ethanol dependence by administering a relatively low dose of vapour for up to seventeen hours a day (Aufère Le Bourhis & Beaugè 1997; Crabbe Harris & Koob 2011). In the soon to be described experiments of this dissertation, it was used to simulate a binge drinking session over only two hours.

The total number of neurons in each brain region is dependant on the balance of two opposing factors: the nominative force of cell acquisition (i.e. proliferation or neural migration) and the reductive force of neuronal death (i.e. apoptosis). Interestingly, ethanol affects both processes resulting in a synergistic effect by simultaneously decreasing proliferation of neuronal precursors and increasing the incidence of cell death when appropriate blood ethanol levels are reached/maintained (Olney et al. 2002; Rice Bullock & Shelton 2004).

1.8 Apoptosis

Apoptosis, as a term, was devised to describe morphological changes which characterize a specific process of cell death; this highly regulated/controlled process is generally a normal part of cell physiology and aging in humans (Elmore 2007). Activation of caspases is an integral part of this process and ensures the degradation of cellular components in a controlled manner with minimal effects on surrounding tissue (Rathore et al. 2015). Caspases are a family of cysteine protease containing zymogens which when activated begin degrading over 600 cellular components (Sollberger et al. 2014; Wyllie Kerr & Currie 1980). Studies have identified 14 different caspases thus far, designated caspase-1 through caspase-14, all with unique cellular and molecular targets (Salvesen & Dixit 1997).

Ethanol induced apoptosis shares many of the same features which are naturally occurring, such as distinct morphological alterations to the cytoskeleton/nucleus as well as various biochemical changes (Wyllie Kerr & Currie 1980). Caspases are an important family of protease enzymes which play essential roles apoptosis (Fan et al. 2005). This study focused on the activity and levels of caspase-3 specifically as it has been shown to

be responsible for cytological alterations which characterize neuronal apoptosis (Clark et al. 2000; D'Mello et al. 2000); as well as, its specific involvement in ethanol induced neurodegeneration (Young et al. 2005).

1.9 Caspase-3

Caspase-3 is known as an effector caspase, meaning that it facilitates the proteolysis leading to apoptosis after the apoptotic signal has been activated by a separate initiator caspase (i.e. caspases 8, 9, & 10; Chen & Wang 2002). Activated caspase-3 is a well validated biomarker of cellular apoptosis in humans (Ward et al. 2008), and it has been found to be the major protease effector protein in the apoptotic process (Olney et al. 2002 a,b). Caspases, particularly caspase-3, are stimulated in a protease cascade that leads to inappropriate activity of key structural proteins and various enzymes important in cell signaling, repair, and homeostasis (Nicholson & Thornberry 1997).

The canonical apoptotic pathway utilizing caspase-3 begins with the release of cytochrome-C from damaged mitochondria, induced by a variety of death stimuli such as oxidative free radicals, ischemic injury, etc., which then activate a complex of apoptosis-activating-factor-1 and caspase-9. This cytochrome-C dependent complex cleaves pro-caspase-3, thereby releasing the active form of caspase-3 (Li et al 1997; Reed 1997). Activated caspase-3 can amplify the cell death pathway upstream either by further inducing the release of cytochrome-c from mitochondria or by cleaving B-cell lymphoma 2 (Bcl-2) converting it from an anti- to pro-apoptotic protein (Cheng et al. 1997). Studies of prenatal effects of ethanol on neuronal survival have indeed found that the balance between caspase-3, Bcl-2, and Bax (the pro-apoptotic version of Bcl-2) is altered and apoptosis is upregulated (Mooney & Miller 2001).

Several insights into the biological role of caspase-3 can be gleaned from observations of caspase-3-knockout mice. These mice have a remarkable phenotype characterized by pronounced skull deformities and ectopic masses of cells which indicate a failure of the apoptotic process during the development of the brain, but surprisingly not in other tissues (Kuida et al. 1996). Therefore, it seems that the actions of caspase-3 are tissue specific, and there are at least two possible explanations for this. Either there is a shortage of proteases similar to caspase-3 in the brain that can substitute for it during apoptosis, or caspase-3 itself is a key mediator of the neural apoptotic pathway (Porter & Janicke 1999). It should be mentioned that although cell death from apoptosis still occurs without the presence of caspase-3 outside of the brain, the hallmark morphological change and DNA fragmentation normally seen are absent (Woo et al. 1998). This implies that DNA fragmentation and chromatin condensation are dispensable with respect to programmed cell death in all tissues, and that this seems to be an incomplete form of apoptosis. Although this incomplete apoptosis has been seen before in cultured cells, it was believed that the cellular disintegration component was necessary *in vivo* to facilitate the removal of dead cells (Jacobson, Weil, & Raff 1997). When exposed to ethanol, caspase-3-knockout mice had an altered time course and cellular morphological features of the apoptotic process, but no preventative effects in the absolute amount of cell death (Young et al. 2005).

Although the above findings show a contribution of caspase-3 in ethanol-mediated neurodegeneration, there must be other cell signaling pathways involved. Caspase-3 is known to cleave NF-kB at the p65 subunit inducing apoptosis and upregulating cell death

(Kang et al. 2001). The connection between the two proteins lead to NF-kB being chosen as a second target to be investigated in this study.

1.10 NF-kB

Nuclear factor kappa-light-chain-enhancer of activated B cells (NF-kB) is part of a major proinflammatory pathway in cells throughout the body by way of its transcriptional regulation of cytokine production, ultimately influencing cell survival (Liu et al. 2017). NF-kB is important in regulating cellular functions as they belong to a class of fast acting transcription factors; they are always present within cells in an inactive state and do not require *de novo* protein synthesis to be activated (Gilmore 1999). Baseline levels of NF-kB in the brain are higher than in peripheral tissue; primarily in glutamatergic neurons of the cerebral cortex (Kaltschmidt et al. 1993, 1994, 1995). There has also been constitutive expression found in other brain regions, including the cerebellum (Schmidt-Ullrick et al. 1996). Of importance to this study is the presence of inducible NF-kB in neuronal synapses which travels to the nucleus during glutamatergic stimulation causing changes in gene expression (Wellman Kaltschmidt & Kaltschmidt 2001).

NF-kB is involved in cellular responses to aversive stimuli such as free radicals, heavy metals, radiation, and pathogenic antigens (Gilmore 2006). Normally bound intracellularly to inhibitor of kappa B (IkB) proteins, NF-kB becomes activated by either canonical or noncanonical signaling pathways (Oeckinghaus & Ghosh 2009). NF-kB can also be activated by protein kinase C (PKC) *in vitro* through the neuokinin 1 receptor (Shirakawa & Mizel 1989).

In the classical/canonical pathway NF-kB activation is initiated by the signal-induced degradation of IkB which is mediated by IkB kinase (IKK); IkB is phosphorylated which tags it for ubiquitin degradation by the cellular proteasome. This process frees the NF-kB complex (p50/RelA) so that it may translocate to the nucleus, modulate gene transcription, and thereby exert its physiological effects of inflammation, immune response, and in some cases cellular proliferation. Activation of NF-kB initiates a negative feedback cycle by inducing expression of its own suppressor, IkB, which binds and thereby re-inhibits NF-kB (Hoffman Natoli & Gosh 2006). In the non-canonical/alternate pathway the initial activation signal comes from a more limited pool of cell-differentiating and developmental stimuli which induce the NF-kB p52/RelB heterodimer. NF-kB inducing kinase (NIK) is activated after receptor ligation and phosphorylates NF-kB p100 precursor protein leading to post-translational modification of the protein to the mature p52 variety (still dependent on IKK). The p52/RelB dimer now travels to the nucleus and binds to DNA altering gene expression. There is also now known to be a third (and perhaps even more) pathway in which p50 homodimers of NF-kB enter the nucleus and affect gene transcription with the help of a cofactor (often Bcl-3; Gilmore 2006). The initial steps of this third pathway are still being elucidated. All of the discussed pathways are thought to be interrelated to a certain degree, as synthesis of constituents of the non-canonical pathway are controlled by the canonical pathway, and generation of the various NF-kB dimers in the cytosol are mechanistically linked (Basak Shih & Hoffmann 2008). Taken together these analyses suggest an integrated NF-kB network drives activation of both RelA and RelB containing dimers and malfunctions in one pathway will cause an aberrant cellular response through all pathways.

Dysregulation of NF-kB has been linked to cancer, improper immune function, and inflammatory/autoimmune diseases (Aksentijevich & Zhou 2017; Dolcet et al. 2005). In addition to its immunomodulatory role, NF-kB also affects the expression of other gene targets, some of which are thought to be involved in the addiction process (Crews at al. 2011). For example, NF-kB also mediates complex behaviors including learning and memory, stress response, and drug reward which are outside the archetypal immune response role (Nennig & Schank 2017). These effects are mediated by the role NF-kB plays in dendritic spine formation (Russo et al. 2009), synaptogenesis (Boersma et al. 2011), dendritic growth (Gutierrez et al. 2005), and modulating synaptic plasticity (Mattson 2005). It seems that transcriptional targets of NF-kB in the nervous system are important for plasticity as these genes have increased expression after learning (Ahn et al. 2008). NF-kB target genes that have been shown to be important for synaptic plasticity include growth factors (e.g. BDNF, NGF; Marini et al. 2004), cytokines (e.g. TNF-α, TNFR; Albensi & Mattson 2000), as well as various kinases (e.g. PKA; Kaltschmidt et al. 2006). It is the inducible RelA form of NF-kB that has been shown to cause secondary neurological damage (Shih Wang & Yang 2015).

Regardless of the functional evidence for NF-kB's transcriptional role in the nervous system, it is still unclear whether this reflects transcriptional activation in neurons themselves. Most experiments in this field have been conducted in mixed-cell environments (i.e. *in vivo*, mixed cell cultures with both neurons and glia); when experiments have been carried out using pure neuronal cultures with physiological endpoints being measured (e.g. electrophysiology), little to no activity of NF-kB was observed (Listwak Rathore & Herkenham 2013). Of course, there could also be issue with

cell culture artifacts, where the isolation of neurons without the influence of surrounding glia could be skewing results. There are also some reports that prior NF-kB activity seen in neurons could be the result of antibody non-specificity (Herkenham et al. 2011). Based on the experiments reviewed above, the p65 form of NF-kB (a.k.a. RelA) was chosen for western blot analysis in the present study. As a side note, the antibody utilized for this study is not one that had issues of non-specificity in the study by Herkenham et al. 2011, and anecdotal reports from previous users are positive.

1.11 Involvement of Protein Kinase C

Protein kinase C (PKC) is a family of enzymes that control the phosphorylation state, and thus the functional status, of other proteins present in several intracellular signal transduction cascades. The activity of PKC is controlled by both increases in concentration of diacylglycerol (DAG) and by intracellular Ca^{2+} (Nishizuka 1986). There are fifteen isozymes making up the PKC family which are divided into three subfamilies depending on which second messenger(s) activates them: classical, novel, and atypical (Nishizuka 1995). The classical isozymes (α, βI, βII, and γ) are activated by both Ca^{2+} and DAG; the novel isozymes (δ, ε, η, and θ) are activated by DAG, but are insensitive to Ca^{2+}; and atypical forms of PKC (ξ and λ) are independent of both DAG and Ca^{2+} for their activation (Mellor & Parker 1998).

Since PKC plays a central role in many cell-signaling pathways, the possibility that the effects ethanol has on neuronal function are mediated by PKC has become an important topic in the field of ethanol research (Stubbs & Slater 1999). In several studies, chronic ethanol exposure has been associated with PKC upregulation. Cultured neuroblastoma-glioma cell lines were treated with ethanol (25-200 mM) for 2-8 days and

were shown to have increased levels of PKC as well as increased phosphorylation activity (Messing Petersen & Henrich 1991; Zhang Rubin & Rooney 1998). Developmental studies found that ethanol exposure upregulated overall PKC activity after 8 days with increased levels of several isozymes (Mahadev & Vemuri 1998). Ethanol also promotes cell death in cerebellar granule neurons by inhibiting the anti-apoptotic activity of insulin like growth factor 1, which is itself inhibited by PKC (Zhang Rubin & Rooney 1998). More recent research on PKC has focused on its role in synaptic remodeling and the induction of protein synthesis; indicating PKC is important in learning and memory function (Jalil, Sacktor, & Shouval 2015; Nelson et al. 2008).

A study conducted by Santerre et al. 2014 examines expression of PKC isoforms across adolescence in response to acute ethanol exposure. Using high dose i.p injections of ethanol (3.5 g/kg), PKC levels were measured one hour after administration. Total PKC isoform expression varies across adolescence, PKC-gamma showed a small dip during mid-adolescence (PNDs 35 & 42). In response to ethanol treatment there was no change in acute PKC levels (the current study saw a chronic increase in PKC in response to ethanol). Results were obtained in cerebral cortex tissue whereas western blotting in the current study was conducted primarily in the cerebellum. Additionally, the dose of ethanol was significantly higher that what was employed in this dissertation.

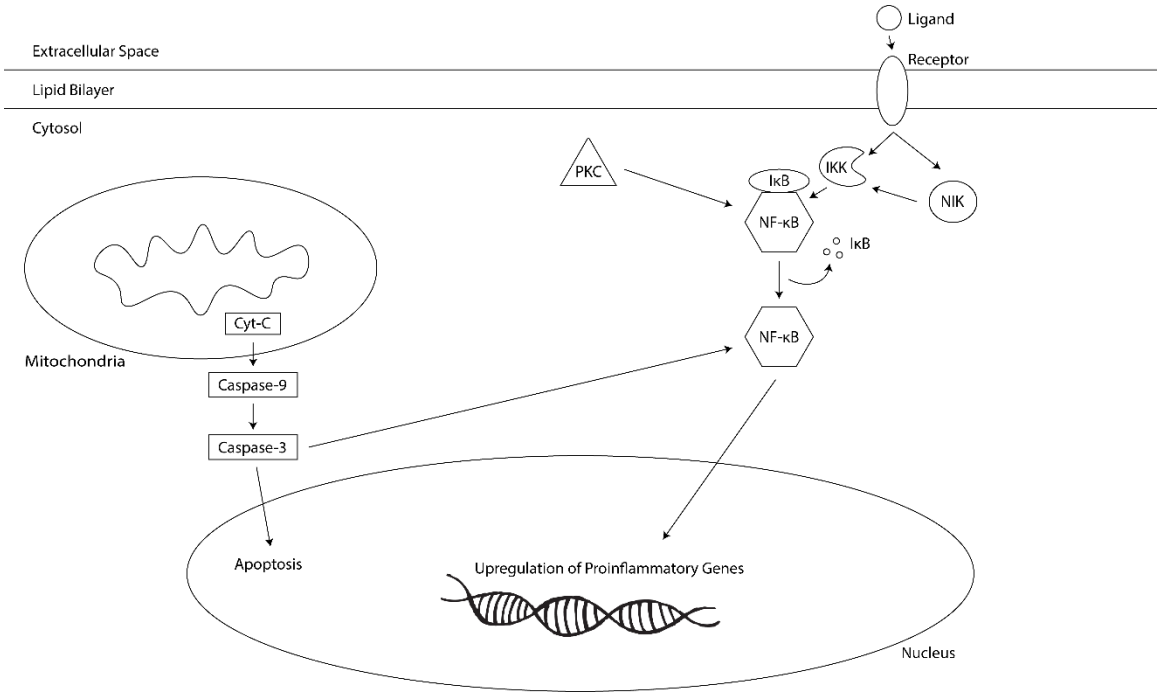

Fig. 1.3 – Diagram depicting the interaction of the three target proteins examined in this dissertation. Legend: Cyt-C = Cytochrome C, IkB = Inhibitor of Kappa B Proteins, IKK = IkB Kinase, NF-kB = Nuclear Factor Kappa-light-chain-enhancer of Activated B Cells, NIK = NF-kB Inducing Kinase, PKC = Protein Kinase C.

Because PKC is intimately involved with the mechanism by which ethanol modulates cellular function, it stands to reason that PKC expression levels and activity may be affected by the model of adolescent binge drinking used in this project. PKC is also known to interact with the other two proteins of interest in this study (i.e. NFkB & Caspase-3) and is an important upstream signaling molecule that can affect cell survival (Fig. 1.3)

1.12 Study Objectives

The *wdl* mouse was utilized for this study since relatively little is known regarding the pathology of the observed ataxia, aside from the involvement of CAR8 (Jiao et al., 2005) and morphological abnormalities which are possibly the cause of decreased functional excitatory signaling (Hirasawa et al., 2007). The localization of the ataxia inducing mutation to mainly the cerebellum in *wdl* mice allows for studies to be conducted with less confounding variables that would occur in the other ataxic animal models whose alterations in Ca^{2+} signaling affect a wide array of brain regions.

Calcium imaging studies have not been conducted in *wdl* mice before and their completion allows for hypothesized suggestions of the involvement of CAR8 with intracellular Ca^{2+} signaling in the *wdl* mutant to be confirmed. These studies also provide insight into the common pathological underpinnings of cerebellar based ataxias.

Given the interconnected relationships between caspase-3, NF-kB, and PKC, as well as their implication in previous studies of various drugs of abuse made the proteins a clear choice to examine in this dissertation (Guerri & Pascual 2010; Nennig & Schank 2017; Russo et al. 2009; Young et al. 2005). In addition to assaying the above protein expression levels, a thorough battery of behavioral tests was utilized to get a

comprehensive overview of the long-term outcomes of adolescent binge drinking. Combining both behavioral and biological assays in the same subjects gives a broad perspective of the potential consequences of binge drinking in humans.

In addition to the valuable data obtained from both; the comparison of results from the two models discussed above will deepen our understanding of cerebellar physiology and how it relates to function. I seek to address the following research questions:

- What are the behavioral implications for a relatively moderate schedule of adolescent binge drinking?
- What are the biological underpinnings of any ethanol-induced behavioral changes?
- Are these changes permanent, or is there an opportunity for recovery?
- How are alterations of intracellular Ca^{2+} signaling influencing neuronal function and ultimately behavior in the *wdl* mouse?
- What changes to cerebellar physiology versus morphology are influencing behavior in the two models?

I hypothesize that there will be substantial behavioral alterations caused by the binge drinking paradigm during the critical neurodevelopmental period of adolescence, and that these changes will be persistent for a significant portion of the subject's lifespan (i.e. several months). Some of these behavioral changes will revert to baseline over time as the brain has been shown to have an impressive ability to adapt and repair. In the *wdl* model the alterations to intracellular Ca^{2+} signaling will have a significant impact on behavior

and this impact will be graded based on the magnitude of the alterations (i.e. more pronounced in the homozygous *wdl* mice than heterozygous mutants). Significant morphological changes in the *wdl* animal will alter the motor output of the cerebellum and LTD occurring there, whereas the physiological changes seen in heterozygous animals will only alter behavior. In the ethanol binge-drinking model there will be significant effects on behavioral output and learning as both physiology and morphology will be altered.

Chapter 2 - Methods

2.1 Waddles Mice/CAR8

2.1.1 Animals

All experiments and mouse husbandry were conducted in accordance with the Canadian Council on Animal Care guidelines and with approval from the Institutional Animal Care Committee of Memorial University. A colony of *wdl* mice was started and maintained in the Animal Care Facility at Memorial University with a breeding pair, originally obtained from Jackson Labs (Bar Harbour, United States), consisting of a homozygous (*wdl/wdl)* female and heterozygous (+/*wdl*) male.

Subjects were divided into three groups based on their genotype (WT, heterozygous *wdl*, and homozygous *wdl*). Both mutant animal and WT controls are from the same genetic background (C57 Black); thereby reducing the possibility of genetic differences, aside from the mutation of interest, affecting obtained results. Heterozygotes are generally utilized as controls since they express only one faulty copy of the gene and therefore do not display the phenotypic ataxia. Despite this a WT group was also included for comparison purposes as the heterozygous mutation may still have a detectable effect on motor output. All mice had food and water available *ad libitum* and were on a 12- hour day/night cycle. Genotyping was unnecessary as the initial breeding pair was genotyped before purchase, and their offspring would have to be either a homozygous or heterozygous mutant. Differentiating heterozygous mice from homozygous mice is relatively simple as only the homozygous animals' display motor difficulties from birth (Harris et al., 2003).

2.1.2 Rota-Rod

Behavioural experiments were conducted to test motor learning skills utilizing a rota-rod apparatus with a previously established accelerating rota-rod (ARR) paradigm (Jones & Roberts, 1968). An ARR paradigm was chosen as it has been shown to better characterize differences between mutant ataxic mouse strains and test for evidence of motor learning, as opposed to the alternative fixed speed rota-rod paradigm which better characterizes motor impairments due to drug exposure (Rustay et al., 2003). Motor learning in mutant groups was defined as a significant increase in mean rota-rod performance (i.e. a higher latency to fall) on the last day of trials (Day 5) as compared to the first day (Zlomuzica et al. 2012). This increase had to be proportional to that experienced by the WT group which would be expected to display normal motor learning. Subjects must display good balance, coordination, and motor planning to remain on the rotating cylinder. Testing groups were divided by both genotype (*wdl/wdl, +/wdl, +/+*) and age (>six months, six months, three months, one month). The greater than six months PNA (post natal age) group had an age range of six to nine months. Groups were composed of both sexes.

All ARR trials were conducted during the late morning (i.e. 10:00 – 11:00). Mice were acclimated to the rota-rod obtained from Harvard Apparatus (Barcelona, Spain), turning at four rotations per minute (RPM) for five minutes prior to data acquisition on the first day of testing. The testing schedule consisted of five trials that were 300 seconds in length on day one, followed by two trials on days two through five, also 300 seconds in length. Animals were returned to their home cage for 45 minutes between every trial. At the beginning of each trial the rota-rod began at a speed of four RPM and gradually

increased to a maximum speed of 40 RPM over the 300 second trial. The time it took each mouse to fall, or their 'latency to fall', was recorded, digitized, and sent to a connected computer for later analysis; thereby, removing some possible human error that would be introduced by manual data collection.

2.1.3 Tissue Preparation

Acute sagittal slices (200-µm thick) were prepared from the cerebellar vermes of young (30 days PNA or less) homozygous/heterozygous *wdl* mice as well as from wild type subjects. Generally, four slices were obtained from each subject and three cells in each slice analyzed; data obtained were averaged 'per slice' for final analysis. Subjects were completely anesthetized via inhalation of isoflurane before being sacrificed by decapitation. The entire brain was then dissected out and the cerebellum placed in ice cold (0-2 ºC) standard aCSF (in mM; 124 NaCl, 5 KCl, 1.25 Na_2HPO_4, 2 $MgSO_4$, 2 $CaCl_2$, 26 $NaHCO_3$, and 10 D-Glucose) bubbled continuously with 95% O_2 and 5% CO_2. The cerebellar vermis was dissected and sliced using a Vibratome (Leica). Slices were transferred from the slicer to a large aCSF bath (500 ml) on small pieces of filter paper and suspended on a mesh screen while the solution was bubbled with 95% O_2 / 5% CO_2 for a short period of post-slicing rest (15 minutes). Slices were then transferred to a smaller bubbled bath (20 ml; 22-24 ºC) and bulk loaded with a cell membrane permeable fluorescent calcium indicator, OG-BAPTA-1-AM, for one hour (50µg; mixed with 8 µl DMSO, 2 µl pluronic acid, and 90 µl aCSF; yielding a final concentration of 200 µM in the bath; Chuquet, Hollender, & Nimchinsky, 2007; Dawitz et al., 2011). Before imaging, the slices were moved a final time to a bubbled container with 20 ml of indicator-free aCSF and allowed to rest for 30 minutes.

2.1.4 Fluorescent Calcium Imaging

Fluorescence excitation was provided by the X-Cite Series 120 illumination source (Mississauga, Canada) at 488 nm and visualized at 507 nm. The fluorescence was imaged using a Sensicam 12-bit cooled CCD camera (Kelheim, Germany) and recordings were performed on a Carl Zeiss Axio Examiner D1 (Oberkochen, Germany). During the test period for agonist wash-in recordings an image was taken, with an exposure time of 80 milliseconds, every five seconds over a total time of seven minutes. During electrical stimulation alone, an image was taken every 3 seconds for a total time of six minutes with an exposure time of 80 milliseconds. When electrical stimulation was combined with AIDA application, an image was taken every 3 seconds for a total of seven minutes, with an exposure time of 80 milliseconds. Data acquisition and analysis were conducted using the Scanalystics IP Lab software (Billerica, United States).

Microscopy was conducted at a total of 100x magnification (objective – 40X; eyepiece – 10X/24), resulting in a field of view diameter of 60 μm. Areas from the GCL were chosen for recording randomly, however areas with no well-loaded cells were avoided. A large area of the GCL was recorded and later regions of interest (ROIs) around well-defined neuronal somas were chosen for analysis.

Slice quality was controlled for in three ways: propidium iodide (PI; which is excluded from healthy cells with intact membranes) was washed in after recording GCs response to glutamate/DHPG which verified there were no problems with membrane integrity (i.e. the level of glutamate utilized did not seem to compromise cell viability). Separate baseline recordings were taken from an area of the slice different from the ROI before glutamate wash-in to confirm signal stability, and [50mM] potassium chloride was

washed into the bath at the end of experiments to confirm the neurons' ability to depolarize and generate a Ca^{2+} signal (Beani et al.,1994).

2.1.5 Electrical and Pharmacological Stimulation

Following bath application of the fluorochrome, a section of the GCL of cerebellar slices was then imaged using a fluorescence microscopy setup for either: baseline activity, response to [100μM] glutamate, [50μM] DHPG (a potent group 1 mGluR agonist), indirect electrical stimulation (60 Hz, for 500 ms, at 3.5 μA; Beani et al., 1994), or thapsigargin [1.5μM; Cayman Chemical, Ontario: Canada]. Additional experiments were conducted using glutamate concurrently while the $GABA_A$ receptor antagonist bicuculline [20μM; Tocris BioScience, Bristol: UK] was also present in the bath.

The stimulating electrode for my indirect stimulation protocol was placed on afferent mossy fiber projections providing excitatory input to GCs (approximately 250 μm below recording area). Electrical stimulation occurred twice during a six-minute recording at the two- and four-minute time points. The stimulation protocol above was chosen because it closely mimics intermittent burst stimulation that GCs would receive *in vivo* (Sola et al., 2004). Both the stimulating and recording electrodes were made of a section of silver-chloride wire (50 μm in diameter). Electrical stimulation success was verified by an extracellular recording electrode approximately 250 μm above the stimulating electrode in the y-plane, next to the section of GCL chosen to be imaged. Extracellular recordings were conducted with glass pipettes (1-3 MΩ) filled with a 3-5 μm tip and filled with aCSF. An additional set of electrical stimulation experiments were conducted with three stimulation points (two, four, and six minutes) over an eight-minute

recording. Furthermore, [100μM] AIDA (a selective group 1 mGluR antagonist) was washed into the bath during the mid-point stimulation point (four minutes) of the experiment described above.

2.1.6 Statistical Analysis

ARR Data – Mean latency to fall was calculated for each age x genotype group on each trial and graphed. A one-way between-subjects analysis of variance (ANOVA) was conducted to compare the effect of age on ARR performance. A two-way repeated measures ANOVA (age x trial) was conducted to detect effects of age and number of trials on motor learning. For subsequent analysis, the values from all trials on a given day were averaged to give a single mean for the entire day of trials (i.e. Trials 1-5 on Day 1 were averaged for each animal to give one overall mean of ARR performance on that day). A Tukey-HSD post-hoc test was used to determine which groups were significantly different with respect to the ANOVA results.

Paired-sample t-tests were used to compare the pooled data of all groups on Day 1 with that of Day 5 in order to detect significant improvement in motor performance which would be indicative of motor learning (Zlomuzica et al. 2012). Day 5 mean values for all groups were also normalized to what could be called baseline values, on Day 1. This normalization of the data was done using a ratio technique, where Day 5 means were divided by Day 1 means to give a value which is easily comparable even between animals with drastically different levels of ARR performance. All statistics were calculated using SPSS (IBM Inc.) with an alpha level of $p. < 0.05$.

Definitions of Quantification Measures - Quantification measures were calculated with the Igor Pro software package by WaveMetrics (Portland, United States). The software utilizes a user defined baseline (in this case the first ten frames of recordings) and user defined treatment window over which the peak of interest occurs. This time window was defined as 10 frames (Frame rate; Glutamate/DHPG = 5 seconds; Electrical Stimulation/AIDA = 3 seconds) before the agonist wash-in. The treatment window was defined as the start of application up to 10 frames after agonist removal (e.g. in the case of glutamate and DHPG application; frames 20-50). The input time frame, during electrical stimulation, for peak detection was 5 frames before and after the electrical stimulation (i.e. frames 35-45, 75-85, and 115-125). Maximum response was defined as the largest increase in signal amplitude seen over the defined stimulation period.

Area-under-the-curve (AUTC) was calculated by multiplying the sum of the y values (% fluorescence change) by the x-interval (frame rate) for a given recording. As described in Chapter 3 (Results), total AUTC measures did not seem to completely describe trends in the recordings where the response appeared bi-phasic. Therefore, in addition to total AUTC being calculated for each recording the Ca^{2+} response to a particular stimulus was broken into two phases (i.e. the direct response to stimulation and the recovery period after stimulation is ceased) and an AUTC measurement was conducted for each of them. Two phase AUTC measurements were conducted for glutamate and DHPG experiments only.

Data were analysed for significance with a one-way between-subjects ANOVA and the Tukey HSD post-hoc test. Data are expressed as mean +/- standard error of the mean (SEM). An alpha level of $p < 0.05$ was set for all statistical analyses.

2.2 Adolescent Binge Drinking Model

2.2.1 Animals

Groups consisted of male Sprague-Dawley rats at two different initial ages to represent approximate early pre-adolescent (PND 26) and adolescent (PND 34) developmental timepoints (Sengupta 2013). Subjects ages were determined to reflect a period of neurodevelopment during which the brain is particularly susceptible to damage (Spear & Brake 1983; Spear 2000; Spear 2013). Male rats begin to sexually mature after weaning beginning on PND 21 and reach maturity by approximately PND 42 (Adams & Boice 1983). Only male rats were utilized due to an outdated idea that cycling hormone levels might affect experimental results. In hindsight this was a mistake, and any future studies should include subjects from both sexes.

Animals were obtained from Charles River Laboratories (Sherbrooke, Quebec; Canada) and given a three-day acclimation period after shipping prior to beginning experiments. All rats were pair housed, provided *ad libitum* food/water, and received environmental enrichment. All experiments were conducted in accordance with the CCAC guidelines and with approval from the Memorial University Institutional Animal Care Committee.

2.2.2 Ethanol Administration

Subjects were assigned randomly to either an experimental or control group. The experimental group was exposed to a mixture of ethanol vapour (2 liters/min) and plain air (5 liters/min) for two hours in a sealed chamber. Control subjects were also placed in the chamber for two hours but received only air (5 liters/min). Control subjects were run first during the day to avoid possible cross contamination of ethanol vapours as much as

possible. Treatment was conducted on PNDs 26-30 for the pre-adolescent model or PNDs 34-38 for the adolescent group, and from 9:00 to 13:00 each treatment day. Subjects were placed into the chamber in two groups of four animals, each group consisted of animals from two of the pair-housed home cages. Blood samples were collected approximately 30 min after ethanol exposure and blood alcohol concentrations (BACs) were measured using a GM7 Micro-stat biochemical analyzer (Analox Instruments, Ltd., UK). A mean BAC of 172 +/- 18 mg/dl was achieved in the treatment group and approximately 0 mg/dl in controls. BAC measurements were obtained from subjects over all five days of ethanol exposure and no significant signs of tolerance were observed over this time. During treatment, ethanol treated animals were closely monitored for proper weight gain and negative health developments because of the treatment (i.e. tremors, piloerection, eye irritation, and respiratory distress).

2.2.3 Behavioral Testing

An initial experiment looked at the performance of a pre-adolescent (n=24) and adolescent (n=24) group on a fixed-speed rota-rod task during/after undergoing ethanol administration. This is a subsequent full study which was conducted with only an adolescent group (n=24) using a battery of behavioral tests: rota-rod (PNDs 32-38, 44, 48, 53, & 68), inverted cage-hang (PNDs 46 & 50), open field (OF; PND 76), elevated plus maze (EPM; PND 78), dark/light box (DLB; PND 79), novel object recognition (NOR: PND 82-85), acoustic startle (AS; PND 86), and fear conditioning (FC: PND 89-92). After the rota-rod and inverted cage-hang tests, subjects were then transferred to a nearby building with facilities necessary for the further behavioral testing and allowed a week to acclimate before they commenced (PNDs 69-76). Therefore, experiments were conducted

from the adolescent period through to the early adulthood (see Figure 2.1 for the experimental timeline).

A limited experiment characterizing withdrawal effects from the ethanol administration paradigm was conducted with a separate group of adolescent subjects (n=24) after the previous testing was completed. This final group was tested for general movement propensity and speed of movement (both before and after ethanol exposure) in an open arena and response in the light-dark box test the day after the last exposure to ethanol (specifications further in this section).

2.2.4 Motor Testing

The rota-rod task is a well-established measure of balance and cerebellar function (Rustay et al. 2003). The rota-rod (Harvard Apparatus; Barcelona, Spain) consists of a rotating rod divided into four lanes which then digitally records the time it takes the animals to fall (latency to fall) at various settings of RPM. Subjects were tested on the rota-rod directly before ethanol/air exposure on all treatment days. Additional trials with no exposure were conducted on either PNDs 36,40,45,60 for the pre-adolescent groups (PND 26) or PNDs 44,48,53,68 for the adolescent groups (PND 34).

The pre-adolescent and adolescent groups from the first set of experiments project were tested only on the fixed speed rota-rod (FSRR), where the RPMs (5, 10, and 15) are set at the beginning of the five-minute trial and do not change. The adolescent group from the main study was tested on an accelerating rota-rod (ARR), where the RPM of the apparatus increased uniformly from 4 to 35 over a five-minute trial.

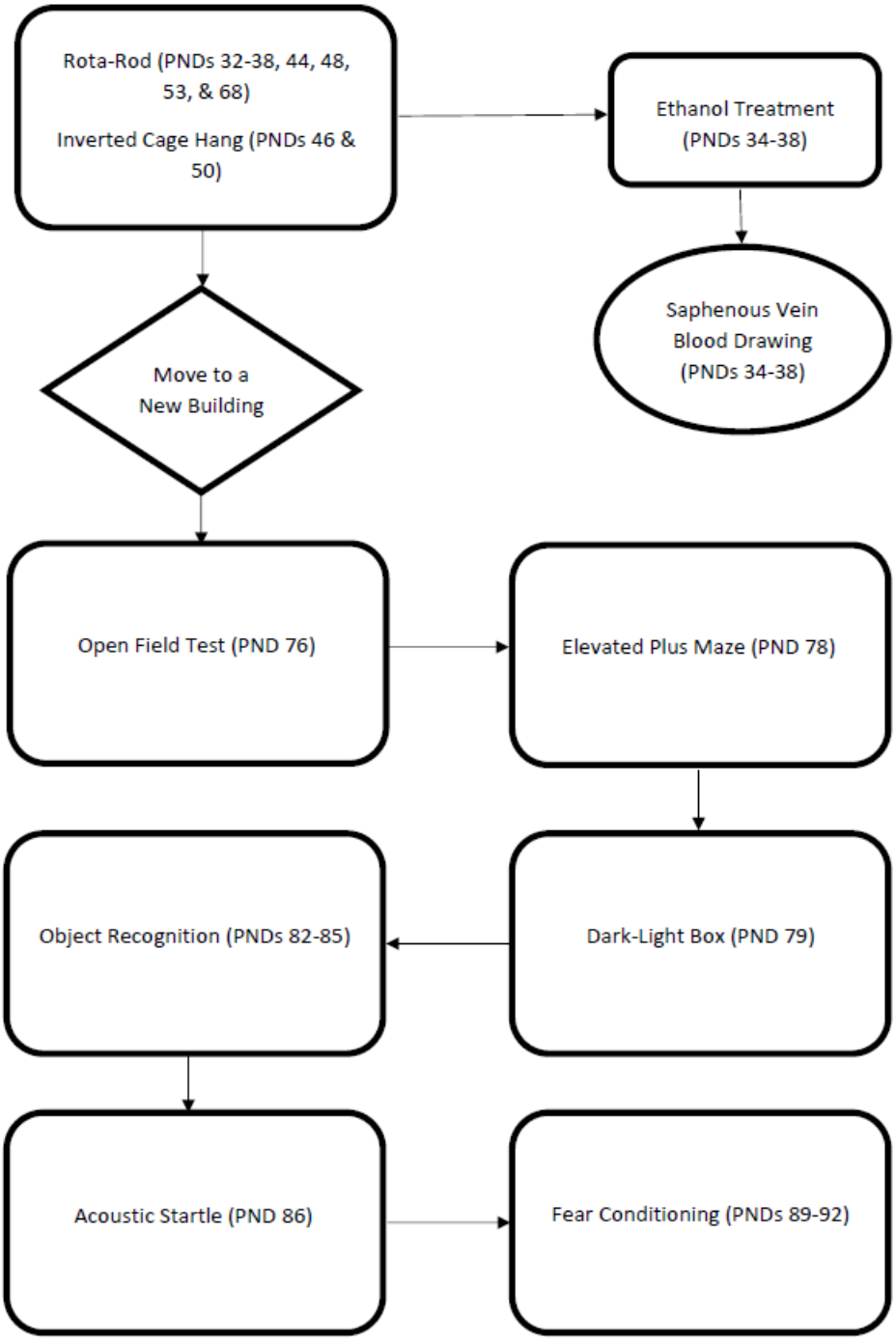

Figure 2.1 – Flowchart for behavioral experiments in the PND 34-38 ethanol treated group.

The second adolescent group was also tested with an inverted cage-hang apparatus. In this test the subject is placed on a metal mesh screen (1.25 cm square spaces) and the screen is then inverted over a pile of soft bedding. The time the animal can remain gripped to the screen when inverted gives a relative indication of muscle tonality/strength (Osmon et al. 2018).

For the withdrawal group only, subject's general tendency to move about and the speed at which they do so was measured in an open arena. The apparatus was a small wooden box (60 cm x 60 cm x 35 cm) painted in black enamel. Both the total amount of distance covered (cm) and the velocity while this movement took place (cm/s) were measured using EthoVision® behavioral tracking software (Noldus Information Technology Inc., Wageningen, The Netherlands).

2.2.5 Open Field

The open field apparatus was a square wooden box (60cm x 60cm x 35cm) painted with black enamel and taped off into a 3x3 grid. Rats were placed in the center of the box to begin the trial and were allowed five minutes to explore while being videotaped. The videos were subsequently scored for total locomotion, time in periphery, and time in center of the open field using the behavioural tracking software. Rats were scored as in the center of the arena when the full body was within the center square demarked by the grid, and in the periphery when all four paws crossed into one of the other squares.

2.2.6 Light-Dark Box

The light/dark box is a single alley apparatus divided into two chambers of equal size (32cm long x 10.5 cm wide x 14.5 cm high). Both chambers are covered by a ventilated plexiglass top with the dark side being rendered opaque with a black plastic lining. The floor and sides on the light side are painted white, while the dark side has a metal mesh floor with the walls painted black. This specific light/dark box has been used in previous studies (Varlinskaya et al. 2020; Kenny et al. 2019; Lau et al. 2016). Testing took place in a dark room with a 100-watt lamp positioned 66 cm above the chamber, producing an illumination on the light side of approximately 590-lux and 20-lux on the dark side. Subjects were placed in the light-side of the box initially for a five-minute trial and had their behavior videotaped for future analysis. Behavior measured included time spent on the light side, time spent on the dark side, and the number of crossings between the two (with all four paws).

The amount of time spent in the light side versus the dark exploits a natural behavior of the rat to get a measure of relative anxiety-like behavior via an unconditioned response. Less time in the light side is indicative of increased anxiety-like behavior as anxiolytic drugs increase time in the light side (Chaouloff Durand & Mormède 1996).

2.2.7 Elevated Plus Maze

The elevated plus maze consists of four arms arranged in the shape of a cross, with two opposite arms considered open (10cm wide x 50cm long) and the other two considered closed (10cm wide x 50cm long x 40 cm high). The four arms join at the center of the maze with a 10 cm squared platform above which was a low-light (30 lux) white light. Subjects were placed in the center platform of the maze facing the same open

arm for a five-minute trial each. Entry into any arm was defined as having all four paws past the opening. Behaviors scored include time in open arm, time in closed arm, and the number of entries into each arm. Final data was expressed as percent of total non-center time. Previous studies looking at intermittent ethanol exposure during early adolescence found significant results using this experimental apparatus (Varlinskaya et al. 2020).

2.2.8 Acoustic Startle

Startle testing was conducted in a commercially available standard startle chamber (San Diego Instruments). The apparatus consists of a cylindrical animal enclosure that sits atop a piezoelectric transducer, the signal from which is recorded by a computer to provide a measure of relative movement intensity by subjects. Rats were first acclimatized to the chamber with a 60 decibel (db) white noise for five minutes. During test trials subjects were exposed to 30 pulses (50 msec each) of white noise at 120 db, rising out of a background of 60 db white noise with a 30 second inter-trial interval. Startle responses were measured over a 250 msec window and averaged for each subject.

2.2.9 Novel Object Recognition

The same testing arena from the open field trials was used for the NOR experiments. Rats were first habituated to the area for 10 minutes over two days prior to pre-training and training trials. During pre-training, subjects were allowed to explore two identical objects (A,A) for three minutes. Memory retention was tested 24 hours later with one familiar object (A) and one novel object (B). Objects were placed 12 cm from each wall and 18 cm from each other during the trials. Positions of objects were counterbalanced within the arena and were rinsed with a 70% ethanol solution between trials. Subjects are given an initial trial to explore two identical objects and are then

placed back in the apparatus one hour later with a similar and novel object. Time spent exploring each object was assessed, which consisted of approaching within 2 cm of the object with the face, sniffing, biting, or pawing the object. Sitting or rearing up on the object was not counted as exploration. A discrimination index was then calculated (exploration of novel object – exploration of familiar object / total exploration time); positive index values indicate the subject explored the novel object more frequently.

2.2.10 Fear Conditioning

All subjects were placed in a Plexiglas shock box (Colbourne Instruments) for two minutes; then a 30 second white noise (90 db) burst was delivered, co-terminating in a two second foot shock (1.5 mA). This procedure is repeated at an inter-stimulus interval of one minute for a total of two shocks over a five-minute trial. Freezing behavior (motionless except for respirations) was monitored at five-second intervals by an observer blinded to the condition.

Cued fear conditioning was tested in subsequent trials for each subject 24 hours after the initial analyses. In these trials there was a three-minute baseline followed by three minutes of the same white noise from the training sessions (no shocks were given). Cue-dependant fear conditioning was determined by subtracting freezing during the baseline condition from that during the white noise. Testing was counterbalanced between groups, and all equipment was rinsed with 70% ethanol between subjects.

2.2.11 Protein Quantification

Samples for western blot analyses were homogenized tissue from either the cerebellar or cerebral regions of experimental animals (PND 34 group). These tissues were harvested approximately 48 hours after the last behavioral test was conducted (PND

94) following rapid decapitation of the animals, and flash frozen using liquid nitrogen. Cerebellar tissue was also collected from *wdl* mice (experimentally naive mice from lab-maintained colony) for comparative analyses. Cerebral tissue was only collected from ethanol treated animals as results obtained with it were inconclusive and the decision was made to focus on the cerebellum only.

Tissues collected were homogenized with ice-cold homogenizing buffer (50 mM Tris, 150 mM sodium chloride, 3.5 mM sodium dodecyl sulphate, 12 mM sodium deoxycholate, and 15 mM Triton X-100, PH 8.0) and protease inhibitor cocktail tablets (Roche, Grenzach-Wylen, Germany). Protein concentrations were measured with the Pierce ™ BCA protein assay kit (Thermo Scientific, USA). Cerebellar and cerebral protein lysates (40 µg/well) were separated by SDS-PAGE (12.5%) under reducing conditions and transferred to a nitrocellulose membrane (Thermo Scientific, USA). Briefly, blots were blocked with blocking buffer for 1 hour at 4°C (5% not-fat dried milk in TBST). After blocking, blots were incubated with anti-caspase-3 polyclonal antibody (1/1000, v/v; catalogue # 9662S, lot # 0018), anti-cleaved caspase-3 monoclonal antibody (1/1000, v/v; catalogue # 9664S, lot # 21), anti-NF-kB monoclonal antibody (1/1000, v/v; catalogue # 8242S, lot # 0009), anti-phospho-NF-kB p65 monoclonal antibody (1/1000, v/v; catalogue # 3033S, lot # 16), anti-PKCγ polyclonal antibody (1/1000, v/v; catalogue # 43806S, lot # 0001), or anti-phospho-PKC (pan) polyclonal antibody (1/1000, v/v; catalogue # 9379S, lot # 0002) (all from Cell Signaling, USA) for 20 hours at 4°C. All blots were also incubated with anti-α/β tubulin polyclonal antibody (1/1000, v/v; catalogue # 2148S, lot # 0007), as a loading control. Blots were washed 3 times with TBST and incubated with HRP conjugated-secondary antibody (1/5000, v/v; catalogue #

7074S, lot # 0026, Cell Signaling, USA) for 1 hour at room temperature. Protein bands were visualized with the commercial Western Lightening© chemiluminescence kit (HRP-catalyzed system; Perkin Elmer, USA).

2.2.12 Statistical Analysis

Results between groups for motor testing were initially analyzed using a mixed-design ANOVA to determine significance of a main effect. Subsequent analyses for motor tests, all other behavioral tests, and western blotting were conducted using the two-tailed independent-samples t-test. The threshold for significance in all experiments was set at $\alpha < 0.05$. All data was analyzed using SPSS (IBM, Armonk, USA).

Chapter 3 – Results

3.1 Waddles Data

A portion of my previous work characterizing the motor dysfunction and cerebellar intracellular Ca^{2+} signaling in the *wdl* mouse was completed for my previously submitted master's thesis as well as a publication (Lamont & Weber, 2015).

3.1.1 Rota-Rod

To characterize the ataxia of homozygous animals while testing for motor learning and to conduct the first known motor testing of heterozygous animals, behavioral testing with the accelerating rota-rod (ARR) paradigm was undertaken. Animals from a *wdl* colony maintained locally were divided into different groups based on genotype and PNA. Groups of different ages were included as previous reports had only included young animals (Jiao et al. 2005) and motor performance data for older animals is not present in the literature. Rota-rod testing was conducted in sets of two trials per day, except for the first day of testing which had five trials (consisting of training and testing rounds). To control for physical exhaustion, all animals were given a 45-minute rest period between trials on the same day in their home cage. However, the animals may still have experienced mental fatigue (i.e. boredom) when undergoing trials after the first on any given day. Data obtained from male and female subjects was not found to be significantly different, therefore results obtained from both sexes were pooled for analysis. A five-day ARR paradigm was utilized to see if motor learning would be displayed by mutants. Motor learning was defined as a significant increase in mean latency to fall on the rota-rod when comparing the first day of trials to the last (Zlomuzica et al. 2012).

A one-way between-subjects ANOVA comparing specific trials revealed significant differences in latency to fall between groups (Day 1 Trial 1 F (2,65) = 114.89, $p < .001$; Day 5 Trial 1 F (2,65) = 144.50, $p < .001$). Post-hoc Tukey-HSD analysis indicated that the homozygous group differed significantly from the WT and heterozygous animals (Day 1 Trial 1 $p < .0001$; Day 5 Trial 1 $p < .001$; Fig. 3.1). The three-month-old WT animals exhibited significantly longer latency to fall when compared with their younger or older cohorts calculated by repeated measures ANOVA (Wilks' Lambda = .109, F (12,24) = 3.22, $p < .001$; Fig. 3.1). Significant differences between one-month old homozygous animals and older cohorts were also observed (Wilks' Lambda = .097, F (12,33) = 1.80, $p < .05$; Fig. 3.1).

To confirm evidence of motor learning, the pooled means from all trials that took place on Day 5 were compared to those on Day 1 for each group. Normalized data show that WT and homozygous subjects had motor improvements which were not seen in the other groups. This was confirmed by a two-way (age x genotype) ANOVA showing a significant main effect of genotype (F (2,74) = 14.39, $p < .001$) as well as a significant interaction effect between genotype and age (F (5,74) = 3.86, $p < .01$). Post-hoc Tukey's test indicated that WT subjects differed significantly from the heterozygous ($p < .001$) and homozygous groups ($p < .001$; Fig. 3.2). Further analysis confirmed that the 1 month postnatal age homozygous group differed from older members of their cohort (F (3,29) = 5.68, $p < .01$), confirmed by Tukey's HSD test, ($p < .01$), as well as from the heterozygous groups (t(24)= -2.11, $p <.05$).

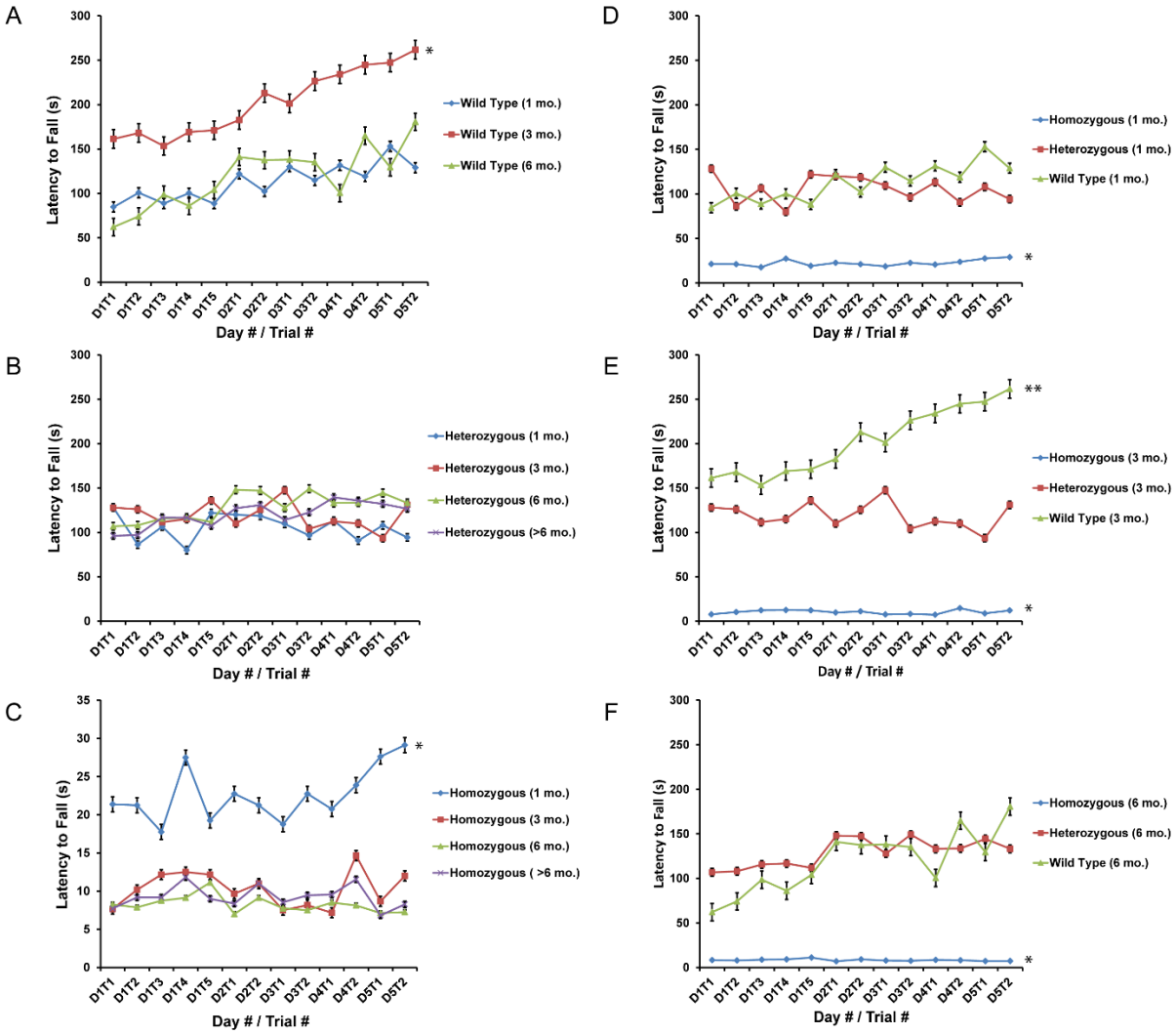

Fig. 3.1 - (A) Mean latency to fall for wild type groups on the ARR (1 mo. PNA, n=16; 3 mo. PNA, n=8; 6 mo. PNA, n=9). The three-month PNA group had a significantly higher latency to fall than other age groups (p < .001). (B) Mean latency to fall for heterozygous groups on the ARR (1 mo. PNA, n=4; 3 mo. PNA, n=4; 6 mo. PNA, n=6; >6 mo. PNA, n=5). (C) Mean latency to fall for homozygous groups on the ARR (1 mo. PNA, n=9; 3 mo. PNA, n=6; 6 mo. PNA, n=8; >6 mo. PNA, n=11). Increased latency to fall in 1 mo. PNA wdl mice versus older cohorts was observed (* p < .001). (D)(E)(F) These are a reorganization of the same data presented in figure components A, B, and C by age instead of genotype. At all age points the homozygous group performed significantly worse that other groups (* p < .001), and at the three-month age point the wild type group performed significantly better than heterozygous animals (** p < .001).*

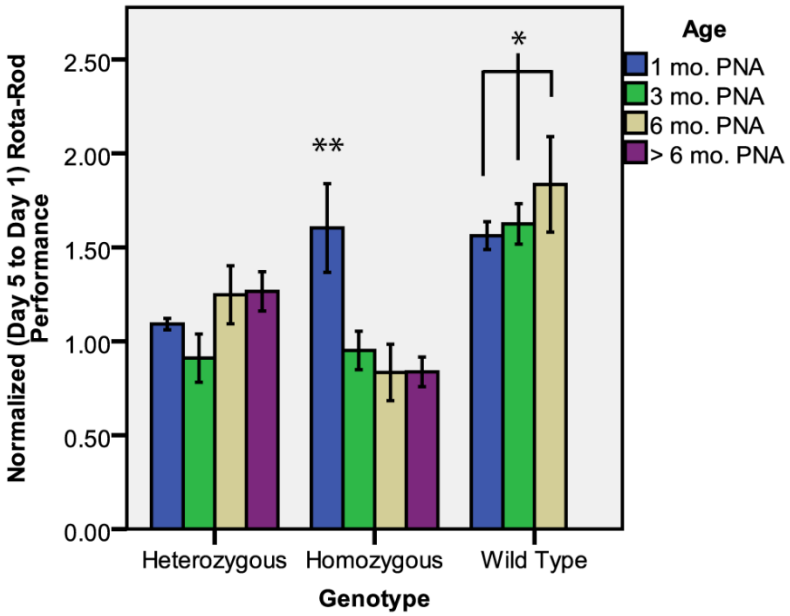

*Fig. 3.2 - Mean latency to fall of all groups on Day 5 of ARR testing normalized to the mean latency to fall on Day 1. The wild type groups had significantly more improvement than the wdl mutant groups (*p < .001). One-month old homozygous animals had a significant improvement in performance over the trials, which was virtually absent in older groups (**p < .01).*

3.1.2 Calcium Imaging

Somatic Ca^{2+} signals from cerebellar GCs were subsequently recorded from a separate cohort using a fluorescent Ca^{2+} indicator. Stimulation with glutamate [100μM] caused variable Ca^{2+} responses. Qualitatively, an interesting oscillatory pattern with an average frequency of 0.04 Hz ± 0.01 was observed during WT recordings in response to glutamate (Fig. 3.3). The maximum response was significantly different between groups (F (2,31) = 3.54, $p < .05$; Fig. 3.3). Post-hoc analysis with the Tukey-HSD test indicated a significant difference between homozygous and heterozygous/WT animals ($p < 0.05$). An area-under-the-curve (AUTC) analysis method was also utilized to determine if total overall Ca^{2+} release was appreciably different from maximal response results. Results turned out to be identical, with WT having a significantly higher AUTC (M = 1756.4, SEM =723.1) than homozygous (M = 236.8, SEM =307.3) or heterozygous (M = - 433.0, SEM =268.9) *wdl* mice (F (2,31) = 5.73, $p < .01$).

An additional set of glutamate experiments were conducted with bicuculline present in the bath to probe the neurotransmitter system mediating the previously described oscillatory patterns in WT Ca^{2+} signaling. Maximum response values were calculated for these recordings (Fig. 3.3), which indicated the WT group was significantly lower than the heterozygous or homozygous groups (F (2,27) = 17.18, $p < .001$). AUTC measurements were also conducted for this experimental condition and they again confirmed findings from maximal response data. In this case, the homozygous group (M = 5291.3, SEM =418.7) was significantly different from the heterozygous (M = 2686.0, SEM =226.5) and WT (M = 1077.6, SEM =280.9) groups (F (2,27) = 35.22, $p < .0001$).

The contribution of intracellular Ca^{2+} stores to the observed Ca^{2+} responses was examined by applying the sarcoplasmic Ca^{2+}-ATPase inhibitor thapsigargin to the bath, which typically leads to a slow increase in $[Ca^{2+}]_i$ due to leakage from the stores. A measure of the difference between the average Ca^{2+} present at the beginning and end of the recordings was taken (Fig. 3.4). A significant difference between groups was detected by a one-way ANOVA (F (2,29) = 27.72, $p < .001$). Post-hoc testing using Tukey's HSD indicated that the homozygous group had a significantly lower, in this case negative, change in baseline compared to WT ($p < .001$) and heterozygous *wdl* ($p < .001$) groups.

To elucidate the role of CAR8 in excitatory synaptic transmission, electrical stimulation was utilized; it allows for relatively precise control over the length, strength, and timing of excitatory synaptic activity. WT groups had a significantly larger response to the first stimulation than the other groups (F (2,23) = 4.45, $p < .05$). Significant differences were detected, when comparing the amplitude difference between the first and second responses to electrical stimulation (Fig. 3.4), between WT and homozygous groups ($t(14)= 5.95$, $p <.001$); as well as WT and heterozygous groups ($t(14)= 3.32$, $p <.005$).

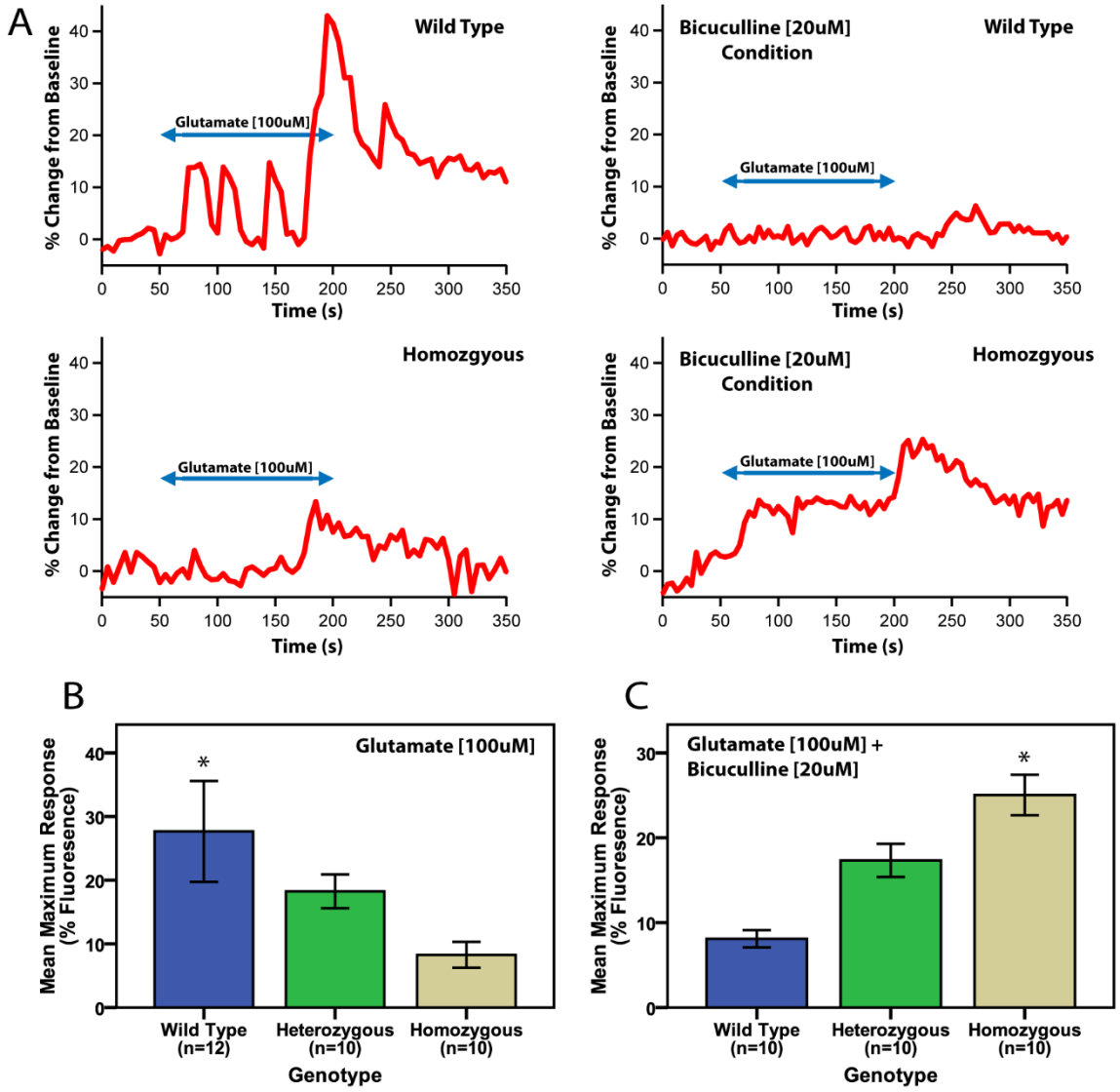

Fig. 3.3 - (A) Representative tracings of homozygous wdl and wild type granule cell somatic Ca^{2+} response (% of baseline) to glutamate [100µM] wash-in, either alone or in the presence of bicuculline. (B) Mean maximum response values reported for all groups; post-hoc analysis indicated that the wild type group was significantly different from the mutant groups ($p < .05$). (C) Response of GCs to glutamate under conditions of GABAA receptor blockade; mean maximum response values reported for all groups. Post-hoc analysis indicated that the homozygous group was significantly different from the wild type group (* $p < .001$).*

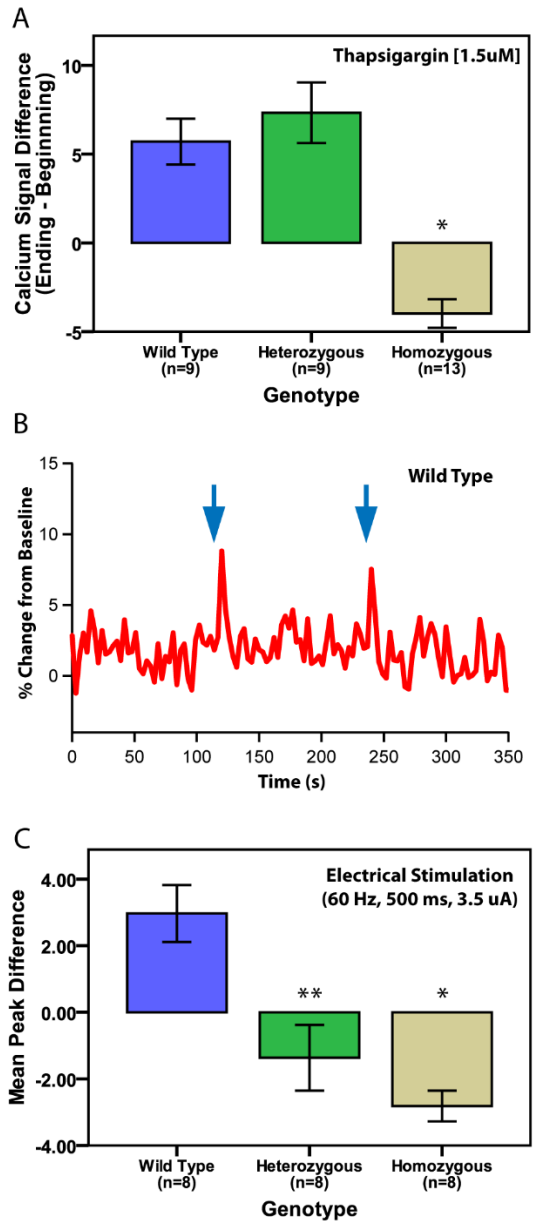

Fig. 3.4 - (A) Difference between average measurements taken at the very end and beginning of recordings when thapsigargin [1.5µM] alone was washed into the bath. Post-hoc testing indicated that the homozygous mutant wdl group had a significantly lower baseline difference ($p < .001$) than wild type or heterozygous wdl groups. (B) Representative tracing from a wild type subject in response to indirect electrical stimulation (60 Hz, for 500 ms, at 3.5 µA), the blue arrows represent stimulation time points. (C) Significant differences were detected, when comparing the amplitude difference between the first and second responses to electrical stimulation (peak 1 - peak 2), between WT and homozygous groups (*$t(14) = 5.95$, $p < .001$); as well as WT and heterozygous groups (**$t(14) = 3.32$, $p < .005$).*

3.1.3 Western Blot - PKC Quantification

Western blotting technique was used to quantify the amount of PKC present in homozygous/heterozygous *wdl* mice, as well as wild type control animals. PKC was chosen as a target protein as it has been shown in prior studies to be involved with CAR8 and regulating Purkinje cell dendritic growth, both of which are linked to the waddle's pathology (Shimobayashi Wagner & Kapfhammer 2016; Gugger et al. 2012). More specifically, previous data have shown that increased PKC activity inhibits dendritic growth and reduced PKC activity promotes it (Metzger & Kapfhammer 2000).
Based on the above evidence, PKC was chosen as a protein of interest and levels of it were measured in homozygous/heterozygous *wdl* mice as well as wild type animals. ANOVA testing indicated significant difference between groups with respect to PKC (F (2,23) = 9.76, $p < .001$), pPKC (F (2,23) = 17.53, $p < .001$), and the pPKC/PKC ratio (F (2,23) = 9.54, $p < .001$; Fig. 3.5). Post-hoc testing was completed to determine which groups were significantly different. Regarding PKC, there were significant differences between homozygous *wdl* mice and both heterozygous ($p = .037$) and wild type ($p = .001$) subjects. Homozygous animals also had significantly higher levels of phosphorylated PKC than heterozygous *wdl* ($p = .001$) and wild types ($p < .001$); this relationship also held for the ratios of pPKC to PKC. A graphical summary of results from experiments with the *wdl* mice are depicted below (Fig. 3.6).

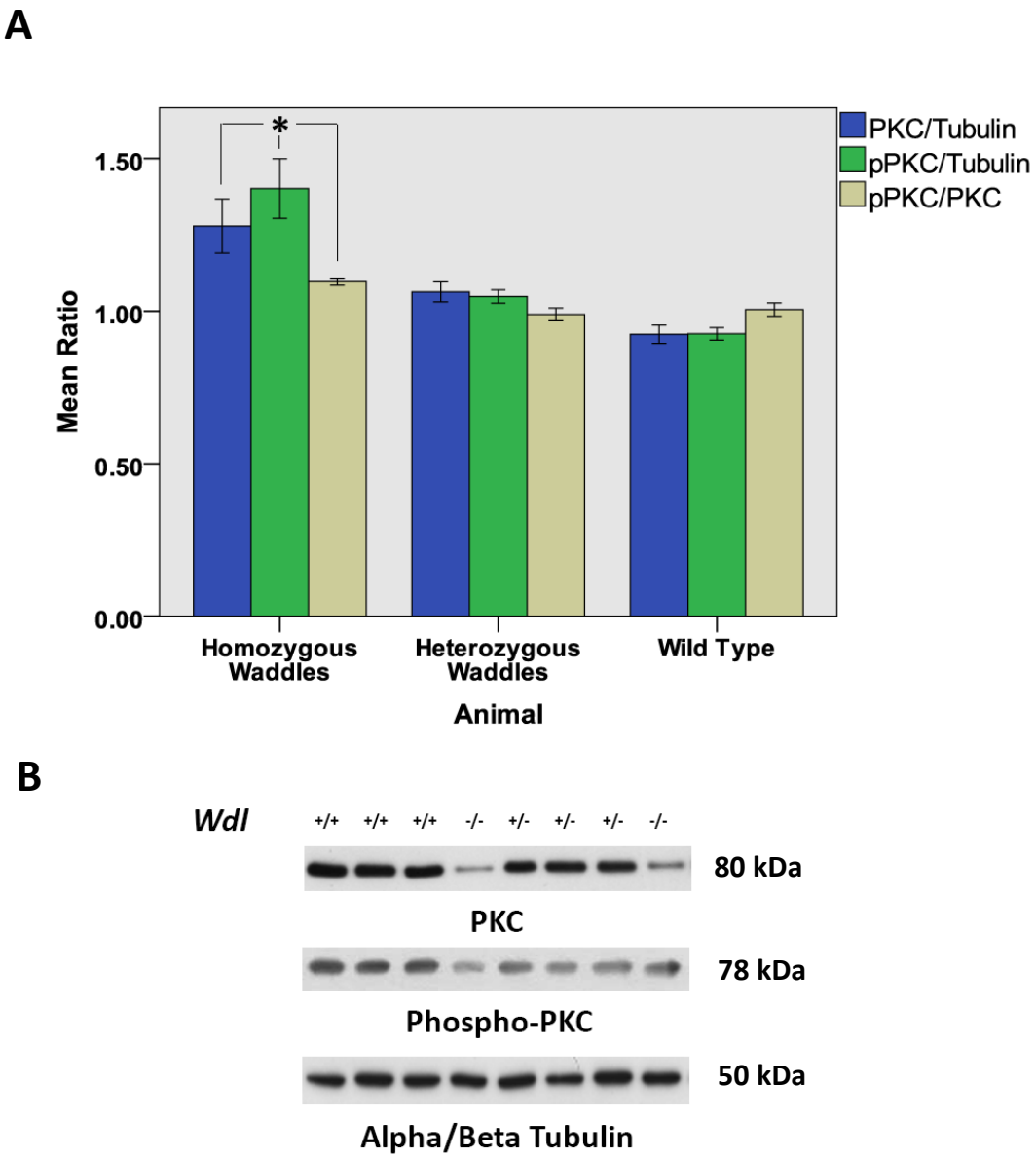

*Fig. 3.5 – (A) Western blot data showed significant differences in PKC (n=8 animals; F (2,23) = 9.76, p < .001) and pPKC (n=8 animals; F (2,23) = 17.53, p < .001) expression levels between groups. There was also a significant difference between groups with respect to the pPKC/PKC ratio (n=8 animals; F (2,23) = 9.54, p < .001). Subjects were between 1 and 6 months of age when samples were collected. Post-hoc testing revealed that it was the homozygous group that had significantly higher protein levels (*p < .05). (B) Representative blot images and approximate molecular weights where: +/+ = homozygous wdl, +/- heterozygous wdl, and -/- wild type mice.*

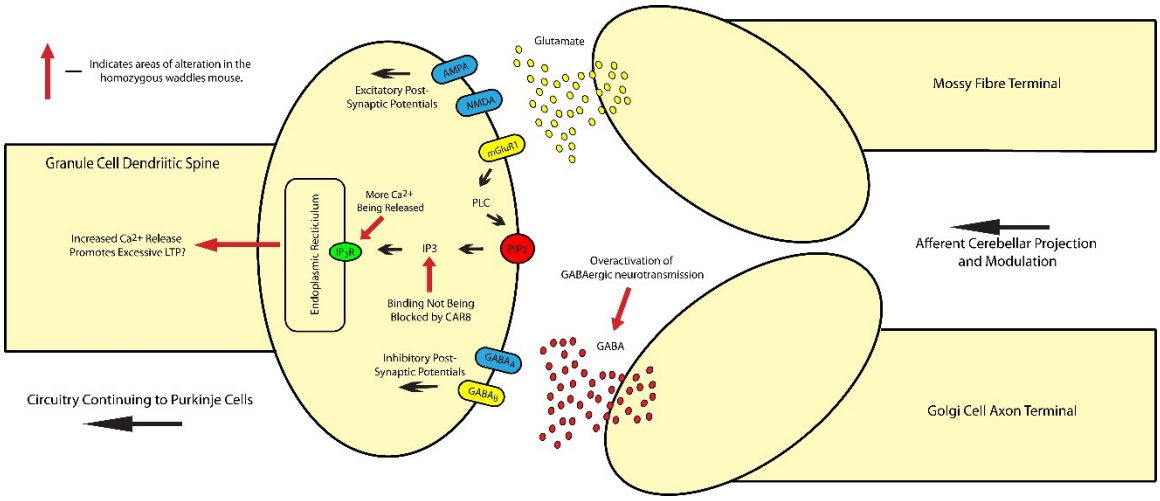

Fig. 3.6 - This is a depiction of the potential mechanisms (see red arrows in diagram) by which mutation of carbonic anhydrase type 8 alters cerebellar granule cell physiology. Legend: AMPA= α-Amino-3-Hydroxy-5-Methyl-4-Isoxazolepropionate, Ca^{2+}=Ionic Calcium, CAR8 = Carbonic Anhydrase Type 8, GABA =Gamma Aminobutyric Acid, $IP_3(R)$= Inositol 1,4,5-trisphosphate (Receptor), $mGluR_1$=Metabotropic Glutamate Receptor Group 1, NMDA= N-Methyl-D-Asparate, PIP_2= Phosphatidylinositol 4,5 Bisphosphate.

3.2 Adolescent Binge Drinking Data

***Note:** Data presented here for the adolescent binge drinking model were recently published (Lamont et al. 2020).

3.2.1 Rota-Rod

An early adolescent group (PND 26) was tested during our initial study had significant differences between control and treated groups at the 15 RPM speed, but not at 5 or 10 RPM. A mixed-design ANOVA with treatment condition (control, ethanol) as a between-subjects factor and testing day (Day 1, 2, 3, 4, 5, 11, 15, 20, or 35) as a within-subjects factor revealed a main effect of the condition ($F(1,10) = 7.98$, $p = .018$) on testing days three ($t(10) = 2.50$, $p = .031$), four ($t(10) = 4.07$, $p = .002$), five ($t(10) = 4.90$, $p = .001$), eleven ($t(10) = 2.67$, $p = .023$), fifteen ($t(10) = 3.50$, $p = .006$), and twenty ($t(10) = 4.30$, $p = .002$); with a return to no between group difference on day thirty-five ($t(10) = 1.03$, $p = .326$; Fig. 3.6A).

Adolescent (PND 34) subjects were also tested on this same paradigm and showed significant differences between groups at 15 RPMs with a main effect of condition ($F(1,10) = 8.89$, $p = .014$). Simple main effect analysis showed that whether the subjects were treated with ethanol had a significant effect on latency to fall from the rota-rod ($p = .018$). Further analyses with a series of independent-samples t-tests revealed significance for testing days two ($t(10) = 2.92$, $p = .015$), three ($t(10) = 2.53$, $p = .030$), four ($t(10) = 2.97$, $p = .014$), five ($t(10) = 2.39$, $p = .038$), eleven ($t(10) = 2.98$, $p = .014$), fifteen ($t(10) = 3.25$, $p = .009$), and twenty ($t(10) = 3.09$, $p = .011$); with a return to no between group difference on day thirty-five ($p = .060$; Fig. 3.6B).

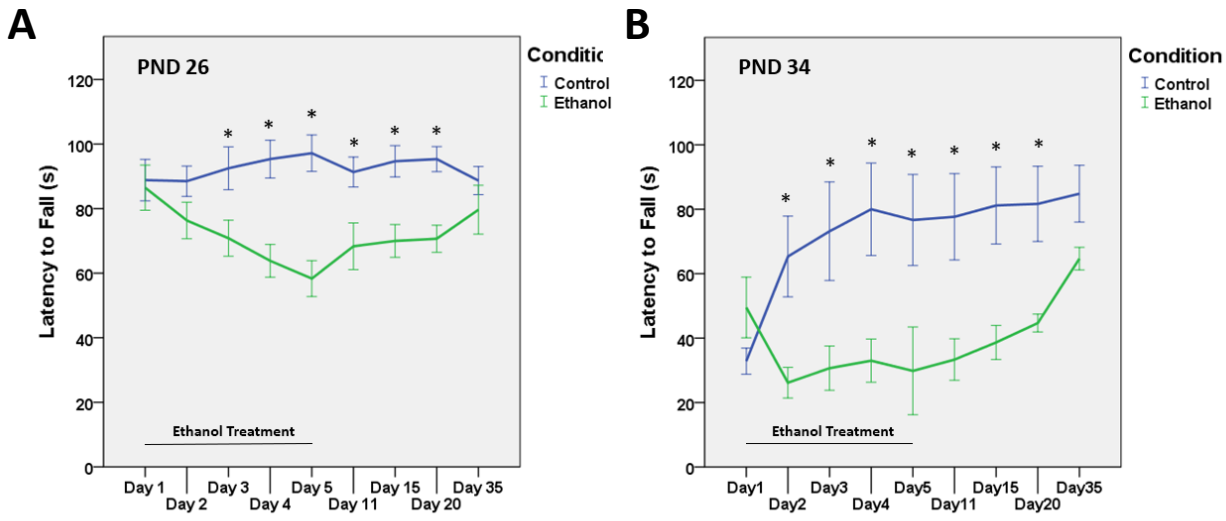

*Figure 3.7 - Fixed-speed rota-rod testing revealed a significant difference between ethanol treated and control subjects in both the pre-adolescent (A; PND 26; n=12 per treatment group; *p < .05 days 3-20) and adolescent (B; PND 34; n=12 per treatment group; *p < .05 days 2-20) age groups. In both graphs "Day 1" corresponds to the first testing day for each group (i.e. Day 1 for adolescent groups was PND 26).*

The experiments in Fig. 3.7 were performed as an initial study to ascertain whether our ethanol administration procedure would affect behavior in the first place. A new adolescent group (PND 34) was subsequently treated with ethanol before a series of behavioral tests. This new group was tested on an accelerating rota-rod paradigm and showed significant differences on PND 39 (F (1,23) = 4.75, p = .040), PND 40 (F (1,23) = 5.38, p = .030), PND 46 (F (1,23) = 5.10, p = .034), and PND 50 (F (1,23) = 4.89, p = .038; Fig. 3.8). No significant difference was found in this group on an inverted cage-hang test (t(22) = 0.110, p = .913; Fig. 3.9). This occludes the possible influence of muscle tonality on previously obtained rota-rod results.

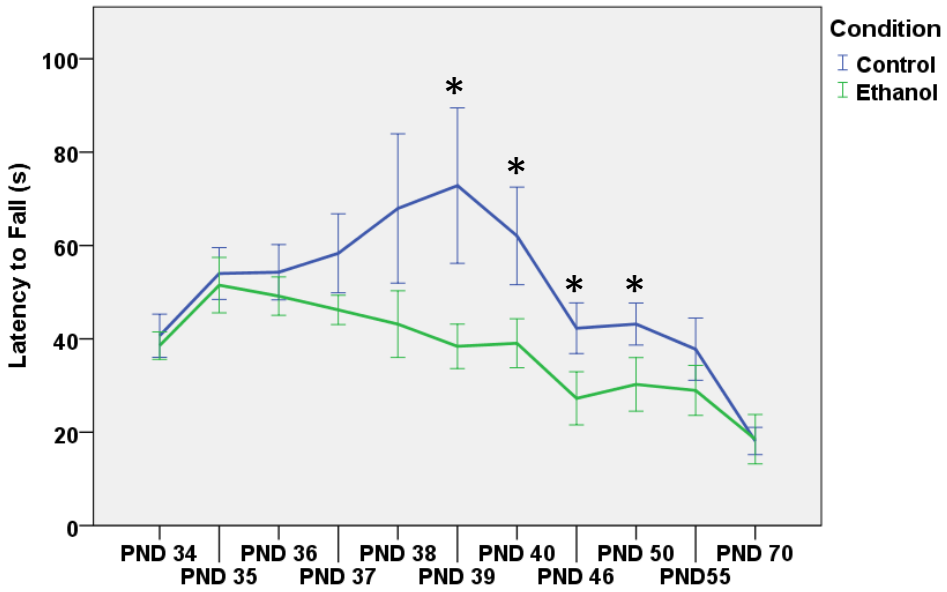

*Fig. 3.8 – Accelerating rota-rod testing of adolescent groups (PND 34; n=12 per group) showed a significant difference between ethanol and control groups on PND 39 (F (1,23) = 4.75, *p = .040), PND 40 (F (1,23) = 5.38, *p = .030), PND 46 (F (1,23) = 5.10, *p = .034), and PND 50 (F (1,23) = 4.89, *p = .038).*

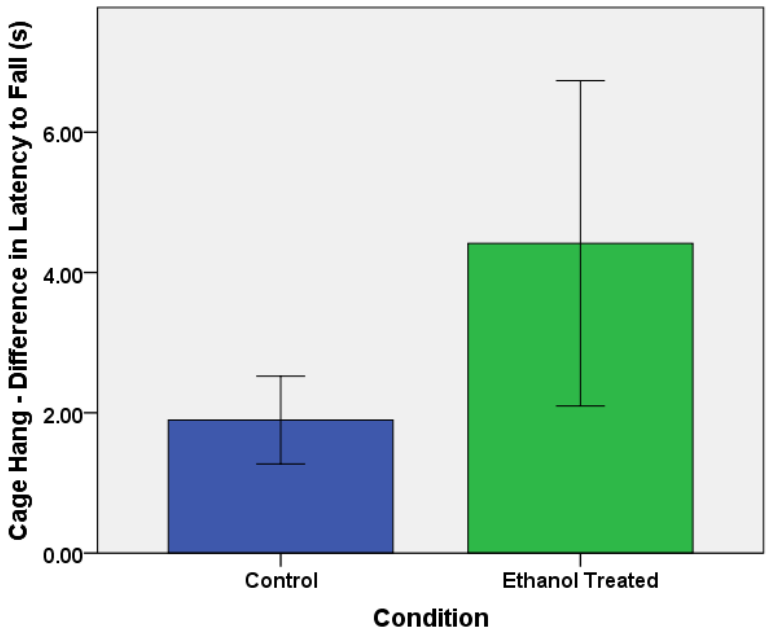

Fig. 3.9 – Adolescent groups (PND 34) were tested on an inverted cage-hang apparatus after treatment to look for any effects on muscle tonality/strength. There was no significant difference between groups in the latency to fall on the inverted cage-hang test (n=12 per group; p = .913).

3.2.2 Open Field

Open field testing was conducted to ensure subjects general propensity for movement was not altered by the ethanol treatment and therefore potentially the cause of differences seen in rota-rod testing. Analyses showed that there was no difference in the total movement of subjects in the arena ($p = 0.21$, Fig. 3.10). There was also no significant difference between the groups with respect to time spent in the center ($p = 0.85$) or periphery ($p = 0.86$) of the open field (data not shown).

A separate group of adolescent animals underwent an identical ethanol exposure paradigm as the PND 34 group and were tested for withdrawal effects shortly after treatment (one day after the last ethanol exposure). There was no withdrawal effect on the subject's propensity for locomotion ($p = .11$) or movement speed ($p = .14$) when this was measured using a simple open arena (Fig. 3.11).

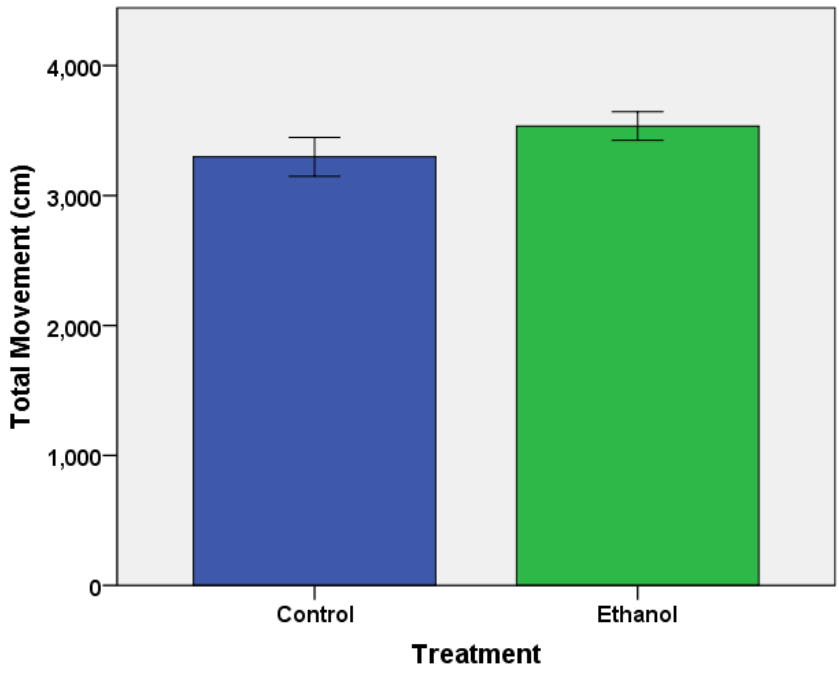

Fig. 3.10 – When PND 34 groups were tested in the open field apparatus, it showed there was no difference between groups with respect to general propensity for locomotion (n=12 per group, p = 0.11).

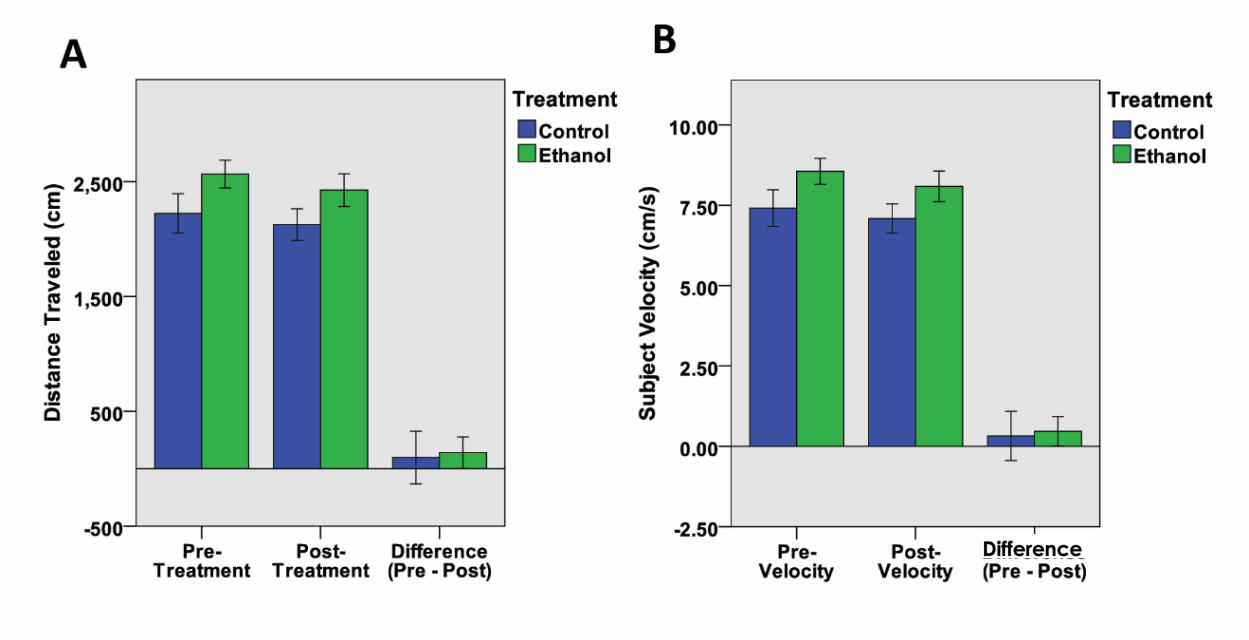

Figure 3.11 – Two groups of PND 34 rats (ethanol treated and control) were tested on the days directly before/after treatment to see if there were any immediate effects on behavior. There was no withdrawal effect on the subject's propensity for locomotion (p = .11) or movement speed (p = .14) when this was measured using a simple open arena. (n=12 per group).

3.2.3 Anxiety-like Behavior

Interestingly, the amount of time spent in the open arm of the EPM was significantly higher in the ethanol treated group when compared to controls ($t(22) = -2.50$, $p = .020$; Fig. 3.12). However, there was no difference between groups with respect to the frequency of crossing between the open/closed arms. Subjects previously treated with ethanol also spent significantly more time in the light side ($t(22) = -2.78$, $p = .011$; Fig. 3.13) of the light dark box. There were no significant differences between groups with respect to the total number of crossings between the light to dark sides. There was an increased preference for the light side of the box noted in the groups being tested for withdrawal effects. Previously seen on PND 79 in the first ethanol treated group, this significant increase appears shortly after treatment as well ($t(22) = -2.65$, $p = .015$; Fig. 3.14). Other studies have found the opposite affect with an increased preference for the closed arms after ethanol treatment (i.e. Varlinskaya et al. 2020); however, there was a significantly higher BACs and a longer time-course of treatment that could explain the discrepancy. Finally, there was no statistically significant difference seen between groups on the open field, acoustic startle, or fear conditioning tests (all $p > .05$; Fig. 3.15).

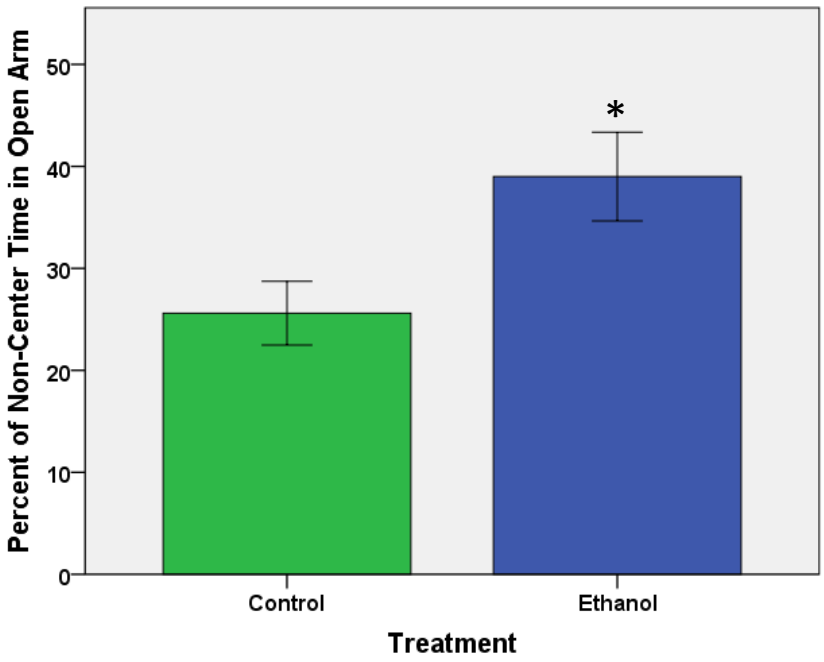

*Fig. 3.12 - Anxiety-like behavior testing revealed significant differences between control and ethanol treated groups in the elevated plus maze (n=12 per group; *p < .05). The ethanol treated group spent a significantly higher percentage of their time in the open arms of the maze, indicating a possible decrease in behavioral inhibition.*

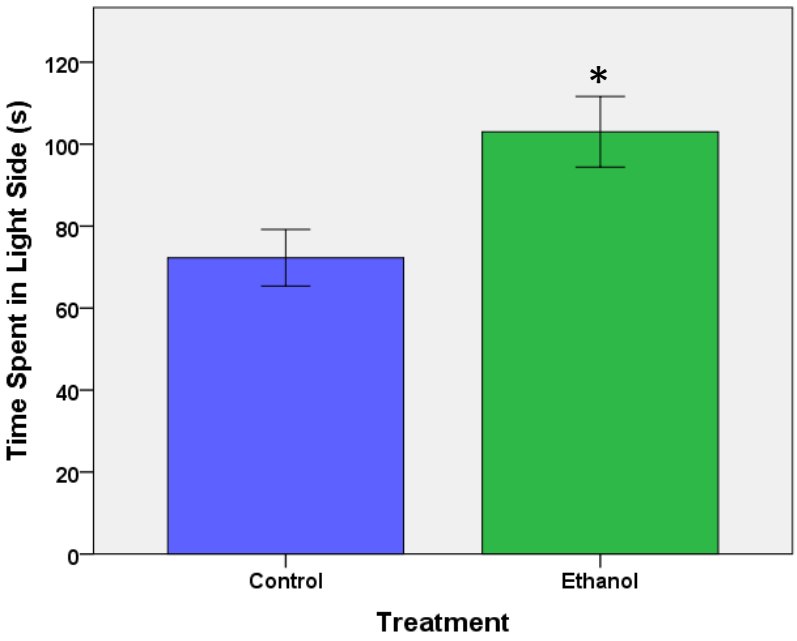

*Figure 3.13 - Anxiety-like behavior testing revealed significant differences between control and ethanol treated groups in the light-dark box (n=12 per group; *p < .05)**.** The ethanol treated group spent significantly more time in the "light" side of the box, indicating a possible decrease in behavioral inhibition.*

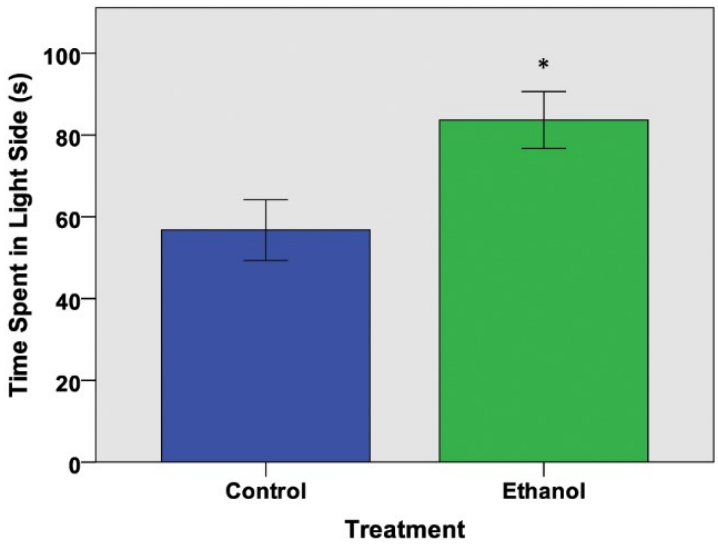

*Figure 3.14 - Experiments with a second adolescent group (PND 34) established that subjects' performance on the light-dark box test was impaired similarly the day after treatment as it was when tested on PND 79 in the first group of adolescent animals (n=12 per group; *p < .05). Therefore, the effect on light-dark box behavior is initiated by the first day post-treatment and persists for at least two months.*

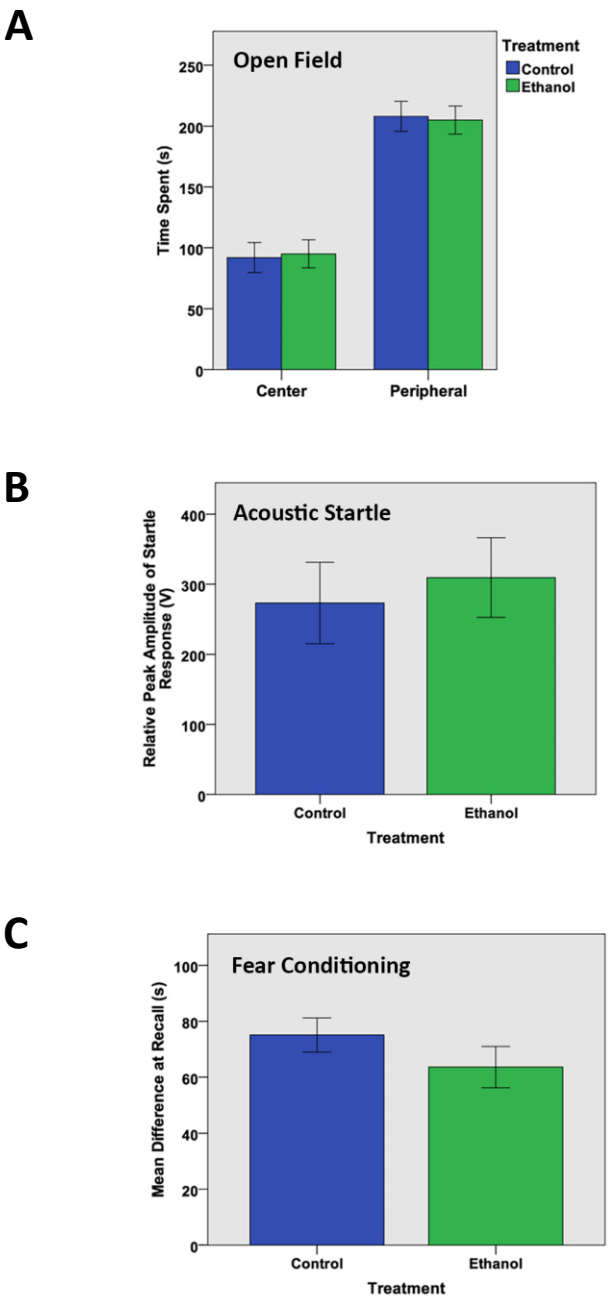

Figure 3.15 – Not all behavioral testing with the adolescent (PND 34) groups yielded significant results when comparing control and ethanol treated groups. There was no statistically significant difference seen between groups on the (A) open field, (B) acoustic startle, or (C) fear conditioning tests (all n=12 per group; p > .05). Meaning that general propensity for locomotion and fear-based memory consolidation were not altered by exposure to ethanol.

3.2.4 Novel Object Recognition

There were no significant differences between the two groups with respect to total exploration time of the objects, either during the training or testing phases of the experiment. Analysis of the discrimination index value showed a significant difference between groups ($t(22) = 2.40$, $p = .025$). A higher value for the control group indicated that they preferred the novel object during the testing trials of NOR, while the ethanol treated group had no strong preference for either object (Fig. 3.11), suggesting a deficit in the ethanol-treated group.

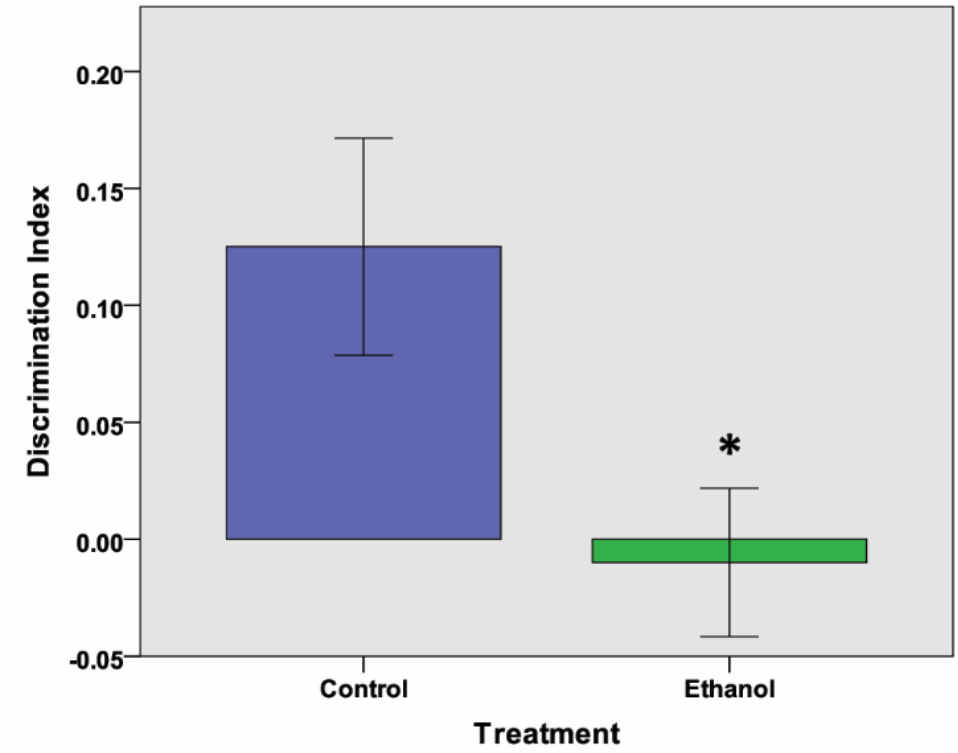

*Figure 3.16 – A discrimination index was calculated (exploration of novel object – exploration of familiar object / total exploration time); positive index values indicate the subject explored the novel object more frequently. Calculated discrimination index values were significantly different between control and ethanol treated groups (n=12 per group; *p < .05); indicating that the ethanol treated group was unable to distinguish between a familiar and novel object after delay on the novel object recognition task.*

3.2.5 Western Blotting

All western blot results were determined to be within the combined linear dynamic ranges of the both the target and loading control. Total caspase-3 levels were significantly elevated in the cerebella of ethanol treated animals compared to control subjects ($t(22) = -2.32$, $p = .030$). Total NF-kB protein levels were also elevated in ethanol treated groups ($t(22) = -2.20$, $p = .038$; Fig. 3.17).

Activated forms of the proteins were also elevated with exposure to ethanol as can be seen in the cleaved form of caspase 3 ($t(14) = -2.73$, $p = .016$) and phosphorylated NF-kB ($t(14) = -2.57$, $p = .022$; Fig. 3.18). These results indicate that neurodegeneration has occurred in the cerebella of animals exposed to ethanol and this is likely related to the behavioral differences observed between groups. PKC was also elevated in both its non-active ($t(14) = -3.18$, $p = .007$) and phosphorylated ($t(14) = -4.38$, $p = .001$) states. There was no significant difference in the ratio of the two forms to one another between groups since both forms of PKC were increased in ethanol treated subjects (Fig. 3.19). All significant blot results in this project were found only in cerebellar tissue. Additionally, there were no significant differences detected when the ratios of activated proteins to base protein level (PKC, Caspase-3, and NF-kB) was compared between groups in cerebellar tissue (Fig. 3.20).

An independent-samples t-test was conducted to compare tubulin densitometry levels between control (M=28325.00, SD=2891.68) and ethanol treated (M=28566.67, SD=2573.84) groups indicating no significant difference ($t(22) = -0.062$, $p = .95$). When homogenized lysates of cerebral cortex were compared for caspase-3 levels, there were no significant differences detected between groups (Fig. 3.21).

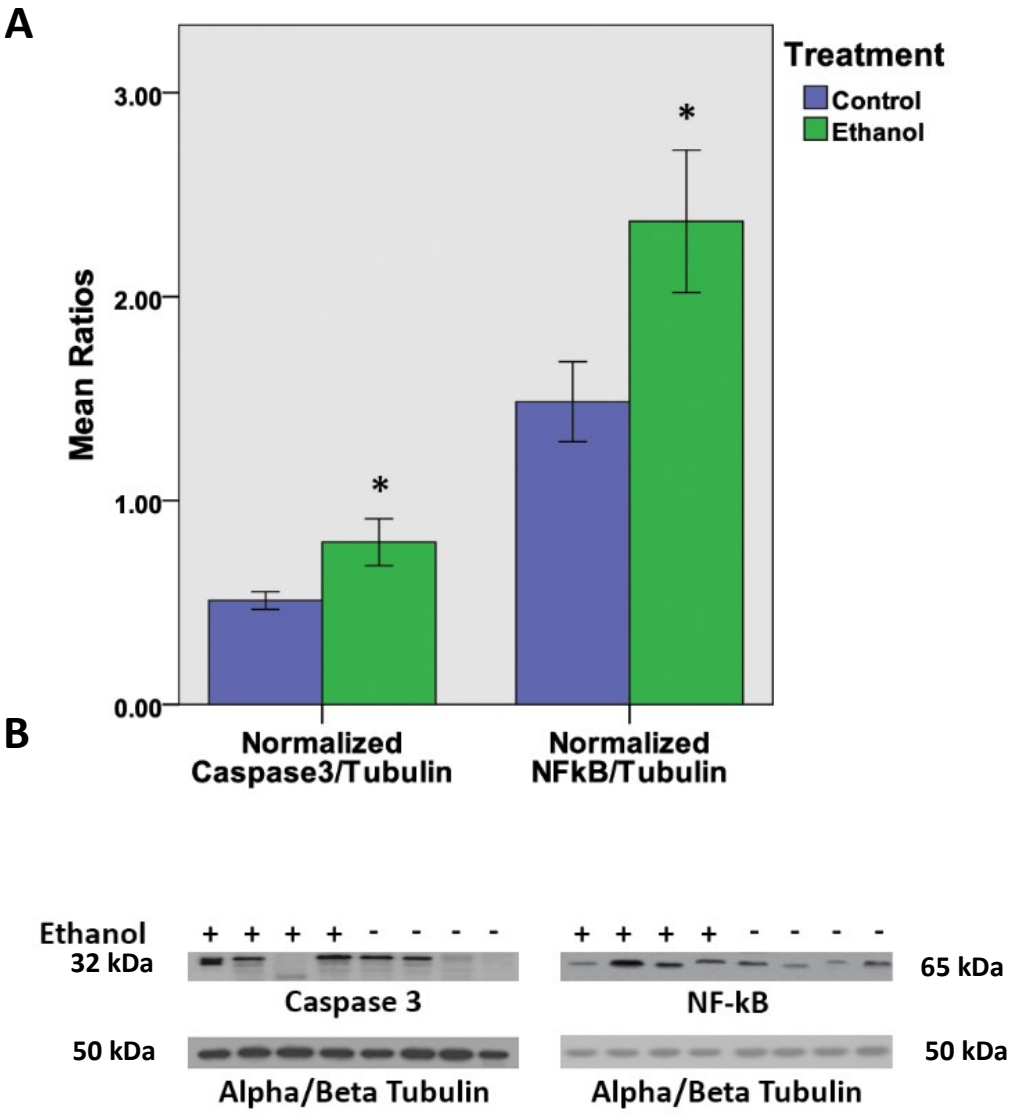

*Figure 3.17 – (A) Significant differences were seen between the control and ethanol groups in the expression levels of the caspase 3 (n=12 per group; *p < .05) and NF-kB (n=12 per group; *p < .05) proteins in the cerebellum. (B) Representative images from western blots examining caspase-3 and NF-kB expression levels in the cerebella of treated/control animals along with alpha/beta tubulin control bands.*

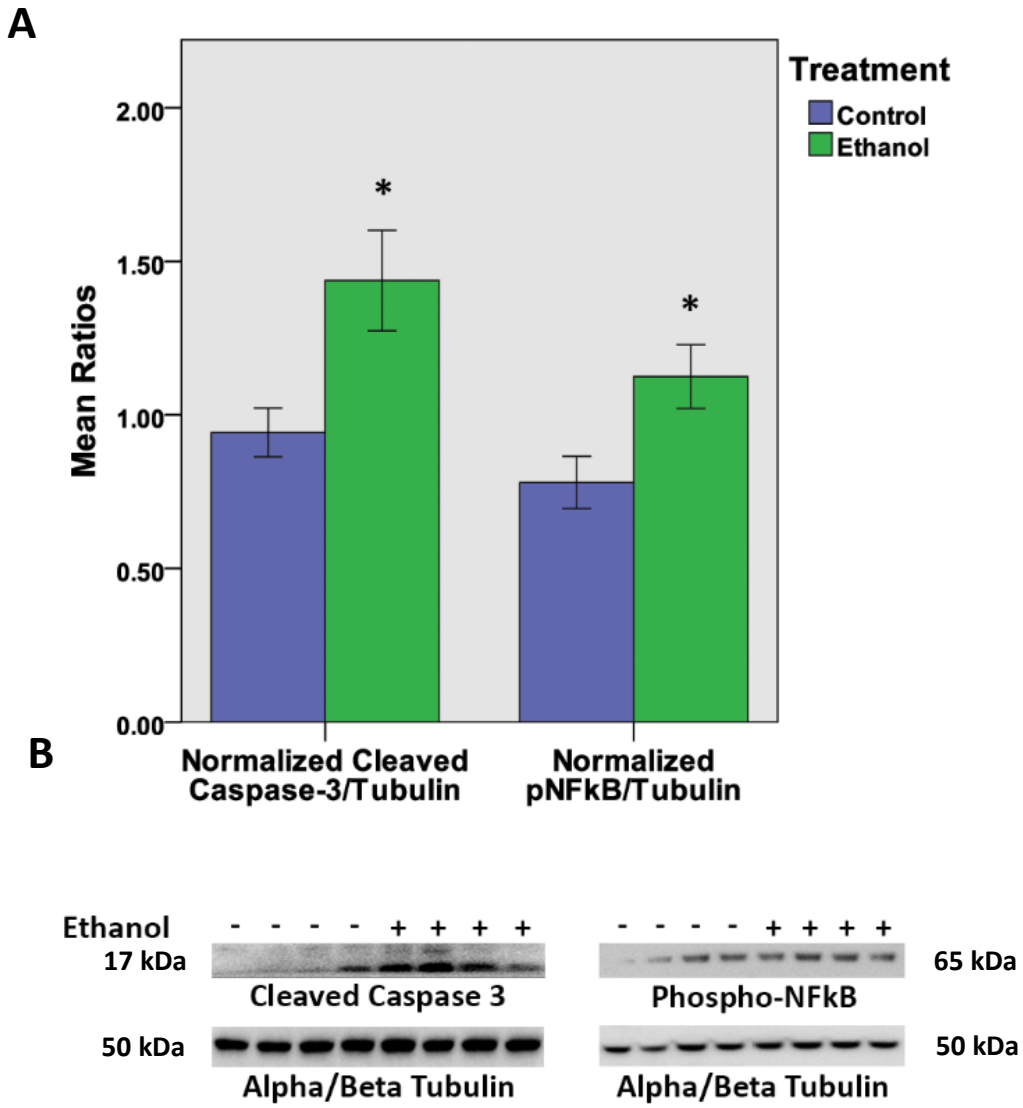

*Figure 3.18 – (A) Activated versions of the proteins of interested are significantly upregulated, as evidenced by increased levels of cleaved caspase-3 (n=12 per group; *p < .05) and phosphorylated NF-kB (n=12 per group; *p < .05) proteins between groups in the cerebellum. (B) Representative images from western blots examining cleaved caspase-3 and phosphorylated NF-kB expression levels in the cerebella of treated/control animals along with alpha/beta tubulin control bands.*

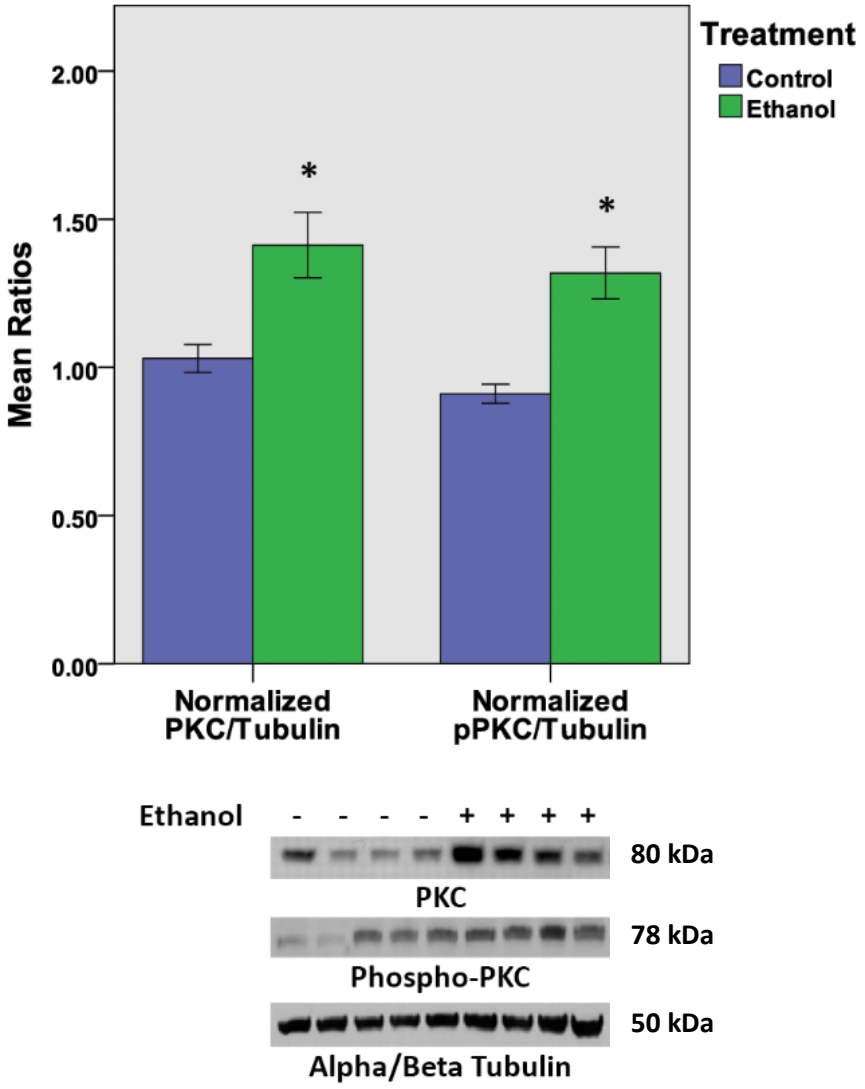

*Figure 3.19 – (A) Levels of both PKC (n=8 per group; t (14) = -3.18, *p < .01) and pPKC (n=8 per group;* t (14) = -4.38, **p < .001) proteins were also elevated in cerebellar tissue when ethanol treated groups are compared to controls. (B) Representative images from western blots examining PKC and phosphorylated PKC expression levels in the cerebella of treated/control animals with an alpha/beta tubulin control band.*

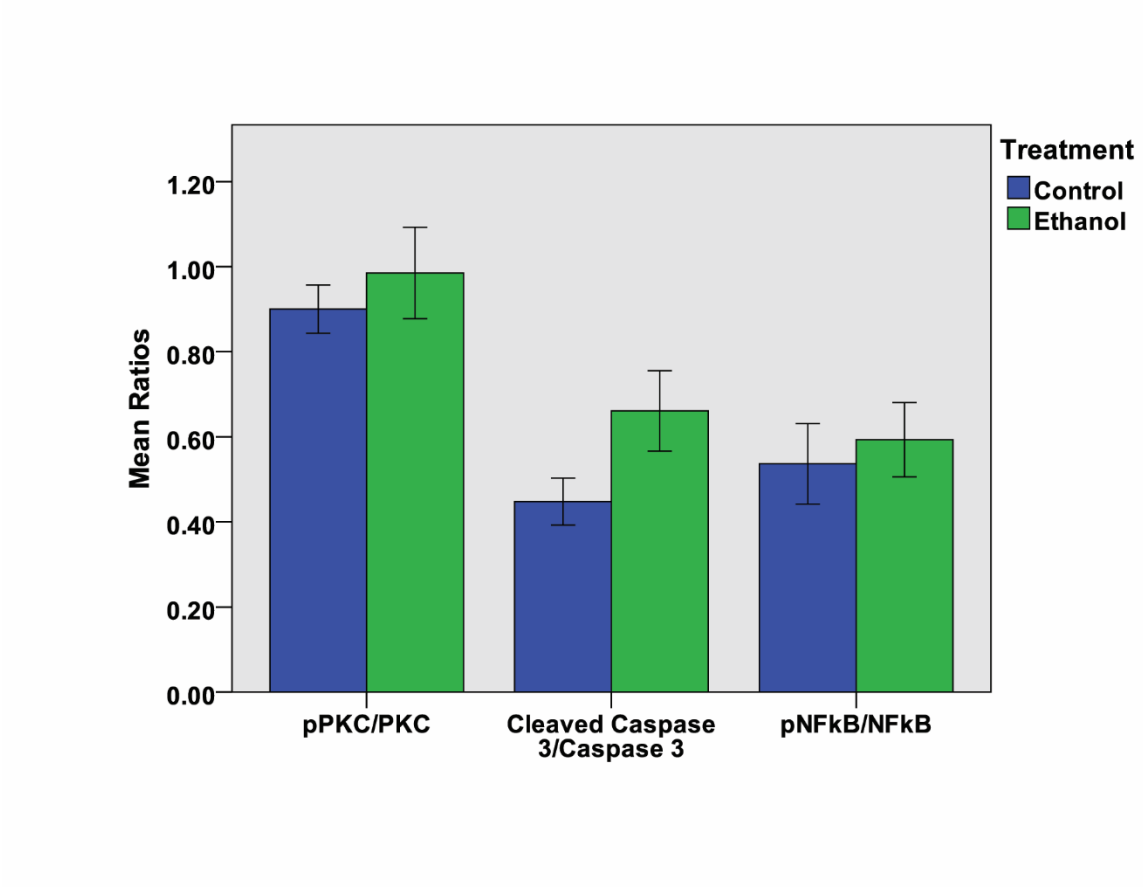

Figure 3.20 - Between group comparison of the ratios of activated to base levels of the proteins examined in this study. No significant differences were noted; the closest was the comparison of caspase 3 proteins (p = .07; n=8 per group).

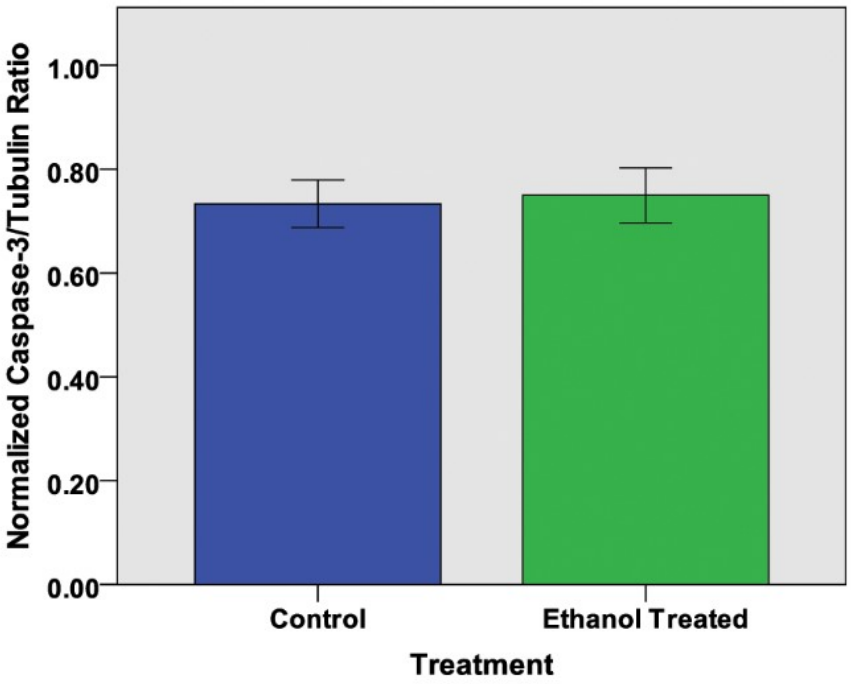

Figure 3.21 - Relative amount of caspase-3 in the cerebral cortex of control versus ethanol treated rats. No significant differences were noted (p = .82; n=8 per group).

3.3 Comparative Analyses of PKC

To bring together the two models in a direct way, PKC levels were compared between the *wdl* mice (both homozygous and heterozygous), wild type mice, ethanol treated rats, and control rats (Fig. 3.22). ANOVA analysis indicates there are significant differences between groups in levels of both PKC (F (4,39) = 8.15, $p < .001$) and pPKC (F (4,39) = 9.98, $p < .001$).

Post-hoc analysis of PKC levels indicated the significant differences are between the: control and ethanol treated groups ($p = .004$*);* the ethanol treated group and the heterozygous *wdl* ($p = .009$), and wild type groups ($p = .001$); the homozygous *wdl* and wild type groups ($p = .008$).

Post-hoc analysis of pPKC levels indicated the significant differences are between the: control and ethanol treated ($p = .001$*)* and homozygous *wdl* groups ($p = .001$); the ethanol treated group and heterozygous *wdl* ($p = .005$), and wild type groups ($p = .007$); the homozygous *wdl* and heterozygous *wdl* ($p = .006$), and wild type groups ($p = .009$). Overall, both the homozygous *wdl* and ethanol treated animals had significantly elevated levels of both PKC and pPKC compared to other groups of subjects (Table 3.1). There was no significant difference detected between the models (i.e. ethanol vs. *wdl*) with respect to PKC (F (1,39) = 2.62, $p = .114$) and pPKC (F (1,39) = 0.03, $p = .865$). This result can be extended to there being no difference between species as well as each model is composed of their respective species (i.e. ethanol = rat & *wdl* = mouse).

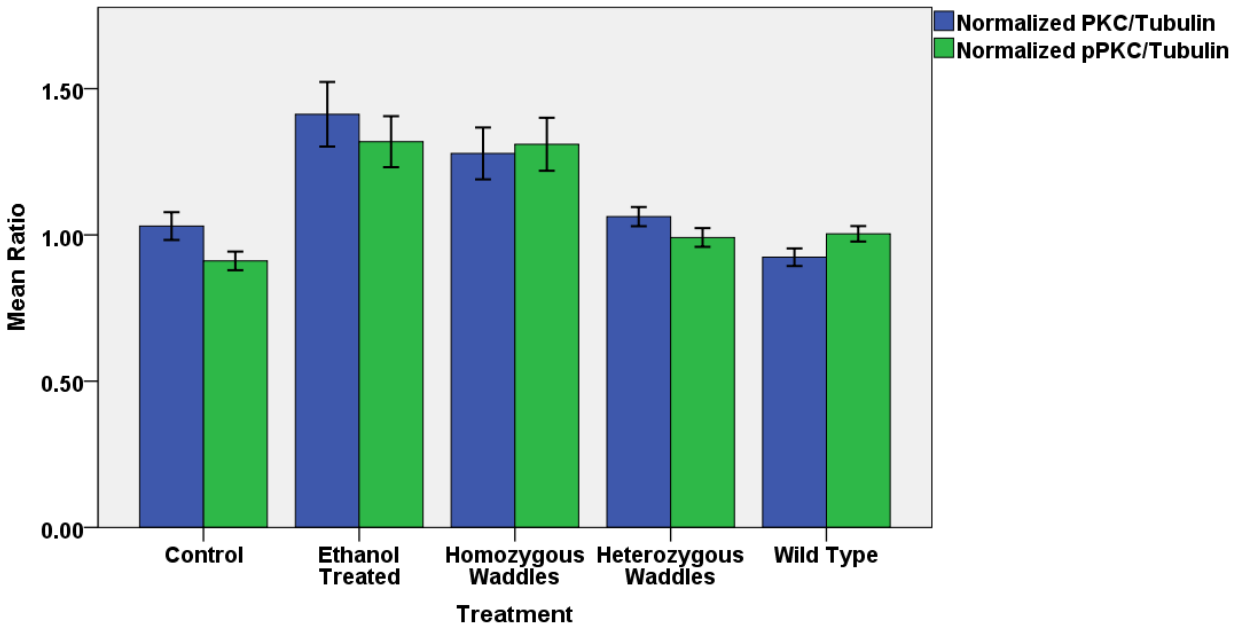

Fig. 3.22 – Comparative graph of the two models (wdl and ethanol) of cerebellar impairment being compared in this dissertation. ANOVA testing revealed significant differences between groups in both PKC ($F(4,39) = 8.15$, $p < .001$) and pPKC ($F(4,39) = 9.98$, $p < .001$) expression levels. Post-hoc testing for PKC indicated these differences were between the: control and ethanol treated groups ($p = .004$); the ethanol treated group and the heterozygous wdl ($p = .009$), and wild type groups ($p = .001$); the homozygous wdl and wild type groups ($p = .008$). Post-hoc analysis of pPKC levels indicated the significant differences are between the: control and ethanol treated ($p = .001$) and homozygous wdl groups ($p = .001$); the ethanol treated group and heterozygous wdl ($p = .005$), and wild type groups ($p = .007$); the homozygous wdl and heterozygous wdl ($p = .006$), and wild type groups ($p = .009$). See table 3.1 for summary of significant comparisons.

Testing Group	Comparison Group	Significance (p-value)
PKC/Tubulin Ratio		
Control	Ethanol	.004
Ethanol	Heterozygous *wdl*	.009
	Wild Type	.001
Homozygous *wdl*	Wild Type	.008
pPKC/Tubulin Ratio		
Control	Ethanol	.001
	Homozygous *wdl*	.001
Ethanol	Heterozygous *wdl*	.005
	Wild Type	.007
Homozygous *wdl*	Heterozygous *wdl*	.006
	Wild Type	.009

Table 3.1 – Summary of significant between-group differences in PKC/Tubulin and pPKC/Tubulin ratios.

Chapter 4 - Discussion

4.1 Experimental Limitations

4.1.1 Behavioral Experiments

With any behavioral methodology there is the recurring issue0nj89i8onj of large amounts of variability in subjects' behavioral performance. Variability in performance can be due to numerous factors including, but not limited to, environmental conditions (i.e. time of day of testing, air pressure, and temperature) and inherent personality variability in subjects (e.g. aggressiveness, sociability, or introversion). This is normally controlled for by relatively large sample sizes where outlying data points from subjects are compensated for by being grouped with those from subjects performing in the normal range, when calculating the means. Therefore, the minimum number of subjects per group in both the ethanol and *wdl* experiments was twelve in behavioral experiments; although this helped us to obtain significant results, the inherent variability in behavioral research could still have affected the statistical analysis of results.

4.1.2 Calcium Imaging

Like any experimental methodology, there are inherent limitations to Ca^{2+} imaging which need to be discussed. One of the major contributors of limitations with this methodology is the choice of fluorescent Ca^{2+} probe to be used. Depending on the dissociation constant of a given probe it may be more suited for either determining the time course of a Ca^{2+} signal or give an accurate reading of Ca^{2+} levels. Probes which dissociate more easily from Ca^{2+}, such as OG-BAPTA-1-AM, are better for determining signal dynamics since they allow for an accurate reading of both the rise and decay phase of a Ca^{2+} peak. Those probes which do not dissociate from Ca^{2+} easily give a more

accurate estimate of absolute Ca^{2+} levels, but since they bind strongly to Ca^{2+}, they will not dissociate quickly enough to accurately indicate the decay phase of a signal (Grienberger & Konnerth 2012).

While analyzing responses from GCs in several conditions, there was a large amount of variability in their responses to various agonists/antagonists. This may be due to an inherent large variability in granule cell morphology, which was determined to affect signaling through a previous computer modeling study (Houston Wisden & Brickley 2012). The authors of this study observed three distinct morphological arrangements of GCs, specifically localization of the axon, which gave three distinct signals when stimulated. This finding explains why there was some significant variability between GCs and indicates the GC population may be more diverse than previously thought.

4.1.3 Western Blotting

The main limitation of the western blot technique, especially when compared with other protein assays, is it being considered a semi-quantitative test. There are companies which supply kits that allow results to be plotted against a standard curve (and thereby become quantifiable), but these are often come with a high expense which is not tenable for many laboratories.

The other major issue which can arise is the potential for non-specificity of both the primary and secondary antibodies (mostly seen when using polyclonal varieties). Antibodies have the potential to bind non-specifically and give false positives. This factor was minimized in the experiments presented here as monoclonal antibodies were employed where possible.

4.2 Waddles Experiments

It was originally hypothesized that the CAR8 mutation significantly altered Ca^{2+} dynamics in the cerebellum. This was thought to be mediated by a loss of inhibition of IP_3 binding to the IP_3R, since the only known function of CAR8 is to inhibit IP_3 binding to its receptor. Within the bounds of this hypothesis only the homozygous animals would have disturbed neuronal signaling as only they displayed ataxia. Conversely, according to this hypothesis heterozygous animals should therefore have neuronal Ca^{2+} within normal limits. However, our findings demonstrate that heterozygous animals also have disturbed Ca^{2+} dynamics and exhibit impaired motor learning. Altered Ca^{2+} dynamics may cause a difficulty with motor learning in both homozygous and heterozygous groups. Additionally, the alterations in Ca^{2+} signaling recorded did not completely match with theoretical predications based on the hypothesis. Possible candidates causing this deviation from the predicted state include compensatory mitochondrial Ca^{2+} sequestration, morphological changes in response to chronically altered Ca^{2+} signaling from birth in the *wdl* mice, and/or a biphasic response of GCs to the altered levels of $[Ca^{2+}]_i$.

4.2.1 Rota-rod

Behavioral testing on the rota-rod apparatus was undertaken to further characterize the ataxic phenotype of both homozygous and heterozygous *wdl* mice (Monville Torres & Dunnett 2006). Homozygous mutants showed a significant age-linked difference in latency to fall from the rota-rod apparatus (Fig. 3.1). When homozygous subjects were examined at one month of age, they performed significantly better than three- or six-month PNA homozygous cohorts (Fig. 3.1). Significant ARR

results may be partially attributable to a difference in body mass between homozygous groups of different ages affecting the ease of balancing. This could not be analyzed with a post-hoc correlational statistic however, as the weights of mice were not recorded during this experiment. This difference in latency to fall indicates that calcium imaging experiments conducted in older versus younger homozygous *wdl* mice may yield significantly different data. The comparison was not conducted in this study as neural tissue from older animals is more sensitive to physiological perturbations during experimentation and generally loads Ca^{2+} indicator much less effectively. Given that motor performance decreased with age but alterations to Ca^{2+} dynamics were present from birth, it may be that it is not the physiological alterations causing ataxia in *wdl* mice; but, instead it is a result of the aberrant morphology of the cerebellar cortex seen in previous studies (Hirasawa et al. 2007).

The three-month old WT group performed significantly better than the one- or six-month old WT groups. This result is not entirely surprising as cerebellar changes continue to occur up until four months postnatally (Altman 1969). Therefore, the superior performance of the three-month-old group may be due to a nearly fully developed cerebellum giving them an advantage over younger animals, while older animals may start to experience an age-related decline in performance. One-month old homozygous animals performed significantly worse than heterozygotes and WT groups of any age (Fig. 3.1). Their outperformance of older homozygous subjects suggests the ataxia is present at birth and worsens during the first several weeks of life. Heterozygous groups did not display any significant motor improvement. Ataxic symptoms specifically affecting motor performance (i.e. those seen in homozygous mutants) have been linked to

morphological abnormalities of the cerebellar cortex (Schonewille et al. 2007) which were described in homozygous *wdl* mice (Hirasawa et al. 2007). A heterozygous mutation in *Car8* may therefore lead to a motor learning deficit without the marked ataxia and altered cerebellar morphology seen in homozygous mice. The lack of significant motor improvement detected in heterozygous groups also brings into question previous reports suggesting that they should be used as controls to homozygous *wdl* mice.

Motor learning was previously defined as significant improvement in the pooled mean of the first day of trials (i.e. five trials total) when the same group was tested on the final two days of the ARR (i.e. two trials per day, four total). A clear trend of increasing latency to fall over the course of the trials was only seen in the one-month old homozygous animals and in the WT group which were each determined to have displayed motor learning. Motor learning in the one-month old homozygous group was established by using a two-way repeated measure ANOVA (time of trial x age) over the last four trials (Fig. 3.1). The results from this ANOVA also confirmed that it was the youngest (1 mo. PNA) homozygous animals who significantly improved their motor performance over time.

As further evidence for motor learning, average latency to fall on Day 5 was normalized to average data from Day 1 for all rota-rod groups individually (Fig. 3.2). These results agreed with the previously conducted ANOVA that motor learning was displayed by the 1-month PNA homozygous and WT groups. There were varying degrees of improvement in the latency to fall, as denoted by a greater normalized value of heterozygous animals, but not to the extent of young homozygotes and WT mice. This lack of consistency in motor performance was only seen in the heterozygous groups; the

homozygous groups either performed consistently poorly or in the case of the one-month old homozygotes, performed consistently until there were persistent improvements. It seems odd at first that young heterozygous animals did not display motor learning, as the 1-month PNA group of the other genotypes did. However, it may be that Ca^{2+} dynamics are further disturbed in young heterozygous animals than in homozygous cohorts since alterations in the timing of neuronal firing is known to affect motor learning whereas ataxic symptoms (i.e. those seen in homozygous mutants) are more generally linked to morphological abnormalities of the cerebellar cortex (Schonewille et al. 2007).

The significantly diminished performance of the 1-month old homozygous animals may be due to the absence of functional CAR8 affecting prenatal development as well as further postnatal development and neuronal synapse maintenance. Compared to rota-rod testing conducted by Jiao et al. (2005), the results obtained here indicate a much lower latency to fall. This can be accounted for by the different methodologies employed; Jiao et al. (2005), utilized a fixed speed rota-rod paradigm, whereas these experiments used the ARR paradigm mentioned previously. The ARR paradigm more accurately characterizes the differences between mutant ataxic mice whereas the alternative fixed speed rota-rod paradigm better characterizes motor impairments due to drug exposure (Rustay et al. 2003). Additionally, the current experiment included the heterozygous group and conducted multiple trials over five days while Jiao et al. (2005) only conducted three trials spaced over the same day which did not allow for motor learning to be investigated.

4.2.2 Calcium Imaging

There were significant differences between the Ca^{2+} signaling in GCs of homozygous mutant *wdl* mice and their WT counterparts (e.g. Fig. 3.3). Results obtained while using DHPG are more pertinent since the known action of CAR8 is on the IP_3 pathway, which is affected directly by group 1 mGluRs (Hirota et al. 2003). Subsequent experiments utilizing electrical stimulation of afferent GCL connections in tandem with a group 1 mGluR antagonist, AIDA, both confirmed and extended the basic hypothesis that there is altered Ca^{2+} signaling in the cerebella of *wdl* mice. This extension is that heterozygous *wdl* mice also experience altered Ca^{2+} signaling and that contrary to previous reports do experience motor difficulties in the form of impaired motor learning.

The first set of imaging experiments were conducted with the excitatory neurotransmitter glutamate as it provides general excitation to neuronal systems *in vivo* (Robinson & Coyle 1987) and is known to stimulate cerebellar GCs. Although it was expected that heterozygotes would show results like WT subjects since they do not display a behavioral phenotype; however, this was not the case. WT animals had a much larger maximum Ca^{2+} response to glutamate stimulation than homozygous *wdl* mutants. Heterozygous animals' maximum response was in between the values from the other two genotypes, but overall closer to the WT response. Differences in the magnitude of the Ca^{2+} response and the speed of that response would have direct functional implication in the GCL. As mentioned earlier the presence of higher or lower $[Ca^{2+}]_i$ drives plasticity either towards LTD or LTP in both the MF-GC and GoC-GC synapses (Gall et al. 2005). Disturbing the balance of 'opposing forces' in plasticity at one of the major input areas into the cerebellum would affect signaling in the entire cerebellar circuitry. The

importance of the GCL in modulating known motor programs such as the VOR was recently postulated (D'Angelo & De Zeeuw 2008). Our results therefore indicate the observed alterations in Ca^{2+} signaling may also affect accurate modulation of stored motor programs.

Qualitative comparison of average tracings from WT and homozygous mutants yielded an interesting observation. The average tracing from the WT group (Fig. 3.3) shows clear oscillations of Ca^{2+} during glutamate application in GCs which is quite uniform and has a very low SEM. This pattern likely reflects the well described GC population oscillation in excitability which is mediated by concurrent activation of GoCs that provide inhibitory input (Dugué et al. 2009). As the GC population is excited by glutamate, GoCs are also stimulated to provide inhibitory input postulated to control GCs from becoming overstimulated and contributes to their information processing abilities (Ito 2006). The pattern dissipates later in the recording (when bath [glutamate] drops), which seems to reflect the GoCs ability to provide feed-back inhibition. The inhibition would maintain the oscillatory pattern being overwhelmed by the strong excitation provided by the exogenous glutamate application. Homozygous mutants, however, have a tracing that shows similar patterns, but lacks the uniformity seen in WT animals (Fig. 3.3). The oscillations in the homozygous tracing are clearly disturbed and these animals also did not show a maximal response even close to that obtained by WT (Fig. 3.3). The disturbed oscillation pattern is most likely to involve GoC, as these cell types are known to express higher levels of CAR8 than GCs and could theoretically be more affected by the mutation. There is a clear dysfunction of the Ca^{2+} signaling in homozygous animals which is due in part to the mutated *Car8* gene. However, this is likely also due to the

possible developmental irregularities. Results of this set of experiments verifies the hypothesis that all three groups differ significantly in their Ca^{2+} signaling and inclusion of all three groups in subsequent experimental paradigms was required. These findings indicate an over-arching disruption in cerebellar circuitry, likely hampering proper neuronal communication as well as leading to morphological abnormalities.

The glutamate experiments yielded useful data, however, there is a lack of external validity since the stimulation paradigms provide a much greater activation than would be encountered *in vivo* (i.e. all cells in the slice are being simultaneously stimulated by the exogenous glutamate washed into the recording bath). Because of this deficiency in external validity a set of experiments using electrical stimulation of mossy fibers (MFs) was conducted. MFs activate synaptic glutamate receptors via endogenous glutamate release onto GCs as would occur *in vivo*. The results of these experiments further verify the basic premise that homozygous subjects respond with different Ca^{2+} dynamics than the WT and heterozygous groups to an equivalent stimulus.

Slices were stimulated at two time-points during recording to see if plasticity of the MF-GC synapses would be induced with this paradigm. Both the heterozygous and homozygous groups had a lower maximum response of their second peak when compared with the first (Figs. 4A). The opposite relationship was observed in the WT group which had an increase in Ca^{2+} response during the second stimulation. The changes in maximal response seen may be due to either Ca^{2+} store depletion or a form of short-term plasticity. A form of plasticity taking place is quite probable as the stimulation paradigm chosen has previously been reported to induce either LTD or LTP in cerebellar GCs dependent on differential $[Ca^{2+}]_i$ activation patterns (Bianchi et al. 1992; Gall et al. 2005). Therefore,

the conflicting bi-directionality of the change in Ca^{2+} response seen between WT and *wdl* groups likely reflects a difference in basal $[Ca^{2+}]_i$ caused by the mutation. Changes in plasticity within the GCL would heavily alter the information processing capabilities of the cerebellum, as a large portion of afferent cerebellar information is transmitted and initially processed here.

Use of thapsigargin allowed for a rough comparison of intracellular Ca^{2+} store size between groups (Fig. 3.4). Both WT and heterozygous *wdl* groups had a similar increase in $[Ca^{2+}]_i$, but the homozygous group had an unexpected drop. This decrease in response to thapsigargin indicates a major disturbance of the intracellular Ca^{2+} store management system. A consistently higher $[Ca^{2+}]_i$, due to increased Ca^{2+} release via IP_3R, may mean there is little Ca^{2+} left stored in the endoplasmic reticulum and therefore no significant amount to leak out in response to thapsigargin.

The average WT tracing from the glutamatergic imaging experiments (Fig. 3.3) has uniform oscillations of Ca^{2+} levels during glutamate application with low SEM. This pattern could reflect a propensity for GC populations to oscillate in excitability, which is mediated by concurrent activation of GoCs that provide inhibitory input. The frequency of the oscillations observed were much lower than those previously described (Dugué et al. 2009). Data from bicuculline experiments provide further evidence of GoC involvement in the altered GC signaling. When the inhibitory input onto GCs is antagonized by bicuculline, responses recorded from *wdl* mice mimicked the responses of WT subjects to glutamate alone. Supporting this conclusion are previous findings that GoCs inhibitory input helps to control signal timing in the GCL of the cerebellum (Dugué et al. 2009; Maex & De Schutter 1998). Abnormal timing in the GCL creates a noisy

signal throughout the cerebellar circuitry (Dizon & Khodakhah 2011), which has previously been linked to the *wdl* motor impairment.

The underlying issue with homozygous animals may not solely be due to the difference in Ca^{2+} dynamics. Results also indicate that alterations in cerebellar circuitry are present in *wdl* mutants, specifically in GoC driven GCL Ca^{2+} oscillations. As well there are clear variations in IP_3-linked intracellular Ca^{2+} pathways, which were more complex than originally hypothesized. Understanding the pathological Ca^{2+} signaling that underlies the *wdl* ataxia furthers our knowledge of other cerebellar ataxias involving aberrant Ca^{2+} signaling (e.g. autosomal dominant cerebellar ataxia/SCA6; Zhuchenko et al. 1997), as well as our comprehension of standard cerebellar Ca^{2+} signaling as it relates to functional motor output.

4.2.3 CAR8, Calcium, and Development

CAR8 is first expressed on day 9.5 of the gestational period in mouse embryos in the neuroepithelium (Lakkis et al. 1997), suggesting that it could be involved with pre-natal neuronal development (Aspatwar et al. 2010). Since cerebellar development continues into the first 30 days after birth for mice (Ito 2006), the effect of CAR8 on development should continue into the postnatal period. The idea is supported by the rota-rod data gathered during this project. The homozygous *wdl* mutants started at a disadvantage on the rota-rod compared to other groups and their performance worsens significantly after the first month of life (Fig. 3.1).

Remarkably, a similar ataxic syndrome is seen in humans with a mutation to a gene which is homologues to the murine *Car8*, *CA8* (Türkmen et al. 2009). The CAR8 protein is heavily conserved through various species and maintains a similar expression

profile in humans (Aspatwar et al. 2010). Humans who suffer from the *CA8* mutation experience ataxia, mild mental retardation, and quadrapedal gait (Türkmen et al. 2009). Insights gained from the study of the *wdl* mutant could eventually be applied to provide relief from this condition in humans and indirectly add to the growing body of research surrounding cerebellar based ataxias. Future studies of the *wdl* mouse could include the Morris water maze as a behavioral assay, since it tests both motor functions (i.e. the swimming itself) as well as cognitive aspects (i.e. spatial memory necessary to locate submerged platform).

The developmental dysfunction seen in *wdl* mutants is almost certainly linked to the altered Ca^{2+} signaling. Differential Ca^{2+} concentrations in the developing cerebellar cortex are known to control parallel fibre and climbing fibre innervation. There is ample research that implicates abnormal cerebellar cortex formation in the phenotypic ataxia of various ataxic mouse models (Rhyu 1999; Hirasawa et al. 2007; Zanjani 2012). In all these cases there are structural alterations of the PF-PC synapse which has been postulated to encode motor learning (Winter Li & Raymond 2012). These structural alterations are thought to be driven by differential Ca^{2+} concentrations and glutamatergic neurotransmission in the cerebellar cortex during development (Ichikawa et al. 2002; Miyazaki et al. 2004; Takeuchi et al. 2005), both of which were found to be disturbed in the *wdl* mouse (Hirasawa et al. 2007). It is important to keep in mind however that one cannot rule out the possibility of a yet undiscovered functional role, outside of the IP_3R, for CAR8 underlying the aberrant phenotype. Gene array studies in the cerebella of *wdl* mice indicate alterations in clusters of genes responsible for vesicle assembly, vesicle transport, signal transduction, and synaptogenesis (Yan et al. 2007). The substantial

number of dysregulated genes in *wdl* mice indicates that CAR8 indeed plays an important physiological role in the cerebellar cortex which is altering gene activation.

Interestingly, heterozygous subjects displayed properties of their GC Ca^{2+} signal that were significantly different from both WT and homozygous animals. This finding was unexpected as heterozygous mutants are normally used as a control in experiments involving *wdl* mice as they display no ataxia. These relatively unexpected findings may be indicative of a biphasic effect which is exerted by CAR8 on intracellular Ca^{2+} dynamics. It is possible that heterozygous animals with only one functional copy of the gene experience Ca^{2+} signaling which is significantly different than WT animals. Homozygous animals therefore have their Ca^{2+} homeostasis disturbed further due to both copies of the *Car8* genes being non-functional, and this initiates a compensatory mechanism (e.g. capacitive Ca^{2+} influx via TRPC channels) causing their signaling to appear similar to WT animals. This phenomenon may also be related to a lower number of functional synapses formed in the ML of homozygous animals (Hirasawa et al., 2007); influencing GCs via a lack of activity at non-functional PF-PC synapses. This would indicate that altered Ca^{2+} signaling may not directly cause the motor deficit by altering neurotransmission; especially since altered Ca^{2+} signaling in GCs is thought to affect motor learning, not cause ataxia (Schonewille et al. 2007) But, may be indirectly causing the ataxia by affecting proper development of the cortex and synapses in homozygous animals.

4.2.4 Western Blots

To draw comparisons between the two models used for this dissertation, western blot assays were performed to determine PKC levels in *wdl* mice (Fig. 3.5). It was

determined that the homozygous *wdl* mice had significantly higher levels of PKC, in both its base and phosphorylated states, than heterozygous and WT groups. These findings are in line with what was observed in ethanol treated animals when examining PKC levels (Fig. 3.19). The alteration of this upstream intracellular signaling protein indicated that cell physiology is being altered significantly in both experimental models.

4.2.5 Conclusions

Wdl mice show a pronounced ataxia due to a lack of CAR8 expression in the cerebellum leading to aberrant synaptic morphology and significantly altered Ca^{2+} signaling. Previous studies indicated the morphology of excitatory synapses was affected, but that there were likely other factors contributing to ataxia (Hirasawa, 2007). This other factor is likely an effect on Ca^{2+} dynamics. My results have shown significant differences in Ca^{2+} signal dynamics between the GCs of homozygous and heterozygous *wdl* mice as well as WT animals in various stimulation conditions that would activate glutamate receptors. These differences in signaling also likely underlie the previously reported developmental abnormalities as Ca^{2+} is known to be heavily involved in cerebellar cortex development (Zanjani 2012).

Behavioral data indicated that very young *wdl* mice display a significantly less severe ataxic phenotype and show motor learning, which was not seen in *wdl* mice over one-month PNA. There was also a lack of motor learning displayed by heterozygous animals over the five days of trials as was expected there was learning in WT mice. A report by Schonewille et al. 2007, indicated disturbed Ca^{2+} signaling in the cerebellum affected motor learning, but not motor performance. Therefore, the fact that both mutant groups (particularly older animals) failed to consistently display motor learning, could be

due to the altered Ca^{2+} signaling. In support of this idea, controlled Ca^{2+} handling by neurons (particularly that mediated via IP_3R and intracellular stores) has been shown to be essential for AMPA receptor trafficking to the post-synaptic membrane and therefore LTP/LTD as well (Nakata & Nakamura 2007). The reason heterozygous animals do not display ataxia is likely that their disturbance in CAR8 functionality is not so severe as to affect earlier cerebellar development but is affecting proper glutamate receptor trafficking.

It seems that CAR8 dysfunction could affect development of the GCL as it is expressed at its highest levels during pre-natal maturation (Aspatwar et al. 2010). The underlying issue with homozygous animals then may not be the originally proposed difference in Ca^{2+} dynamics, but morphological abnormalities in the cerebellar cortex. Continuation of this research line will produce important information regarding the mechanisms of CAR8 function in the cerebellum, and will aid, specifically, in determining the cause of the altered cellular physiology producing ataxia in *wdl* mice. Conclusions from experiments with the *wdl* mice are graphically summarized here (Fig. 3.6).

4.3 Ethanol Experiments

Our lab group previously found long-term adverse effects of ethanol administration in adolescent rats on motor function, which were evident weeks after exposure (Forbes et al. 2013). In this previous study a binge drinking paradigm was used, in which animals received intraperitoneal injections of ethanol (total of eight injections over a two-week period) that resulted in very high BACs of 303.2 +/- 24.5 mg/dl (in males). In the current study, exposure to ethanol vapours for two hours resulted in BACs

of 172 +/- 18 mg/dl, which we believe is a more realistic BAC that would be achieved by adolescent individuals who are participating in binge drinking. The exposure paradigm was chosen to mimic binge-drinking episodes at an age when the brain is still undergoing rapid development. In addition to being able to achieve the proper dose, the ethanol vapour administration method also mimics a realistic time course of ethanol consumption. Whereas more invasive methods (i.e. oral gavage, injections, etc.) deliver a bolus dose of ethanol resulting in a quick and intense spike in BAC, the vapour chamber methodology results in a slow climb of BAC over the course of administration.

Previous studies using vapour administration of ethanol have only monitored the effects of chronic exposure to alcohol (Becker & Hale 1993; McCool & Chappell 2015; Nentwig et al. 2019; Topper & Valenzuela 2014), whereas the present study utilized a relatively short exposure paradigm of five days. What is considered a relatively low amount of ethanol for binge drinking (enough to reach a BAC ≈160 mg/dl) was administered over the course of five days, and yet we still saw deficits that persisted into adulthood two months after the last alcohol exposure. Unlike what is commonly noted in chronic ethanol exposure studies, we did not observe any obvious signs of physical withdrawal in this model. There were no effects on overall movement the day after the last exposure. We did observe a significant increase in time spent in the light side of the box one day after the last alcohol exposure. However, it is difficult to determine if this was a true withdrawal effect, especially as this effect was maintained when tested on PND 79. The light-dark box has been used previously to examine withdrawal effects in animals (McCool & Chappell 2015). These results indicate that binge drinking during adolescence produces persistent behavioral and biological alterations that can last well

into adulthood even after alcohol exposure has ceased. However, these changes are due to long-term changes to either neuronal physiology or morphology and not physical withdrawal.

4.3.1 Assays of Locomotion (FSRR, ARR, OF, ICH)

Motor testing showed significant deficits caused by ethanol administration on the rota-rod task (Fig. 3.7) It is interesting that this was the only deficit that recovered over time after the cessation of ethanol administration. The cerebellum is known to have a large capacity for regeneration of GCs which may explain the recovery. In this case, it is unlikely Purkinje cells are being destroyed in significant numbers as they cannot regenerate (Ito 2006).

Experiments with the adolescent group and a separate adolescent group on the accelerating rota-rod did not show any significant differences (Figs. 3.4 & 3.5), which was surprising since it is believed to be a more difficult task than the fixed-speed rota-rod. A persistent downward trend in latency to fall was noted with all groups tested which may explain why there were no significant differences between groups. This coupled with the increasing weight of animals and lack of practice at the task in between later trials would cause the observed results.

4.3.2 Novel Object Recognition

Previous studies have found that pre-natal exposure to ethanol can affect object recognition and spatial learning (Kim et al. 1997), it can decrease performance on a NOR task when given acutely (Ryabinin Miller & Durrant 2002), and that chronic ethanol intake can produce object memory deficits in adult rats before going through alcohol withdrawal (Garcia-Moreno et al. 2002). These results are the first, to my knowledge,

which demonstrate that a relatively short exposure to ethanol during adolescence can not only produce these deficits, but that they persist long after the acute effects of ethanol consumption are over. This highlights the high susceptibility of the brain to alcohol induced damage during a critical stage of neurodevelopment.

4.3.3 Assays of Anxiety-like Behavior (DLB, EPM, AS, FC)

It has been established that high levels of behavioral inhibition in childhood predict an increased chance of developing anxiety disorders later in life (Biederman et al. 2001; Campbell-Sills Liverant & Brown 2004). Behavioural inhibition relates to the tendency to experience distress and to withdraw from unfamiliar situations, people, or environments. Where a decrease of behavioral inhibition is a well-known consequence of acute ethanol consumption in humans (de Wit Crean & Richards 2000), it is plausible the altered behavior seen in this study is a long-term extension of this effect. Therefore, the ethanol treated group responses in the anxiety-like behavior testing (i.e. EPM & DLB) may reflect a chronic decrease of behavioral inhibition or increase in risk taking behaviour, but further testing would need to be done in order to confirm this.

4.3.4 Western Blots

Increases to both pro-inflammatory (NF-kB) and pro-apoptotic (capase-3) protein expression in the cerebellum, even at sixty days post-exposure, indicates a biological basis for the accompanying aberrant behavioral features. Studies in hippocampal brain slice cultures found that ethanol exposure increases NF-kB binding to DNA which in turn induce the production of proinflammatory cytokines TNFα, MCP-1, and IL-1β (Zou & Crews 2010). It was interesting that there was a broad-based increase of cellular protein production in all western blots run from the ethanol treated group. Previous studies have

shown that the phosphorylation state of NF-kB can be affected by other drugs of abuse (Zhang et al. 2011). Like these findings, Pascual et al. (2007) found long-term motor dysfunction and increased levels of inflammatory mediators (cyclooxygenase-2 and inducible nitric oxide synthase) in brain tissue using a model of intermittent ethanol exposure in adolescent rats. A lack of statistically significant differences seen in cerebral tissue western blotting was likely due to the large variety of brain regions which were homogenized together. In future experiments the brain needs to be dissected into smaller regions (i.e. hippocampus, prefrontal cortex, etc.) prior to flash freezing the tissue to facilitate a more detailed analysis. Additionally, the inclusion of other methodologies (i.e. immunohistochemistry, fluorescent imagine, etc.) would have made a stronger case for the occurrence of apoptosis in this model. However, due to time constraints these experiments were not undertaken.

While ethanol consumption is correlated with decreased pro-inflammatory protein production; either chronic consumption or consumption with extenuating factors will lead to increased production of these proteins in adults (Szabo et al. 2007). Even though the fully-developed adult physiology can tolerate acute ethanol intake, the fact that adolescent brains are still undergoing development seems to make them more susceptible to long-term behavioral alterations especially in the domain of learning and memory (Crews et al. 2000; Guerri & Pascual 2010).

4.3.5 Conclusions

Previous studies in this area have mainly used oral gavage or intraperitoneal injections to administer doses of ethanol. This set of experiments relied on a less invasive technique where the ethanol is vaporized and absorbed by the animal through mucus

membranes. Unlike previous studies examining the effects of adolescent binge-drinking, this project found persistent changes in behavior and protein expression levels long after treatment had ceased. Previous studies have noted an increase in caspase-3 expression beginning immediately following ethanol exposure (e.g. Han et al. 2005). However, our work is the first to show increased levels long after ethanol administration has ceased (Figs. 3.17 & 3.18).

There are two hypothesized mechanisms by which alcohol damages the adolescent brain; blockade of NMDA receptors (Lovinger White & Weight 1989) and by direct stimulation of $GABA_A$ receptors (Harris et al. 1995). Low-intensity stimulation of glutamatergic NMDA receptors increase intracellular Ca^{2+} levels (Yano et al. 1998) normally protecting against apoptosis from ischemic injuries (Babcock et al. 1999). Therefore, the antagonistic activity of ethanol at NMDA receptors may lower intracellular Ca^{2+} levels and increase the risk of apoptotic signaling cascades. Susceptibility to apoptosis due to changes in Ca^{2+} signaling is another similarity between this model and the *wdl* mice, as our data indicates lower levels of intracellular Ca^{2+} in homozygous *wdl* animals. Additionally, other studies have indicated lower numbers of GCs in *wdl* mice which could be linked to increased apoptosis (Shimobayashi Wagner & Kapfhammer 2016).

Adolescent binge ethanol exposure had effects on the cerebellum up to sixty days after treatment, which is considered early adulthood in rats (Sengupta 2013) and thus extending the findings of existing studies focused on acute outcomes. In addition to the persistent behavioral deficits/changes, protein quantification indicated increased expression of the NF-kB/pNF-kB, caspase-3/cleaved caspase-3, and PKC/pPKC proteins.

The complex interaction of the expression levels of these proteins with the behavioural output of subjects is highlighted by these findings as only certain domains of memory (i.e. object recognition) and motor performance (i.e. balance/coordination) were affected by the binge-drinking paradigm while others were spared (i.e. fear related memory consolidation and muscle tonality/strength). Although there are some limitations to the external validity of the model with respect to the timing of alcohol consumption, we believe it is a reasonable approximation of human behavior seen in adolescents today (Johnston et al. 2018). Future studies should focus on determining the specific sensitive period during which the brain is most susceptible to these alterations and how these alterations might be inhibited by blocking the effects of the proteins whose expression has been increased as a result of treatment.

Comparison of the two models utilized in this dissertation yields several interesting conclusions. Levels of PKC and its activated form (i.e. pPKC) are elevated in the two experimental conditions that experience motor dysfunction (i.e. homozygous wdl mice & adolescent ethanol treated subjects). Ca^{2+} signaling in the cerebellum clearly plays an important role in motor output and disturbances in its balance will significantly affect behavioral output (especially when considering a neurodevelopmental perspective). Alteration of the upstream signaling molecule PKC can inherently have substantial effects on numerous downstream cellular processes due to its position in the cellular cascade. In both models, PKC was determined to have increased expression levels in its active and inactive forms when motor dysfunction was present. Taken as a whole, these results highlight the sensitive nature of the postnatal neurodevelopmental period, and how

important controlled intracellular Ca^{2+} dynamics and conservation of upstream cellular signaling molecules are to the proper functional output of the cerebellum.

References

Adams N, Boice R (1983) A longitudinal study of dominance in an outdoor colony of domestic rats. *Journal of Comparative Psychology*, 97(1), 24-33.

Ahn HJ, Hernandez CM, Levenson JM, Lubin FD, Liou HC, Sweatt JD (2008) c-Rel, an NF-kB family transcription factor, is required for hippocampal long-term synaptic plasticity and memory formation. *Learning & Memory*, 15(7): 539-549.

Aksentijevich I, Zhou Q (2017) NF-kB pathway in autoinflammatory diseases: dysregulation of protein modifications by ubiquitin defines a new category of autoinflammatory diseases. *Frontiers in Immunology*, 8: 399.

Alba A, Kano M, Chen C, Stanton ME, Fox GD, Herrup K, Zwingman TA, Tonegawa S (1994) Deficient cerebellar long-term depression and impaired motor learning in mGluR1 mutant mice. *Cell*, 79(2): 377-388.

Albensi BC, Mattson M (2000) Evidence for the involvement of TNF and NF-kB in hippocampal synaptic plasticity. *Synapse*, 35(2): 151-159.

Albus J (1971) A theory of cerebellar function. *Mathematical Bioscience,* 10: 25–61.

Alling C (1999) The biological mechanisms underlying alcohol dependence. *Lakartidningen,* 96(28-29): 3248-3252.

Altman J (1969) Autoradiographic and histological studies of postnatal neurogenesis. III. Dating the time of production and onset of differentiation of cerebellar microneurons in rats. *Journal of Comparative Neurology*, 136(3), 269-293.

Aspatwar A, Tolvanen MEE, Ortutay C, Parkkila S (2010) Carbonic anhydrase related protein VIII and its role in neurodegeneration and cancer. *Current Pharmaceutical Design*, 16: 3264-3276.

Aufrère G, Le Bourhis B, Beaguè F (1997) Ethanol intake after chronic intoxication by inhalation of ethanol vapour in rats: behavioural dependence. *Alcohol*, 14(3), 247-253.

Baba A, Yasui T, Fujisawa S, Yamada R, Yamada M, Nishiyama N, Ikegaya Y (2003) Activity-evoked capacitative Ca^{2+} entry: implications in synaptic plasticity. *Journal of Neuroscience*, 23(21): 7737-7741.

Babcock AM, Liu H, Paden CM, Churn SB, Pittman AJ (1999) In vivo glutamate neurotoxicity is associated with reductions in calcium/calmodulin-dependent protein kinase II immunoreactivity. *Journal of Neuroscience Research*, 56: 36-43.

Basak S, Shih VF, Hoffmann A (2008) Generation and activation of multiple dimeric transcription factors within the NF-kB signaling system. *Molecular and Cellular Biology*, 28(10): 3139-3150.

Beani L, Tomasini C, Govoni B, Bianchi C (1994) Fluorometric determination of electrically evoked increase in intracellular calcium in cultured cerebellar granule cells. *Journal of Neuroscience Methods*, 51(1): 1-7.

Becker HC, Hale RL (1993) Repeated episodes of ethanol withdrawal potentiate the severity of subsequent withdrawal seizures: an animal model of alcohol withdrawal "kindling". *Alcohol Clin Exp Res.* 17(1): 94-8.

Belmeguenai A, Botta P, Weber JT, Carta M, De Ruiter M, De Zeeuw CI, Valenzuela CF, Hansel C (2008) Alcohol impairs long-term depression at the cerebellar parallel fibre-Purkinje cell synapse. *Journal of Neurophysiology*, 100: 3167-3174.

Bianchi C, Beani L, Antonelli T, Vedovato M, Calo G, Tomasini C (1992) A simple method for electrical field stimulation of cultured granule cells. *Journal of Neuroscience Methods*, 45(3): 175-182.

Biederman J, Hirshfeld-Becker DR, Rosenbaum JF, Herot C, Friedman D, Snidman N, Kagan J, Faraone SV (2001) Further evidence of association between behavioral inhibition and social anxiety in children. *American Journal of Psychiatry*, 158(10): 1673-1679.

Bliss T, Collingridge G (1993) A synaptic model of memory: long-term potentiation in the hippocampus. *Nature*, 361(6407): 31-39.

Boersma MC, Dresselhaus EC, De Biase LM, Mihalas AB, Bergles DE, Meffert MK (2011) A requirement for nuclear factor-kappaB in developmental and plasticity-associated synaptogenesis. *Journal of Neuroscience*, 31: 5414-5425.

Bortolotto Z, Fitzjohn S, Collingridge G (1999) Roles of metabotropic glutamate receptors in LTP and LTD in. *Current Opinion in Neurobiology*, 9(3): 299-304.

Bruno V, Copani A, Knöpfel T, Kuhn R, Casabona G, Dell'Albani P, Nicoletti F (1995) Activation of metabotropic glutamate receptors coupled to inositol phospholipid hydrolysis amplifies NMDA-induced neuronal degeneration in cultured cortical cells. *Neuropharmacology*, 34(8): 1089-1098.

Campbell-Sills L, Liverant GI, Brown TA (2004) Psychometric evaluation of behavioral inhibition/behavioral activation scales in large sample of outpatients with anxiety and mood disorders. *Psychological Assessment*, 16(3): 244-254.

Carobrez AP, Bertogilo LJ (2005) Ethological and temporal analyses of anxiety-like behavior: The elevated plus-maze model 20 years on. *Neuroscience & Biobehavioral Reviews*, 29: 1193-1205.

Chaouloff F, Durand M, Mormède P (1996) Anxiety- and activity-related effects of diazepam and chlordiazepoxide in the rat light/dark and dark/light tests. *Behavioral Brain Research*, 85: 27-35.

Chen M, Wang J (2002) Initiator caspases in apoptosis signaling pathways. *Apoptosis*, 7(4): 313-319.

Cheng EH-Y, Krisch DG, Clem RJ, Ravi R, Kastan MB, Bedi A, Ueno K, Hardwick JM (1997) Conversion of Bcl-2 to a bax-like death effector by caspases. *Science* 278: 1966-1968.

Chuquet J, Hollender L, Nimchinsky E (2007) High-resolution in vivo imaging of the neurovascular unit during spreading depression. *Journal of Neuroscience*, 27(15): 4036-4044.

Clark RS, Kochanek PM, Watkins SC, Chen M, Dixon CE, Seidberg NA, Melick J, Loeffert JE, Nathaniel PD, Jin KL, Graham SH (2000) Caspase-3 mediated neuronal death after traumatic brain injury in rats. *Journal of Neurochemistry*, 74(2): 740-753.

Collingridge G, Singer W (1990) Excitatory amino acid receptors and synaptic plasticity. *Trends in Pharmacological Sciences*, 11(7): 290-296.

Coesmans M, Weber J, De Zeeuw C, Hansel C (2004) Bidirectional parallel fiber plasticity in the cerebellum under climbing fiber control. *Neuron*, 44(4), 691-700.

Coutinho V, Knöpfel T (2002) Metabotropic glutamate receptors: electrical and chemical signaling properties. *The Neuroscientist*, 8(6): 551-561.

Crews FT. Braun CJ, Hoplight B, Switzer III RC, Knapp DJ (2000) Binge ethanol consumption causes differential brain damage in young adolescent rats compared with adult rats. *Alcoholism: Clinical and Experimental Research,* 24(11): 1712-1723.

Crews F, Nixon K, Kim D, Joseph J, Shukitt-Hale B, Qin L, Zou J (2006) BHT blocks NF-kappaB activation and ethanol-induced brain damage. *Alcoholism: Clinical and Experimental Research*, 30(11): 602-612.

Crews FT, Zou J, Qin L (2011) Induction of innate immune genes in brain create the neurobiology of addiction. *Brain Behavior & Immunity*, 25: S4-12.

Dachour A, Hoffmanm A, Deitrich R, de Witte P (2000) Effects of ethanol on extracellular amino acid levels in high-and low-alcohol sensitive rats: a microdialysis study. *Alcohol*, 35: 548-553.

D'Angelo E, Rossi P, Armano S, Taglietti V (1999) Evidence for NMDA and mGlu receptor-dependent long-term potentiation of mossy fiber–granule cell transmission in rat cerebellum. *Journal of Neurophysiology*, 81(1), 277-287.

D'Angelo E, De Zeeuw C (2008) Timing and plasticity in the cerebellum: focus on the granular layer. *Trends in Neurosciences*, 32(1): 30-40.

Daniel H, Levenes C, Crépel F (1998) Cellular mechanisms of cerebellar LTD. *Trends in Neurosciences*, 21(9): 401-406.

Daniell LC, Leslie SW (1986) Inhibition of fast phase calcium uptake and endogenous norepinephrine release in rat brain region synaptosomes by ethanol. *Brain Research*, 377(1): 18-28.

Daoudal G, Debanne D (2003) Long-term plasticity of intrinsic excitability: learning rules and mechanisms. *Learning & Memory*, 10(6): 456-465.

Dawitz J, Kroon T, Hjorth J, Meredith R (2011) Functional calcium imaging in developing cortical networks. *Journal of Visualized Experiments*, 56.

Dean P, Porrill J (2010) The cerebellum as an adaptive filter: a general model? *Functional Neurology*, 25(3): 173-180.

De Bellis MD, Narasimhan A, Thatcher DL, Keshavan MS, Soloff P, Clark DB (2005) Prefrontal cortex, thalamus, and cerebellar volumes in adolescents and young adults with adolescent-onset alcohol use disorders and comorbid mental disorders. *Alcoholism: Clinical and Experimental Research*, 29:1590-1600.

De Wit H, Crean J, Richards JB (2000) Effects of d-amphetamine and ethanol on a measure of behavioral inhibition in humans. *Behavioral Neuroscience*, 114(4): 830-837.

DeZeeuw C, Yeo C (2005) Time and tide in cerebellar memory formation. *Current Opinion in Neurobiology*, 15: 667-674.

Dizon MJ, Khodakhah K (2011) The role of interneurons in shaping Purkinje cell responses in the cerebellar cortex. *Journal of Neuroscience*, 31(29): 10463-10473.

D'Mello SR, Kuan CY, Flavell RA, Rakic P (2000) Caspase-3 is required for apoptosis-associated DNA fragmentation but not for cell death in neurons deprived of potassium. *Journal of Neuroscience Research*, 59: 24-31.

Dobbing J, Sands J (1979) Comparative aspects of the brain growth spurt. *Early Human Development*, 3: 79-83.

Dodgson S, Tashian R, Gross G, Carter N (1991) The carbonic anhydrases: cellular physiology and molecular genetics. Springer-Plenum, New York.

Doulcet X, Llobet D, Pallares J, & Matias-Guiu X (2005) NF-kB in development and progression of human cancer. *European Journal of Pathology*, 446(5): 475-482.

Draski L, Nash D, Gerhardt G (1994) CNS monoamine levels and motoric behaviors in the hotfoot ataxic mutant. *Brain Research*, 645(1): 69-77.

Dugué G, Brunel N, Hakim V, Schwartz E, Chat M, Dieudonné S (2009) Electrical coupling mediates tunable low-frequency oscillations and resonance in the cerebellar Golgi cell network. *Neuron*, 61(1): 126-139.

Eccles JC, Ito M, Szentagothai J (1967) The cerebellum as a neuronal machine. Springer-Verlag, Berlin.

Elmore S (2007) Apoptosis: A review of programmed cell death. *Toxicology Pathology*, 35: 495-519.

Faas G, Adwanikar H, Gereau I, Saggau P (2002) Modulation of presynaptic calcium transients by metabotropic glutamate receptor activation: a differential role in acute depression of synaptic transmission and long-term depression. *Journal of Neuroscience*, 22(16): 6885-6890.

Fan TJ, Han LH, Cong RS, Liang J (2005) Caspase family proteases and apoptosis. *Acta Biochimica et BioPhysica Sinica*, 37(11): 719-727.

Forbes A, Cooze J, Malone C, French V, Weber JT (2013) Effects of intermittent binge alcohol exposure on long-term motor function in young rats. *Alcohol*, 47: 95-102.

Gall D, Prestori F, Sola E, D'Errico A, Roussel C, Forti L, D'Angelo E (2005) Intracellular calcium regulation by burst discharge determines bidirectional long-term synaptic plasticity at the cerebellum input stage. *Journal of Neuroscience*, 25(19): 4813-4822.

Garcia-Moreno LM, Conejo NM, Capilla A, Garcia-Sanchez O, Senderek K, Arias JL (2002) Chronic ethanol intake and object recognition in young and adult rats. *Progress in Neuro-Psychopharmacology and Biological Psychiatry*, 26(5): 831-837.

Garwicz M (2002) Spinal reflexes provide motor error signals to cerebellar modules—relevance for motor coordination. *Brain Research Reviews*, 40(1-3): 152-165.

Gilmore TD (1999) The Rel/NF-kB signal transduction pathway: introduction. *Oncogene*, 18(49): 6824-6844.

Gilmore TD (2006) Introduction to NF-kB: players, pathways, perspectives. *Oncogene*, 25(51): 6680-6684.

Guerri C, Pascual M (2010) Mechanisms involved in the neurotoxic, cognitive, and neurobehavioral effects of alcohol consumption during adolescence. *Alcohol*, 44: 15-26.

Gugger OS, Hartmann J, Brinbaumer L, Kapfhammer JP (2012) P/Q-type and T-type calcium channels, but not type 3 transient receptor potential cation channels, are involved in inhibition of dendritic growth after chronic metabotropic glutamate receptor type 1 and protein kinase C activation in cerebellar Purkinje cells. *European Journal of Neuroscience*, 35: 20-33.

Gutierrez H, Hale VA, Dolcet X, Davies A (2005) NF-kB signalling regulates the growth of neural processes in the developing PNS and CNS. *Development*, 132(7): 1713-1726.

Han JY, Joo Y, Kim YS, Lee YK, Kim HJ, Cho GJ, Choi WS, Kang SS (2005) Ethanol induces cell death by activating caspase-3 in the rat cerebral cortex. *Molecules and Cells*, 20(2), 189-195.

Hansel C, Artola A, Singer W (1997) Relation between dendritic Ca^{2+} levels and the polarity of synaptic long-term modification in the rat visual cortex neurons. *European Journal of Neuroscience*, 9: 2309-2322.

Hansel C, Linden D (2000) Long-term depression of the cerebellar climbing fibre-Purkinje neuron synapse. *Neuron*, 26: 239-247.

Hansel C, Linden D, D'Angelo E (2001) Beyond parallel fiber LTD: the diversity of synaptic and non-synaptic plasticity in the cerebellum. *Nature Neuroscience*, 4: 467-476.

Hamelink C, Hampson A, Wink DA, Eiden LE, Eskay RL (2005) Comparison of cannabidiol, antioxidants, and diuretics in reversing binge ethanol-induced neurotoxicity. *Journal of Pharmacology and Experimental Therapeutics*, 314(2), 780-788.

Harris B, Ward-Bailey P, Johnson K, Bronson R, Davisson M (2003) A new mutation, waddles (wdl), on mouse Chromosome 4. Mouse Mutant Resources Web Site. The Jackson Laboratory: Bar Harbor, Maine. MGI Direct Data Submission.

Harris RA, Proctor WR, McQuilkin SJ, Klein RL, Mascia MP (1995) Ethanol increases GABAA responses in cells stably transfected with receptor subunits. *Alcoholism: Clinical and Experimental Research*, 19: 226-232.

Herkenham M, Rathore P, Brown P, Listwak SJ (2011) Cautionary notes on the use of NF-kB p65 and p50 antibodies for CNS studies. *Journal of Neuroinflammation*, 8(1): 141.

Hirasawa M, Xu X, Trask R, Maddatu T, Johnson B, Naggert JK, Nishina PM, Ikeda A (2007) Carbonic anhydrase related protein 8 mutation results in aberrant synaptic morphology and excitatory synaptic function in the cerebellum. *Molecular and Cellular Neuroscience*, 35: 161-170.

Hiroko N, Nakamura S (2007) Brain-derived neurotrophic factor regulates AMPA receptor trafficking to post-synaptic densities via IP3R and TRPC calcium signaling. *FEBS Letters*, 581(10): 2047-2054.

Hirota J, Ando H, Hamada K, Mikoshiba K. (2003) Carbonic anhydrase-related protein is a novel binding protein for inositol 1,4,5-trisphosphate receptor type 1. *Journal of Biochemistry*, 372: 435-441.

Hoebeek FE, Stahl JS, Van Alphen AM, Schonewille M, Luo C, Rutteman M, van den Maagdenberg AMJM, Molenaar PC, Goossens HHLM, Frens MA, De Zeeuw CI (2005) Increased noise level of purkinje cell activities minimizes impact of their modulation during sensorimotor control. *Neuron*, 45(6): 953-965.

Hoffmann PL, Rabe CS, Moses F, Tabakoff B (1989) N-methyl-D-aspartate receptors and ethanol: Inhibition of calcium flux and cyclic GMP production. *Journal of Neurochemistry*, 52(6): 1937-1940.

Hoffmann A, Natoli G, Ghosh G (2006) Transcriptional regulation vis the NF-kB signaling module. *Oncogene*, 25(51): 6706.

Houston C, Wisden W, Brickley S (2012) Axon location determines the input selectivity of cerebellar granule cells. *2012 Neuroscience Meeting Planner*. New Orleans, LA: Society for Neuroscience. Program No. 648.17: Online.

Ikonomidou C, Bittigau P, Ishimaru MJ, Wozniak DF, Koch C, Genz K, Price MT, Stefovska V, Horster F, Tenkova T, Dikranian K, Zorumski CF, Olney JW, Wozniak DF (2003) Ehanol-induced apoptotic neurodegeneration and fetal alcohol syndrome. *Science*, 287: 1056-1060.

Jacobson MD, Weil M, Raff MC (1997) Programmed cell death in animal development. *Cell* 88: 347-354.

Ichikawa R, Miyazaki T, Kano M, Hashikawa T, Tatsumi H, Sakimura K, Watanabe M (2002) Distal extension of climbing fiber territory and multiple innervation caused by aberrant wiring to adjacent spiny branchlets in cerebellar Purkinje cells lacking glutamate receptor δ2. *Journal of Neuroscience*, 22(19): 8487-8503.

Ito M, Kano M (1982) Long-lasting depression of parallel fibre-Purkinje cell transmission induced by conjunctive stimulation of parallel fibres and climbing fibres in the cerebellar cortex. *Neuroscience Letters*, 33(3): 253–258.

Ito M (2006) Cerebellar circuitry as a neuronal machine. *Progress in Neurobiology*, 78: 272-303.

Jalil SJ, Sacktor TC, Shouval HZ (2015) Atypical PKCs in memory maintenance: the roles of feedback and redundancy. *Learning & Memory*, 22(7): 344-353.

Jiao Y, Yan J, Zhao Y, Donahue LR, Beamer WG, Li X, Roe BA, Ledoux MS, & Gu W (2005) Carbonic anhydrase-related protein VIII deficiency is associated with a distinctive lifelong gait disorder in waddles mice. *Genetics*, 171: 1239-1246.

Johnston LD, Miech RA, O'Malley PM, Bachman JG, Schulenberg JE, Patrick ME (2018) Monitoring the Future national survey results on drug use: 1975-2018: Overview, key findings on adolescent drug use. Ann Arbor: Institute for Social Research, The University of Michigan.

Jones BJ, Roberts DJ (1968) The quantitative measurement of motor inco-ordination in naïve mice using an accelerating rotarod. *Journal of Pharmacy and Pharmacology*: 20, 302-304.

Kaltchmidt C, Kaltschmidt B, Baeuerle PA (1993) Brain synapses contain inducible forms of the transcription factor NF-kappa B. *Mechanisms of Development*, 43: 135-147.

Kaltchmidt C, Kaltschmidt B, Baeuerle PA (1995) Stimulation of ionotropic glutamate receptors activates transcription factor NF-kappa B in primary neurons. *Proceedings of the National Academy of Sciences of the USA*, 92: 9618-9622.

Kaltchmidt C, Kaltschmidt B, Neumann H, Wekerle H, Baeuerle PA (1994) Constitutive NF-kappa B activity in neurons. *Molecular and Cellular Biology*, 14: 3981-3992.

Kaltschmidt B, Ndiaye D, Korte M, Pothion S, Arbibe L, Prullage M, Pfeiffer J, Lindecke A, Staiger V, Israel A, Kaltschmidt C (2006) NF-kB regulates spatial memory formation and synaptic plasticity through protein kinase A/CREB signaling. *Molecular and Cellular Biology*, 26(8): 2936-2946.

Kandel E, Schwartz J, Jessell T (Eds.). 2000. *Principles of Neural Science,* Vol. 4, pp. 837-840. New York: McGraw-Hill.

Kohda K, Inoue T, Mikoshiba K (1995) Ca^{2+} release from Ca^{2+} stores, particularly from ryanodine-sensitive Ca^{2+} stores, is required for the induction of LTD in cultured cerebellar Purkinje cells. *Journal of Neurophysiology*, 74(5): 2184-2188.

Kuida K, Zheng TS, NA S, Kuan C-Y, Yang D, Karasuyama H, Rakic P, Flavell RA (1996) Decreased apoptosis in the brain and premature lethality in CPP32-deficient mice. *Nature* 384: 368-372.

Kurihara H, Hashimoto K, Kano M, Takayama C, Sakimura K, Mishina M, Watanabe M (1997) Impaired parallel fiber→ Purkinje cell synapse stabilization during cerebellar development of mutant mice lacking the glutamate receptor δ2 subunit. *Journal of Neuroscience*, 17(24): 9613-9623.

Lakkis M, O'Shea K, Tashian R (1997) Differential expression of the carbonic anhydrase genes for CA VII (Car7) and CA-RP VIII (Car8) in mouse brain. *Journal of Histochemistry & Cytochemistry*, 45(5): 657-662.

Lalonde R, Strazielle C (2001) Motor performance and regional brain metabolism of spontaneous murine mutations with cerebellar atrophy. *Behavioural Brain Research*, 125(1): 103-108.

Lamont MG, Weber JT (2012) The role of calcium in synaptic plasticity and motor learning in the cerebellar cortex. *Neuroscience and Biobehavioral Reviews*, 36(4):1153-1162.

Lamont MG, Weber JT (2015) Mice deficient in carbonic anhydrase type 8 exhibit motor dysfunctions and abnormal calcium dynamics in the somatic region of cerebellar granule cells. *Behavioral Brain Research*, 286: 11-16.

Lamont MG, McCallum P, Head N, Blundell J, Weber JT (2020) Binge drinking in male adolescent rats and its relationship to persistent behavioral impairments and elevated proinflammatory/proapoptotic proteins in the cerebellum. *Psychopharmacology*, 1-11.

Lazzari C, Peggion C, Stella R, Massimino M, Lim D, Bertoli A, Sorgato M (2011) Cellular prion protein is implicated in the regulation of local Ca^{2+} movements in cerebellar granule neurons. *Journal of Neurochemistry*, 116: 881-890.

Lev-Ram V, Wong S, Storm D, Tsien R (2002) A new form of cerebellar long-term potentiation is postsynaptic and depends on nitric oxide but not cAMP. *Proceedings of the National Academy of Sciences*, 99(12): 8389-8393.

Li P, Nijhawan D, Budihardjo I, Srinivasula SM, Ahmad M, Alnemri ES, Wang X (1997) Cytochrome c and dATP-dependent formation of Apaf-1/caspase-9 complex initiates an apoptotic protease cascade. *Cell*, 91: 479-489.

Lisman J, Zhabotinsky A (2001) A model of synaptic memory: a CaMKII/PP1 switch that potentiates transmission by organizing an AMPA receptor anchoring assembly. *Neuron*, 44: 191-201.

Listwak SJ, Rathore P, Herkenham M (2013) Minimal NF-kB activity in neurons. *Neuroscience*, 250: 282-299.

Liu S, Cull-Candy S (2005) Subunit interaction with PICK and GRIP controls Ca^{2+} permeability of AMPARs at cerebellar synapses. *Nature Neuroscience*, 8(6): 768-775.

Liu T, Zhang L, Joo D, Sun S (2017) NF- kB signaling in inflammation. *Signal Transduction and Targeted Therapy*, 2: 17023.

Lovinger DM, White G, Weight FF (1989) Ethanol inhibits NMDA-activated ion current in hippocampal neurons. *Science*, 243: 1721-1724.

Maex R, De Schutter E (1998) Synchronization of Golgi and granule cell firing in a detailed network model of the cerebellar granule cell layer. *Journal of Neurophysiology*, 80: 2521-2537.

Mahadev K, Vemuri MC (1998) Selective changes in protein kinase C isoforms and phosphorylation on endogenous substrate proteins in rat cerebral cortex during pre- and postnatal ethanol exposure. *Archives of Biochemistry and Biophysics*, 356: 249-257.

Malenka R, Nicoll R (1999) Long-term potentiation – a decade of progress? *Science*, 285: 1870-1874.

Mandolesi G, Autuori E, Cesa R, Premoselli F, Cesare P, Strata P (2009) GluRδ2 expression in the mature cerebellum of hotfoot mice promotes parallel fiber synaptogenesis and axonal competition. *Public Library of Science ONE*, 4(4): e5243.

Manto M, Jissendi P (2012) Cerebellum: links between development, developmental disorders and motor learning. *Frontiers in Neuroanatomy*, 6: 1.

Marini AM, Jiang X, Wu X, Tian F, Zhu D, Okagaki P, Lipsky RH (2004) Role of brain-derived neurotrophic factor and NF-kB in neuronal plasticity and survival: From genes to phenotype. *Restorative Neurology and Neuroscience*, 22(2): 121-130.

Marr D (1969) A theory of cerebellar cortex. *Journal of Physiology*, 202(2): 437-470.

Massey P, & Bashir Z (2007) Long-term depression: multiple forms and implications for brain function. *Trends in Neurosciences*, 30(4): 176-184.

Mattson, MP (2005) NF-kB in the survival and plasticity of neurons. *Neurochemical Research*, 30(6-7): 883-893.

McCool BA, Chappell AM (2015) Chronic intermittent ethanol inhalation increases ethanol self-administration in both C57BL/6J and DBA/2J mice. *Alcohol* 49(2): 111-20.

Medina J, Nores W, Mauk M (2002) Inhibition of climbing fibres is a signal for the extinction of conditioned eyelid responses. *Nature*, 416(6878): 330–333.

Melloe H, Parker PJ (1998) The extended protein kinase C superfamily. *Biochemical Journal*, 332(2): 281-292.

Messing RO, Petersen PJ, Henrich CJ (1991) Chronic ethanol exposure increases levels of protein kinase C delta and epsilon and protein kinase C-mediated phosphorylation in cultured neural cells. *Journal of Biological Chemistry*, 266: 23428-23432.

Metzger F, Kapfhammer JP (2000) Protein kinase C activity modulates dendritic differentiation of rat Purkinje cells in cerebellar slice cultures. *European Journal of Neuroscience*, 12: 1993-2005.

Mitsumura K, Hosoi N, Furuya N, Hirai H (2011) Disruption of metabotropic glutamate receptor signaling is a major defect at cerebellar parallel fibre-Purkinje cell synapses in staggerer mutant mice. *Journal of Physiology*, 589(13): 3191-3209.

Miyazaki T, Hashimoto K, Shin HS, Kano M, Watanabe M (2004) P/Q-type Ca2+ channel alpha1A regulates synaptic competition on developing cerebellar Purkinje cells. *Journal of Neuroscience*, 24(7): 1734-1743.

Monville, C, Torres E, Dunnett S (2006) Comparison of incremental and accelerating protocols of the rotarod test for the assessment of motor deficits in the 6-OHDA model. *Journal of Neuroscience Methods*, 158(2): 219-223.

Mooney SM, Miller MW (2001) Effects of prenatal exposure to ethanol on the expression of bcl-2, bax, and caspase 3 in the developing rat cerebreal cortex and thalamus. *Brain Research*, 911: 71-81.

Moroni F, Lombardi G, Thomsen C, Leonardi P, Attucci S, Peruginelli F, Torregrossa S, Pellegrini-Giampiettro D, Luneia R, Pelliccian R (1997) Pharmacological characterization of 1-aminoindan-1,5-dicarboxylic acid, a potent mGluR1 antagonist. *Journal of Pharmacology and Experimental Therapeutics*, 281(2): 721-729.

Mulkey R, Malenka R (1992) Mechanisms underlying induction of homosynaptic long-term depression in area CA1 of the hippocampus. *Neuron*, 9: 967-975.

Nagase T, Ito KI, Kato K, Kaneko K, Kohda K, Matsumoto M, Hoshino A, Inoue T, Fujii S, Kato H, Mikoshiba K (2003) Long-term potentiation and long-term

depression in hippocampal CA1 neurons of mice lacking the IP3 type 1 receptor. *Neuroscience*, 117(4): 821-830.

Nelson TJ, Sun MK, Hongpaisan J, Alkon DL (2008) Insulin, PKC signalling pathways, and synaptic remodeling during memory storage and neuronal repair. *European Journal of Pharmacology*, 585(1): 76-87.

Nennig SE, Schank JR (2017) The role of NF-*k*B in drug addiction: beyond inflammation. *Alcohol and Alcoholism*, 52(2): 172-179.

Nentwig TB, Starr EM, Chandler LJ, Glover EJ (2019) Absence of compulsive drinking phenotype in adult male rats exposed to ethanol in a binge-like pattern during adolescence. *Alcohol* 79: 93-103.

Nicholson DW, Thornberry A (1997) Caspases: killer proteases. *Trends in Biochemical Sciences*, 22: 299-306.

Nieus T, Sola E, Mapelli J, Saftenku E, Rossi P, D'angelo E (2006) LTP regulates burst initiation and frequency at mossy fiber–granule cell synapses of rat cerebellum: experimental observations and theoretical predictions. *Journal of Neurophysiology*, 95(2): 686-699.

Nishizuka Y (1986) Studies and perspective of protein kinase C. *Science*, 233(4761): 305-312.

Nishizuka Y (1995) Protein kinase C and lipid signaling for sustained cellular responses. *The FASEB Journal*, 9(7): 484-496.

Nixon K, Crews FT (2002) Binge ethanol exposure decrease neurogenesis in adult rat hippocampus. *Journal of Neurochemistry*, 83(5): 1087-1093.

Nutt DJ (1996) Addiction: brain mechanisms and their treatment implications. *The Lancet*, 347: 31-36.

Oeckinghaus A, Ghosh S (2009) The NF-kappaB family of transcription factors and its regulation. *Cold Spring Harbour Perspectives in Biology*, 1(4): 1-14.

Okubo Y, Kakizawa S, Hirose K, Iino M (2001) Visualization of IP3 dynamics reveals a novel AMPA receptor-triggered IP3 production pathway mediated by voltage-dependent Ca^{2+} influx in Purkinje cells. *Neuron*, 32: 113–122.

Olney JW, Tenkova T, Dikranian K, Muglia LJ, Jermakowicz WJ, D'Sa C, Roth KA (2002) Ethanol-induced caspase-3 activation in the in vivo developing mouse brain. *Neurobiological Disease*, 9: 205-219.

Olney JW, Tenkova T, Dikranian K, Qin YQ, Labruyere J, Ikonomidou C (2002) Ethanol-induced apoptotic neurodegeneration in the developing C57BL/6 mouse brain. *Developmental Brain Research*, 133: 115-126

Osmon KJ, Vyas M, Woodley E, Thompson P, Walia JS (2018) Battery of behavioral tests assessing general locomotion, muscular strength, and coordination in mice. *Journal of Visual Experiments*, 131: e55491.

Pascual M, Blanco AM, Cauli O, Minarro J, Guerri C (2007) Intermittent ethanol exposure induces inflammatory brain damage and causes long-term behavioral alterations in adolescent rats. *European Journal of Neuroscience*, 25: 541-550.

Phillips SC, Cragg BG (1982) A change in susceptibility of rat cerebellar purkinje cells to damage by alcohol during fetal, neonatal and adult life. *Neuropathology and Applied Neurobiology*, 8: 441-454.

Piochon C, Irinopoulou T, Brusciano D, Bailly Y, Mariani J, Levenes C (2007) NMDA receptor contribution to the climbing fiber response in the adult mouse Purkinje cell. *Journal of Neuroscience*, 27(40): 10797-10809.

Piochon C, Levenes C, Ohtsuki G, Hansel C (2010) Purkinje cell NMDA receptors assume a key role in synaptic gain control in the mature cerebellum. *Journal of Neuroscience*, 30(45): 15330-15335.

Porter AG, Janicke RU (1999) Emerging roles of caspase-3 in apoptosis. *Cell Death and Differentiation*, 6: 99-104.

Rahman S, Neuman R (1996) Characterization of metabotropic glutamate receptor-mediated facilitation of N-methyl-D-aspartate depolarization of neocortical neurones. *British Journal of Pharmacology*, 117(4): 675-683.

Ramos A, Pereira E, Martins GC, Wehrmeister TD, Izídio GS (2008) Integrating the open field, elevated plus maze and light/dark box to assess different types of emotional behaviors in one single trial. *Behavioral Brain Research*, 193: 277-288.

Randall A, Tsien R (1995) Pharmacological dissection of multiple types of Ca^{2+} channel currents in rat cerebellar granule neurons. *Journal of Neuroscience*, 15(4): 2995-3012.

Rathore S, Datta G, Kaur I, Malhotra P, Mohmmed A (2015) Disruption of cellular homeostasis induces organelle stress and triggers apoptosis like cell-death pathways in malaria parasite. *Cell Death & Disease*, 6(7): e1803.

Reed JC (1997) Cytochrome c: Can't live with it – can't live without it. *Cell*, 91: 559-562.

Renzi M, Farrant M, Cull-Candy S (2007) Climbing-fibre activation of NMDA receptors in Purkinje cells of adult mice. *Journal of Physiology*, 585(1): 91-101.

Rhyu I, Abbott L, Walker D, Sotelo C (1999) An ultrastructural study of granule cell/Purkinje cell synapses in tottering (tg/tg), leaner (tg^{la}/tg^{la}) and compound heterozygous tottering/leaner (tg/tg^{la}) mice. *Neuroscience*, 90(3): 717-728.

Rice AC, Bullock MR, Shelton KL (2004) Chronic ethanol consumption transiently reduced adult neural progenitor cell proliferation. *Brain Research*, 1011(1): 94-98.

Rinaldo L, Hansel C (2010) Ataxias and cerebellar dysfunction: involvement of synaptic plasticity deficits? *Functional Neurology*, 25(3): 135-139.

Robinson M, Coyle J (1987) Glutamate and related acidic excitatory neurotransmitters: from basic science to clinical application. *The FASEB Journal*, 1(6): 446-455.

Rose C, Konnerth A (2001) Stores not just for storage: intracellular calcium release and synaptic plasticity. *Neuron*, 31(4): 519-522.

Ross DH, Medina MA, Cardenas HL (1974) Morphine and ethanol: Selective depletion of regional brain calcium. *Science*, 186(4158): 63-65.

Russo SJ, Wilkinson MB, Mazei-Robison MS, Dietz DM, Maze I, Krishnan V, Renthal W, Graham A, Brinbaum SG, Green TA, Robison B (2009) Nuclear factor kappa B signaling regulates neuronal morphology and cocaine reward. *Journal of Neuroscience*, 29: 3529-3537.

Rustay N, Wahlsten D, Crabbe C (2003) Influence of task parameters on rotarod performance and sensitivity to ethanol in mice. *Behavioural Brain Research*, 141:237-249.

Ryabinin AE, Miller MN, Durrant S (2002) Effects of acute alcohol administration on object recognition learning in C57BL/6J mice. *Pharmacology Biochemistry and Behavior*, 71(1-2): 307-312.

Salin P, Malenka R, Nicoll R (1996) Cyclic AMP mediates a presynaptic form of LTP at cerebellar parallel fibre synapses. *Neuron*, 16: 797-803.

Salvesen GS, Dixit VM (1997) Caspases: intracellular signaling by proteolysis. *Cell*, 91: 443-446.

Sánchez-Campusano R, Gruart A, Delgado-García J (2007) The cerebellar interpositus nucleus and the dynamic control of learned motor responses. *The Journal of Neuroscience*, 27(25): 6620-6632.

Santerre JL, Gigante ED, Landin JD, Werner DF (2014) Molecular and behavioral characterization of adolescent protein kinase C following high dose ethanol exposure. *Psychopharmacology*, 2331(8): 1809-1820.

Schmahmann J (2004) Disorders of the cerebellum: ataxia, dysmetria of thought, and the cerebellar cognitive affective syndrome. *Journal of Neuropsychiatry and Clinical Neurosciences*, 16(3): 367-378.

Schmidt-Ullrich R, Memet S, Lilienbaum A, Feuillard J, Raphael M, Israel A (1996) NF-kappa B activity in transgenic mice: developmental regulation and tissue specificity. *Development*, 122: 2117-2128.

Schonewille M, Wulf P, Farrant M, Wisden W, De Zeeuw C (2007) Interneurons in the molecular layer of the cerebellum are required for consolidation of motor

learning. *2007 Neuroscience Meeting Planner*. San Diego, CA: Society for Neuroscience. Program No. 190.13. Online.

Schonewille M, Belmeguenai A, Koekkoek S, Houtman S, Boele H, van Beugen B, Gao Z, Badura A, Ohtsuki G, Amerika W, Hosy E, Hoebeek F, Elgersma Y, Hansel C, De Zeeuw C (2010) Purkinje cell-specific knockout of the protein phosphatase PP2B impairs potentiation and cerebellar motor learning. *Neuron*, 67(4): 618-628.

Schummers J, Bentz S, Browning MD (1997) Ethanol's inhibition of LTP may not be mediated solely via direct effects on the NMDA receptor. *Alcoholism: Clinical and Experimental Research*, 21: 404-408.

Sengupta P (2013) The laboratory rat: Relating its age with human's. *International Journal of Preventative Medicine*, 4(6): 624-630.

Shih RH, Wang CY, Yang CM (2015) NF-kappaB signaling pathways in neurological inflammation: A mini review. *Frontiers in Molecular Neuroscience*, 8: 77.

Shimobayashi E, Wagner W, Kapfhammer JP (2016) Carbonic anhydrase 8 expression in Purkinje cells is controlled by PKCγ activity and regulates Purkinje cell dendritic growth. *Molecular Neurobiology*, 53: 5149-5160.

Shirakawa F, Mizel SB (1989) In vitro activation and nuclear translocation of NF-kappa B catalyzed by cyclic AMP-dependent protein kinase and protein kinase C. *Molecular and Cell Biology*, 9: 2424-2430.

Sola E, Prestori F, Rossi P, Taglietti V, D'Angelo E (2004) Increased neurotransmitter release during long-term potentiation at mossy fibre-granule cell synapses in rat cerebellum. *The Journal of Physiology*, 557(3): 843-861.

Sollberger G, Strittmatter GE, Garstkiewicz M, Sand J, Beer HD (2014) Caspase-1: the inflammasome and beyond. *Innate Immunity*, 20(2): 115-125.

Spear LP, Brake SC (1983) Periadolescence: age-dependent behavior and psychopharmacological responsivity in rats. *Developmental Psychobiology*, 16(2): 83-109.

Spear LP, (2000) The adolescent brain and age-related behavioral manifestations. *Neuroscience & Biobehavioral Reviews*, 24(4): 417-463.

Spear LP, (2013) Adolescent neurodevelopment. *Journal of Adolescent Health*, 52(2): S7-S13.

Steele A, Lindquist S, Aguzzi A (2007) The prion protein knock-out mouse. *Prion*, 1(2): 83-93.

Streissguth AP, O'Malley K (2000) Neuropsychiatric implications and long-term consequences of fetal alcohol spectrum disorders. *Seminars in Clinical Neuropsychiatry*, 5: 177-190.

Stoodley C, Schmahmann, J (2010) Evidence for topographic organization in the cerebellum of motor control versus cognitive and affective processing. *Cortex*, 46(7): 831-844.

Stubbs CD, Slater SJ (1999) Ethanol and protein kinase C. Alcoholism*: Clinical and Experimental Research*, 23(9): 1552-1560.

Szabo G, Mandrekar P, Oak S, Mayerle J (2007) Effect of ethanol on inflammatory responses. *Pancreatology*, 7(2-3): 115-123.

Takeuchi T, Miyazaki T, Watanabe M, Mori H, Sakimura K, Mishina M (2005) Control of synaptic connection by glutamate receptor δ2 in the adult cerebellum. *Journal of Neuroscience*, 25(8): 2146-2156.

Tajuddin N, Moon KH, Marshall SA, Nixon K, Neafsey EJ, Kim HY, Collins MA (2014) Neuroinflammation and neurodegeneration in adult rat brain from binge ethanol exposure: abrogation by docosahexaenoic acid. *PLoS One*, 9(7): e101223.

Taniuchi K, Nishimori I, Takeuchi T, Fujikawa-Adachi K, Ohtsuki Y, Onishi S (2002) Developmental expression of carbonic anhydrase-related proteins VIII, X, and XI in the human brain. *Neuroscience*, 112(1): 93-99.

Teixeira FB, da Silva Santana LN, Bezerra FR, De Carvalho S, Fontes-Junior EA, Prediger RD, Crespo-Lopez ME, Maia CSF, Lima RR (2014) Chronic ethanol exposure during adolescence in rats induces motor impairments and cerebral cortex damage associated with oxidative stress. *PloS One*, 9(6).

Topper LA, Valenzuela CF (2014) Effect of repeated alcohol exposure during the third trimester-equivalent on messenger RNA levels for interleukin-1β, chemokine (C-C motif) ligand 2, and interleukin 10 in the developing rat brain after injection of lipopolysaccharide. *Alcohol,* 48(8): 773-80.

Türkmen S, Guo G, Garshasbi M, Hoffmann K, Alshalah A, Mischung C, Robinson P (2009) CA8 mutations cause a novel syndrome characterized by ataxia and mild mental retardation with predisposition to quadrupedal gait. *PLoS Genetics*, 5(5): e1000487.

Urrutia A, Gruol DL (1992) Acute alcohol alters the excitability of cerebellar Purkinje neurons and hippocampal neurons in culture. *Brain Research*, 569(1): 26-37.

Varlinskaya EI, Hosova D, Towner T, Werner DF, Spear LP (2020) Effects of chronic intermittent ethanol exposure during early and late adolescence on anxiety-like behaviors and behavioral flexibility in adulthood. *Behavioral Brain Research*, 378: 112292.

Ward TH, Cummings J, Dean E, Greystoke A, Hou JM, Backen A, Randon M, Dive C (2008) Biomarkers of apoptosis. *British Journal of Cancer*, 99: 841-846.

Weber J, Rzigalinski B, Ellis E (2001) Traumatic injury of cortical neurons causes changes in intracellular calcium stores and capacitative calcium influx. *Journal of Biological Chemistry*, 276(3): 1800-1807.

Wellmann H, Kaltschmidt B, Kaltschmidt C (2001) Retrograde transport of transcription factor NF-kappa B in living neurons. *Journal of Biological Chemistry*, 276: 11821-11829.

Winter O, Li L, Raymond J (2012) Is motor learning encoded by structural alterations in cerebellar parallel fibers? *2012 Neuroscience Meeting Planner*. New Orleans, LA: Society for Neuroscience. Program No. 477.27: Online.

Woo M, Hakem R, Soengas MS, Duncan GS, Shahinian A, Kagi D, Hakem A, McCurrach M, Khoo W, Kaufman SA, Senaldi G, Howard T, Lowe SW, Mak TW (1998) Essential contribution of caspase-3/CPP32 to apoptosis and its associated nuclear changes. *Genes & Development*, 12: 806-819.

Wyllie AH, Kerr JF, Currie AR (1980) Cell death: the significance of apoptosis. *International Review of Cytology*, 68:251-306.

Yan J, Jiao Y, Jiao F, Stuart J, Donahue L, Beamer W, Gu W (2007) Effects of carbonic anhydrase VIII deficiency on cerebellar gene expression profiles in the wdl mouse. *Neuroscience Letters*, 413(3): 196-201.

Yano S, Tokumitsu H, Soderling TR (1998) Calcium promotes cell survival through CaM-K kinase activation of the protein-kinase-B pathway. *Nature*, 396, 584-587.

Young C, Roth KA, Klocke BJ, West T, Holtzman DM, Labruyere J, Qin YQ, Dikranian K, Olney JW (2005) Role of caspase-3 in ethanol-induced developmental neurodegeneration. *Neurobiology of Disease*, 20:608-614.

Zagha E, Manita S, Ross W, Rudy B (2010) Dendritic $Kv_{3.3}$ potassium channels in cerebellar Purkinje cells regulate generation and spatial dynamics of dendritic Ca2+ spikes. *Journal of Neurophysiology*, 103(6): 3516-3525.

Zanjani H, Vogel M, Mariani J (2012) Morphometric and quantitative analysis of cerebellar Purkinje and granule cells in the hotfoot ($Grid2^{ho/ho}$) mutant mice. *2012 Neuroscience Meeting Planner*. New Orleans, LA: Society for Neuroscience. Program No. 652.01: Online.

Zhang FX, Rubin R, Rooney TA (1998) Ethanol induces apoptosis in cerebellar granule neurons by inhibiting insulin-like growth factor 1 signaling. *Journal of Neurochemistry*, 71: 196-204.

Zhang X, Cui Y, Jing J, Cui Y, Xin W, Liu X (2011) Involvement of p38/NF-kB signaling pathway in the nucleus accumbens in the rewarding effects of morphine in rats. *Behavioral Brain Research*, 218(1): 184-189.

Zheng T, Li W, Zhang A, Altura BT, Altura BM (1998) Staurosporine and H7 attenuate ethanol-induced elevation in [Ca^{2+}]i in cultured canine cerebral vascular smooth muscle cells. *Neuroscience Letters*, 241(2-3): 139-142.

Zhuchenko O, Bailey J, Bonnen P, Ashizawa T, Stockton DW, Amos C, Dobyns WB, Subramony SH, Zoghbi HY, Lee CC (1997) Autosomal dominant cerebellar ataxia (SCA6) associated with small polyglutamine expansions in the α 1A-voltage-dependent calcium channel. *Nature Genetics*, 15(1): 62-69.

Zlomuzica A, Burghoff S, Schrader J, Dere E (2012) Superior working memory and behavioural habituation but diminished psychomotor coordination in mice lacking the ecto-5′-nucleotidase (CD73) gene. *Purinergic Signalling*: 1-8.

Zou J, Crews F (2010) Induction of innate immune gene expression cascades in brain slice cultures by ethanol: key role of NF-kappaB and proinflammatory cytokines. *Alcoholism: Clinical and Experimental Research*, 34(5): 777-489.